



University
of Glasgow

<https://theses.gla.ac.uk/>

Theses Digitisation:

<https://www.gla.ac.uk/myglasgow/research/enlighten/theses/digitisation/>

This is a digitised version of the original print thesis.

Copyright and moral rights for this work are retained by the author

A copy can be downloaded for personal non-commercial research or study,
without prior permission or charge

This work cannot be reproduced or quoted extensively from without first
obtaining permission in writing from the author

The content must not be changed in any way or sold commercially in any
format or medium without the formal permission of the author

When referring to this work, full bibliographic details including the author,
title, awarding institution and date of the thesis must be given

Enlighten: Theses

<https://theses.gla.ac.uk/>
research-enlighten@glasgow.ac.uk

ELASTIC BUCKLING OF LATTICED AND

THIN WALLED COLUMNS.

STUDIES IN OVERALL AND COMPONENT STABILITY.

by

ROBERT M. KENEDI B.Sc. A.R.T.C.

ProQuest Number: 10646995

All rights reserved

INFORMATION TO ALL USERS

The quality of this reproduction is dependent upon the quality of the copy submitted.

In the unlikely event that the author did not send a complete manuscript and there are missing pages, these will be noted. Also, if material had to be removed, a note will indicate the deletion.



ProQuest 10646995

Published by ProQuest LLC (2017). Copyright of the Dissertation is held by the Author.

All rights reserved.

This work is protected against unauthorized copying under Title 17, United States Code
Microform Edition © ProQuest LLC.

ProQuest LLC.
789 East Eisenhower Parkway
P.O. Box 1346
Ann Arbor, MI 48106 – 1346

I N D E X.

	<u>Page.</u>
ABSTRACT _____	<u>1.</u>
CONTENTS _____	<u>3.</u>
PART I - LATTICED COLUMNS. _____	<u>9.</u>
PART II - THIN WALLED COLUMNS. _____	<u>50.</u>
BIBLIOGRAPHY _____	<u>74.</u>
ACKNOWLEDGEMENTS _____	<u>77.</u>
APPENDICES _____	<u>78.</u>

ABSTRACT.

Columns in general can be regarded as built up of components. These components may be of different structural form, such as the column legs and the latticing of a Latticed Column, or may be of the same form, such as the flange and web plates of a Thin Walled Column. In any one case failure may occur either by integral column action - "Overall Instability" or by failure of one of the components - "Component Instability".

The contents of the thesis are divided into two main parts. Part I presents a review of published Analytical and Experimental Investigations of Latticed Columns, followed by a short critical discussion. This reveals, on the experimental side, the lack of complete column distortion data and on the theoretical side, the absence of stability analysis of the column leg components as distinct from the panel elements.

The review is followed by the presentation of the experimental work carried out on a model latticed column, from which the complete distortion of the column legs were obtained by measurement of the lateral deflections at 18 points along their length.

Using the experimental work as a guide an analysis is developed, which gives the buckling load of Latticed Columns based on the stability of the column legs. Account is taken of the action of lateral loads on the column legs, the magnitude of these loads being dependent on the elasticity of the latticing.

In its application, the critical stress given by this treatment is taken as the "ideal column" buckling stress of the Perry-Robertson formula, which is then utilised to compute actual failure stresses. Values calculated in this manner are compared with the published experimental results of other investigators.

Part II gives a brief survey of the relevant published theories of flexural and torsional integral column stability, and flexural plate stability under compressive actions.

The thesis then presents the experimental work carried out on thin walled columns consisting of some 70 tests to destruction of 3 ft. long channel section specimens. The tests were designed to cover the complete range of integral column and plate component failure. Special study was made of the conditions obtaining under simultaneous overall column and plate component collapse.

The characteristics of flange plate failure were further investigated on two 12 ft. long channel section columns tested to destruction. Complete edge deflection data for the flanges together with a stress survey of the flange surface are presented.

The experimental buckling stress results of the plate failure range, are analysed on the basis of the classic plate buckling theory, leading to the evaluation of the degree of edge fixity of the flange plates.

This is followed by a comparison of the experimental results with calculated distributions given by the Perry-Robertson formula - the plate critical stress being taken as the "ideal column" buckling stress - and by the present day stress basis of American design.

The findings of the investigations presented in the thesis fall into two categories, namely/

namely

- (1) Specific characteristics - appertaining to details of theoretical and experimental behaviour. These are given in the Summaries at the end of each section.
- (ii) General features amounting to a substantiation of the Perry - Robertson formula. While developed originally for the "Overall" type of failure it is shown to be applicable to the "Component" failure range also, provided the values of the imperfection factor and the "ideal column" buckling stress correspond to the characteristics of the weakest column component.

The theory of Latticed Columns presented in Section III of Part I has been accepted for publication in the Journal of the Royal Technical College, Glasgow.

The work carried out by the author, presented in Section II (1) of Part II was used in a paper published by the Institution of Structural Engineers under joint authorship with Dr. C. M. Moir (28).

CONTENTS.

PART I.

LATTICED COLUMNS.

SECTION I - REVIEW OF LATTICED COLUMN INVESTIGATION

	<u>Page.</u>
<u>Introduction.</u>	
(a) <u>Analyses based on Stability.</u>	<u>11.</u>
Solid Column Development applied directly to Latticed Columns - Dinnik. Solid Column Formulae corrected for the effect of Shear adapted to Latticed Struts - Timoshenko. Formulae based on Structural Actions in Latticed Columns as distinct from Solid Columns - Muller, Breslau, Engesser, Prandtl, Kayser. Treatment developed on the basis of an equivalent column with a continuous elastic web - Pippard.	
(b) <u>Analyses based on Maximum Stress.</u>	<u>14.</u>
Solid Column Development applied directly to latticed columns. - Ayrton, Perry, Robertson. Treatment developed on the basis of superposed bending action due to lateral deflection - Krohn, Engesser, Saliger, Gerard, Brik. Formulae based on the "Krohn effect" and incorporat- ing allowance for initial irregularities - Salmon.	
(c) <u>Experimental Investigations.</u>	<u>16.</u>
Overall Column Behaviour - Talbot & Moore, Howard & Buchanan; American Society of Civil Engineers Steel Structure Research Committee; Holt, comprising:- The Lack of Integral Action. Mode of Failure of Test Columns. The Effect of the Bracing. Imperfections in Columns and their Estimation - Ayrton, Perry, Robertson, Smith, Salmon, A.S.C.E. Research Committee, Baker, Howard & Buchanan, Christie, Lilly, comprising:- Eccentricity of Load - Actual and Equivalent Initial Curvature - Actual and Equivalent. Reduction in Strength - the effect of past history of the material.	
(d) <u>Empirical Formulae.</u>	<u>18.</u>
Straight Line Formulae - Holt. Parabolic Formulae - Voss. Rankine-Gordon Type Formulae - Cooper, Schneider, Hutt.	
(e) <u>Discussion.</u>	<u>19.</u>
<u>Contrast of the Analytical Developments.</u> <u>Integral Structure versus Connected System.</u> <u>The Four Component Strength Criteria.</u> <u>Reclassification of the Analyses presented</u> <u>based on Component Strength.</u>	
<u>General Features of the Experiments. /</u>	

General Features of the Experiments.

Lack of Integral Action.
 The Meaning of "Local" Failure.
 Column Distortion Data.
 The Influence of the Mode of Failure on the
 Effect of Imperfections.

Summary and Outline of the Research Programme.SECTION II. - EXPERIMENTAL WORK ON A MODEL COLUMN.(a) Experimental Appliances. 23.

Description of Model.
 Apparatus
 Measuring Devices.
 Method of Testing.

(b) Experimental Results. 23.

Deflected Form of Column Legs.
 Relative Deflection of Column Legs.
 Panel Point Deflection v. Column Load.
 Centre of Panel Deflection v. Column Load.
 Centre of Panel Deflection relative to Line of
 Panel Points v. Column Load.
 Distribution of Δ = (Leg Deflection / Column
 Load) along Column Legs.

(c) Discussion of Experimental Results. 24.

Distorted Form of Column Legs.
 Overall and Panel Unit Shape.
 Relative Movement between Column Legs - "Barrelling"
 and Contraction.
 Local Bending of Panel Elements.
 Variation of Δ with Load.
 Active and Passive Column Legs.

(d) Column Model Behaviour. 30.

The Column as a Unit.
 The Individual Column Legs.
 The Panel Element.
 The Lattice System.

SECTION III. - LATTICED COLUMN ANALYSIS AND APPLICATIONS1. ANALYSIS.

Notation.

General Assumptions.

(a) Eccentric Loading - Buckling in the Plane of the Lattice. 34.

Equivalent Column.
 Derivation of the Equations.
 Hyperbolic Buckling Load Relation.
 Buckling with Legs Deflecting to the same Side.
 Buckling with Legs Deflecting to Opposite Sides.
 Limiting Buckling Load Value at "Full" Eccentricity.
 Variation with the Factors β and n^2 .
 Buckling Load Variation with Eccentricity.

(b)	<u>Eccentric Loading - Buckling Perpendicular to the Plane of the Latticing.</u>	Page. 38.
	Assumptions. Force Actions on Column Legs. Second Order Quantities. Buckling Load Formulae.	
(c)	<u>Concentric Loading.</u>	38.
	Reduction of the Eccentric Load Equation. Alternative Modes of Buckling. Minimum Buckling Load Value. Variation with the Factors β and n^2 .	
(d)	<u>Calculation of the Equivalent Web Constant.</u>	39.
	In the Plane of the Latticing. Perpendicular to the Plane of the Latticing.	
(e)	<u>Summary.</u>	42.
	The Perry-Robertson Formula and the Value of P_e . The Overall Column Strength. The Column Leg Component Strength. The Panel Element Strength.	

SECTION III - LATTICED COLUMN ANALYSIS AND APPLICATIONS.

2. APPLICATIONS.

(a)	<u>Analysis of Collected Experimental Results.</u>	45.
	Method of Calculation of Theoretical Failure Stress. The Evaluation of P_e based on the Theory of Section III (1). The Use of the Perry-Robertson Formula. The Equivalent Slenderness Ratio and Allowance for Imperfections. Table of Test Specimens' particulars and Discussion. Table of Experimental and Calculated Results and Discussion.	
(b)	<u>Summary.</u>	49.
	Overall and Column Component Strength. Selection of the Relevant P_e Value. Allowance for Imperfections in Built Up Columns. The Applicability of the Perry-Robertson Formula.	

PART II.

THIN WALLED COLUMNS.

SECTION I - THE COMPOSITE BEHAVIOUR OF THIN WALLED COLUMNS.

(a)	<u>Overall Column Stability Under Concentric End Load.</u>	52.
	Flexural Instability - Euler. Torsional Instability - Lundquist, Fligg, Thomas.	

(b)	<u>Plate Component Stability Under Lengthwise Compression.</u>	<u>Page</u> 53.
	Flexural Instability - Bryan, Timoshenko. The Effect of Edge Conditions. Contrast of the Elastic Critical Load and the Ultimate Load - v. Karman. The Effective Width - Winter.	
(c)	<u>Optimum Conditions - Equal Overall and Component Strength.</u>	54.
	"Column" v. "Plate" Failure. The Combined Column - Plate Failure Curve. The Dimension Ratios L/r and b/t . The Relation $b/t = \text{constant} \times L/r$ for Maximum Strength. Structures of Maximum Strength and Minimum Weight - Cox and Smith. The Use of the Perry-Robertson Formula.	
<u>SECTION II - EXPERIMENTAL WORK AND ANALYSIS OF RESULTS.</u>		
<u>1. MODEL SCALE INVESTIGATION</u>		
(a)	<u>Experimental Appliances.</u>	57.
	Description of Specimens and Range. Apparatus. Method of Testing.	
(b)	<u>Experimental Results.</u>	57.
	Typical Modes of Failure. Table of Typical Results. Graph of Experimental Failure Stress against the Slenderness Ratio L/r . Graph of Experimental Failure Stress Against the Plate Ratio b/t .	
(c)	<u>Analysis and Discussion of Results.</u>	59.
	Variation of the Experimental Failure Stress with L/r and b/t . Relative Scatter of Column v. Plate Failure Results. The "Optimum" Range - Simultaneous Column and Plate Component Collapse. Logarithmic Interpolation of "Peak" Values. Comparison of the Experimental and Theoretical Straight Line Variation of b/t with L/r for Optimum Conditions. Flange Plate Edge Support under Optimum Conditions. Column Behaviour in the Plate Component Failure Range. Comparison of the Experimental Average Stress Curve with the Theoretical Plate Stress Curves. The Variation of the Edge Fixity Coefficient K_2 . The Value of the Perry-Robertson Imperfection Coefficient η for Plate Failure. Comparison of the Perry-Robertson Stress Form with the Lower Scatter Boundary of the Experimental Failure Stress Curve.	

(d) Summary......

Page.

65.

Maximum Strength and Simultaneous Integral
Column and Plate Component Collapse.
Plate Component Edge Support Corresponding to
Simultaneous Collapse.
Plate Component Edge Fixity Variation with the
b/t Ratio.
The Application of the Perry-Robertson Formula
to Plate Component Failure.

SECTION II.

EXPERIMENTAL WORK AND ANALYSIS

OF RESULTS.

2. FULL SCALE INVESTIGATION.

(a) Experimental Appliances......67.

Description of Specimens and Range.
Apparatus.
Measuring Devices.
Method of Testing.

(b) Experimental Results......67.

Mode of Distortion and Failure.
Deflected form of the Flanges.
Variation of the Flange Deflections with the
Axial Load.
Longitudinal and Transverse Stress Survey of
Flanges (In Appendix No. 4).

(c) Analysis and Discussion of Results......68.

Deflected Form of the Flanges.
Development of Form.
Number of Half Waves.
Magnitude of Deflections.
Flange Deflection Variation with Axial Load at
Particular Points.
"Stationary" Tendency.
Reversal of Deflection Direction.
"Running Away" Tendency.
Derivation of the Elastic Buckling Load from the
Flange Deflections.
The Southwell-Lundquist Straight Line Plot.
Elastic Buckling Stress Comparison - Full
Scale v. Model Scale.

(d) Summary......73.

The Elastic Buckling Load to Collapse Load Margin.
Application of the Southwell Lundquist Plot to
Plate Buckling Analysis.
Comparison of Full Scale and Small Scale Behaviour.
The Absence of Scale Effect in the Elastic Range.

	<u>Page.</u>
BIBLIOGRAPHY.....	<u>74.</u>
ACKNOWLEDGEMENTS....	<u>77.</u>

APPENDICES.

1. Solution of the Eccentric Load Equations for Latticed Columns by Fourier Sine Transformation.....	<u>78.</u>
2. Numerical Example of Buckling Load Analysis for a Latticed Column.....	<u>81.</u>
3. Summary of Tensile Test Results on Material of Specimens used in the Experimental Work.....	<u>87.</u>
4. Stress Survey of the Flanges of a 12 ft. Thin Walled Column Specimen with a Note on Collapse Load.....	<u>89.</u>
5. Note on the Design of Concentrically Loaded Thin Walled Columns.....	<u>97.</u>
6. Flange Deflection Variation with Axial Load.....	<u>100.</u>

P A R T I.

LATTICED COLUMNS.

SECTION I - REVIEW OF LATTICED COLUMN INVESTIGATIONS.

<u>Introduction.</u>	<u>Page.</u>
(a) <u>Analyses based on Stability.</u>	<u>11.</u>
Solid Column Development applied directly to Latticed Columns - Dinnik.	<u>11.</u>
Solid Column Formulae corrected for the effect of Shear adapted to Latticed Struts - Timoshenko.	<u>12.</u>
Formulae based on Structural Actions in Latticed Columns as distinct from solid columns - Muller, Breslau, Engesser, Prandtl, Kayser.	<u>12.</u>
Treatment developed on the basis of an equivalent column with a continuous elastic web - Pippard.	<u>13.</u>
(b) <u>Analysis based on Maximum Stress.</u>	<u>14.</u>
Solid Column Development applied directly to latticed columns - Ayrton, Perry, Robertson.	<u>14.</u>
Treatment developed on the basis of superposed bending action due to lateral deflection - Krohn, Engesser, Saliger, Gerard, Brik.	<u>14.</u>
Formulae based on the "Krohn effect" and incorporating allowance for initial irregularities - Salmon.	<u>15.</u>
(c) <u>Experimental Investigations.</u>	<u>16.</u>
Overall Column Behaviour - Talbot & Moore, Howard & Buchanan; American Society of Civil Engineers Steel Structure Research Committee; Holt. comprising:-	
The Lack of Integral Action.	
Mode of Failure of Test Columns.	
The Effect of the Bracing.	<u>16.</u>
Imperfections in Columns and their Estimation - Ayrton, Perry, Robertson, Smith, Salmon, A.S.C.E Research Committee, Baker, Howard and Buchanan, Christie, Lilly, comprising:-	
Eccentricity of Load - Actual and Equivalent	
Initial Curvature - Actual and Equivalent.	
Reduction in Strength - the effect of past history of the material.	<u>17.</u>
(d) <u>Empirical Formulae.</u>	<u>18.</u>
Straight Line Formulae - Holt.	
Parabolic Formulae - Voss.	
Rankine - Gordon Type Formulae - Cooper, Schneider, Eutt.	
(e) <u>Discussion.</u>	<u>19.</u>
<u>Contrast of the Analytical Developments.</u>	<u>19.</u>
Integral Structure versus Connected System.	
The Four Component Strength Criteria.	
Reclassification of the Analyses presented based on Component Strength.	
<u>General Features of the Experiments.</u>	<u>20.</u>
Lack of Integral Action.	
The Meaning of "Local" Failure.	
Column Distortion Data.	
The Influence of the Mode of Failure on the Effect of Imperfections.	
<u>Summary and Outline of the Research Programme.</u>	<u>21.</u>

* Numbers in brackets following the name of an Author
give the appropriate reference in the Bibliography.

Introduction.

The review presented in the following pages has been assembled to indicate the broad lines followed by investigators rather than to collate all contributions to the subject. The treatment of its subject matter may be described as stating the line of investigation and quoting selected analyses as illustrations. As such it makes no claim to comprehensiveness of detail but attempts a classification of fundamental approach.

On the whole the lines of attack of column investigations fall under the main headings -

- Analyses based on stability.
- Analyses based on Maximum Stress.
- Experimental Investigations.
- Empirical formulae based on experimental investigations.

Each of these sections can be further subdivided depending on the actual method used in arriving at formulae offered as applicable to built up columns. Some of these are "corrected" solid column formulae, while others are based directly on an assumed behaviour of the built up form considered.

No line of attack is restricted to any particular historical period. Examples of all the four main lines of investigation can be found in any period following the classic contribution of Euler to column theory. In view of this a certain amount of arbitrary selection had to be exercised when choosing the analyses thought "typical" of any one line.

The review concludes with a discussion contrasting and summarising the significant features of theory, experiments and practice.

(a) Analyses based on Stability.

Solid Column Development Applied directly to Latticed Struts.

Solid column formulae have been applied extensively to built up columns, despite the fact that integral action of the column as a whole is but rarely obtained in practice.

Such an approach is typified by the development originally proposed by Dinnik (4)* for a column whose Moment of Inertia varies exponentially along its length.

The Moment of Inertia at any distance from a fixed origin is given as

$$I_x = I_1 \left(\frac{x}{a} \right)^n$$

where

I_1 = Moment of Inertia at top of strut.
 a = Distance of top of strut from fixed origin.

Using various values of n , various shapes of columns may be obtained. The assumption $n = 2$ for example can be taken to represent the case of a built up column consisting of four angles connected by diagonals.

The critical load for any column of this type is given by

$$P_c = m \frac{E I_2}{L^2}$$

where m = factor depending on n ; I_1 and I_2
 I_2 = Moment of Inertia at bottom of column
 L = Length of column

The form of P_c can be extended to cover the case of a strut whose middle portion is prismatical and whose end portions may be

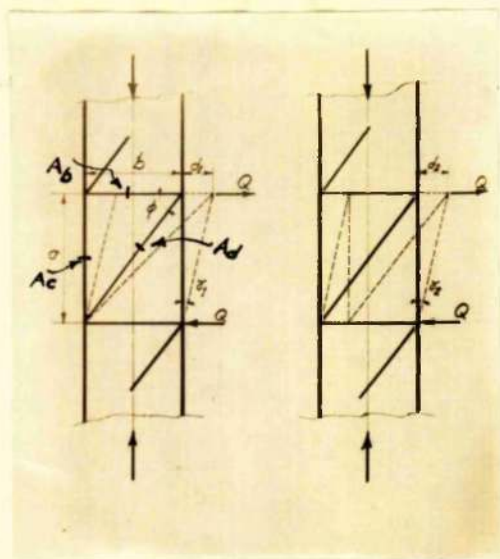


Fig. 1.

of various shapes (as defined by n) by combining the relevant differential equations of prismatical and varying section bars.

Solid column formulae corrected for the effect of shear adapted to latticed struts.

The Euler critical load of a solid column, P_e is diminished in the ratio $1 + \frac{1}{cA/AG}$ owing to the action of the shearing forces where $\frac{1}{c} =$ shear deflection factor

($\frac{10}{9}$ for circular, $\frac{6}{5}$ for rectangular sections)

A = Cross Sectional Area of Column
G = Modulus of Rigidity

Timoshenko (19) applies this form to latticed and battened struts of many panels. Considering the latticed bar shown in Fig.1. it is seen that the angular displacement produced by the shearing force Q is

$$\theta = \theta_1 + \theta_2 = \frac{d_1 + d_2}{a} = \frac{Q}{\sigma/Q A_d E \sin \phi \cos^2 \phi} + \frac{Qb}{a A_b E}$$

defining c/AG as σ/Q

gives the critical load as

$$P_c = P_e / \{ 1 + P_e (1/A_d E \sin \phi \cos^2 \phi + b/a A_b E) \}$$

This form is applied to single and double bracing with or without horizontal members after appropriate interpretation of the quantities A_b and A_d

From the equation for P_c it can be seen that, if A_b and A_d are very small in comparison with A_c the latticed strut becomes considerably weaker than a solid strut with the same value of EI.

It is relevant to remark here that experiments have shown that where a column is definitely subjected to shear force the effect is marked. For ordinary cases however this is compensated for by bracing stiffness, which introduces secondary bending stresses of over-riding importance.

Formulae based on Structural Actions in Latticed Columns as Distinct from Solid Columns.

The secondary bending stresses referred to in the previous paragraph have been taken into account by Muller Breslau (13) in a very complete analysis. The approach considers the deformation of the panels due to shear, the consequent bending moments at the panel points and the deformation of the web bracing.

The results of the original analysis are complicated and apply only to long columns. The equations have however been simplified by means of reduction coefficients and for short columns, they are modified to suit Tetmajer's straight line. The expression for the critical load is similar to the Euler expression except that I is replaced by a function depending on areas and I's of the component parts.

$$\text{Thus } P_c = \frac{\pi^2 EI}{L^2} \xi_1 \xi_2 \quad \text{where}$$

ξ_1 and ξ_2 are coefficients depending on the strength of the bracing and the number and arrangement of the panels.

The main point brought out by the theory is that the effect of the shearing force on the ultimate strength of well designed columns is negligible.

The analyses of Engesser, Prandtl, Kayser and others may be

regarded as less complete forms of the Muller Breslau analyses.

Treatment developed on the basis of an equivalent column with a continuous elastic web.

A recent example of the utilisation of the equivalent web device was given by Pippard (11) in his analysis of the critical load of battened columns.

The analysis assumes that

- (1) There is no relative movement between column shafts and batten plates at their junction.
- (11) The column as a whole reaches its critical load before any component of it fails.

The theory is then worked out for an equivalent column whose shafts are joined by a continuous web which can apply flexural restraint to the flanges but is incapable of transmitting stress along the axis of the column.

Expressions for slopes and relative deflections at the ends of a web element are obtained from simple beam theory and the differential equation for the case is obtained from the Elastic Beam equation

$$EI \frac{d^2 y}{dx^2} = -M$$

The characteristics of the equivalent column web are obtained in terms of the actual batten plate bracing, by assuming that the slopes and displacements in the actual column at the attachments of the batten plates are the same as at the corresponding points in the equivalent column.

The critical load is given by

$$P_c = \frac{2 \left\{ \pi^2 \frac{I_c}{L^2} + 6 \frac{I_c}{I} \left(1 + 4 \frac{K^2}{\rho^2} \right) Z \right\}}{\pi^2 \frac{I_c}{L^2} + \left(24 \frac{I_c}{I} \frac{K^2}{\rho^2} \right) Z} Q$$

where $Z = \begin{cases} 1 + \operatorname{cosec} \theta & \text{if } n \text{ is even} \\ \text{or } 1 + \cot \theta & \text{if } n \text{ is odd} \end{cases} \quad \theta = \frac{\pi}{2(n-1)}$

l = Distance between centroids of column shafts.

I = Moment of Inertia of one column shaft.

K = Radius of Gyration corresponding to I

L = Length of column

I_c = Moment of Inertia of batten plate.

Q = Euler load for one column shaft.

n = Number of batten plates.

It is shown that if the batten plates are spaced so as to touch each other P_c tends to $2Q$ if n is large i.e. the batten plates have no effect; and P_c tends to P_e for the column if "solid" indicating full stiffening action by the bracing. For practical use it is suggested that P_e in the Perry Robertson formula be based on P_c as given by the above expression.

The foregoing - although - outwith the scope of the thesis has been included as the only example known to the author utilising the device of the "continuous" elastic web. It is interesting from this point of view, as a somewhat similar approximation is utilised in the analysis of Latticed Columns presented in Section III.

It is relevant to remark at this stage that an analysis of

batten plate columns has been given by Timoshenko (19) buckling being assumed to take place due to shear only. This implies that rotation of the batten plates - included in Pippard's Analysis - are neglected. Timoshenko presents the analysis as a further application of the solid column formula, "corrected" for shear, while Karman and Biot (9) analyse the same problem using difference equations for the slopes.

(b) Analyses based on Maximum Stress.

Solid Column Development Applied Directly to Latticed Columns.

The most satisfactory formula for the determination of the strength of struts at the present time is based upon an analysis of the initial curvature problem by Ayrton and Perry (1). The approach is based on the inclusion of the effects of initial curvature (E_1) and eccentricity (E_2) in the derivation of the elastic line. This yields as the equation of the elastic line

$$y_0 = \frac{E_1}{1 - P/P_R} + E_2 \sec \frac{\pi}{2} \sqrt{P/P_R}$$

Use of the approximation of $\sec \frac{\pi}{2} \sqrt{P/P_R} = \frac{1.12}{1 - P/P_R}$

allows the effects of E_1 and E_2 to be combined as an equivalent initial curvature of $E = \frac{6}{5} E_2 + E_1$

The maximum bending moment given by $P y_0$ yields the maximum ^{fibre} stress as

$$P_m = \frac{1}{2} \left\{ P_y + P_e \left(1 + \frac{E_c}{K^2} \right) - \sqrt{ \left(P_y + P_e \left(1 + \frac{E_c}{K^2} \right) \right)^2 - 4 P_y P_e } \right\}$$

where

P_m	=	Maximum Stress
P_y	=	Yield stress of the material (or max. allowable stress)
P_e	=	Euler critical stress for column.
c	=	Extreme fibre distance.
K	=	Relevant radius gyration.

The value to be taken for the equivalent curvature E , to obtain consistency with test figures was determined by Robertson (12) on the basis of extensive investigations. As a result the "Perry-Robertson" formula is now the basis of column design in this country. The formula as used in the British Standard Specification No. 449 is

$$P_c = \frac{P_y + (\eta + 1) P_e}{2} - \sqrt{ \left(\frac{P_y + (\eta + 1) P_e}{2} \right)^2 - P_y P_e }$$

with the eccentricity factor $\eta^2 = 0.0034/K$ for solid columns. The load factor suggested for use on the basis of P_c is 2.36.

It should be noted at this stage that the formula can equally well be applied to struts other than solid if the values of P_e and η relevant to the particular type of column are known. The value of the former can be determined theoretically -- such an analysis is put forward in Section III for latticed columns -- while the value of the latter must of necessity be experimental. A value for η quoted recently by Pippard (11) for batten plate columns was -
 0.00154K.

Treatment developed on the basis of superposed bending action due to lateral deflection.

The first rational theory of this type was developed by Krohn (13). The reasoning is as follows:- For a given deflection in the plane of the web, for a concentric column load P , the load on each flange - originally $P/2$ - is altered by an amount (additive on the concave side and subtractive on the convex side) which can be expressed in terms of the deflection. This is referred to as the "Krohn Effect". Consequently the loads on the elementary columns between the panel points of the bracing can be found. It is assumed that the strength

of these panel elements defines the strength of the column as a whole.

The treatment gives the lateral deflection in terms of the constants in Tetmajer's straight line formula for solid columns - interpreting these as stress values, yielding

$$P_f = P \frac{A_f}{A} \frac{272}{272 - 4K}$$

where

P_f	=	Flange force
P	=	Column Load
A_f	=	Flange Area
A	=	Column Area

For "normal" column proportions $A_f = \frac{1}{2} A$ and $K = \frac{d}{2}$ where d = distance between centres of Gravity of the flanges. The flange force reduces to

$$P_f = P \frac{68d}{136d - L}$$

thus in short columns P_f tends to $\frac{1}{2} P$. The validity limit of Tetmajer's straight line is $L/K = 105$ giving the validity of Krohn's formula as $P_f = 0.81P$.

Krohn's formula was modified by Engesser, extended by Saliger and put in a generalised form by Gerard and others. Brik (13) drew attention to the fact that although Krohn's assumption of $K = d/2$ is practically true for normal sections, if the distance between the flanges is small the K value may differ considerably from $d/2$.

Formulae based on the "Krohn Effect" and incorporating Allowances for initial irregularities.

A very exhaustive analysis is given by Salmon (13) for a nominally concentrically loaded latticed column, subject to various imperfections and buckling in the plane of latticing.

The treatment assumes, elastic uniplanar bending with small curvature and lateral deflections. The weight of the column itself is neglected and the imperfections allowed for include lack of homogeneity of the elastic properties, eccentricity of loading due to imperfections and a parabolic initial curvature.

The equation of the elastic line is given as

$$\frac{d^2}{dx^2} (y - y_1) + \frac{Py}{\frac{d^2}{n_1 + m} (b - P \frac{n_1 m}{n_1 + m})} = 0$$

where

y_1	=	the initial curvature.
y	=	the deflection of the column
b	=	length of the panel element.
d	=	distance between C.G.s of the flanges.

$$\left. \begin{aligned} n_1 &= \frac{d}{a_1 E_1} \\ n_2 &= \frac{d}{a_2 E_2} \end{aligned} \right\} \begin{aligned} &\text{where } a_1, a_2, E_1 \text{ and} \\ &E_2 \text{ are the areas and Young's} \\ &\text{Moduli of the flanges respectively.} \end{aligned}$$

Solving the differential equation for y where $y_1 = e_2 + e_1 (1 - 4 \frac{x^2}{L^2})$

representing eccentricity of loading and a parabolic initial curvature the maximum deflection is

$$y_0 = (e_2 + \frac{8e_1}{\alpha^2 L^2}) \sec \frac{\alpha L}{2} - \frac{8e_1}{\alpha^2 L^2}$$

The maximum flange force under working conditions corresponding to this is

$$P_f = P (\frac{1}{2} + 1.3 \frac{e_1 + e_2}{d}) \quad \text{for } P/P_e = \frac{1}{5}$$

The maximum fibre stress then becomes

$$p = \frac{2P}{d} \left[\frac{1}{2} + 1.3 \frac{e_1 + e_2}{d} \right] \left[1 + 1.3 \frac{e}{k_2} (e_1 + e_2) \right]_f$$

where the terms within the second bracket refer to the flange element between panel points considered as a column.

In the analysis shortening effects due to bending transmitted by the lattice bars are neglected. This is justifiable from a practical point of view particularly as the "upper" working load limit is taken as $\frac{1}{5} P_e$.

(c) Experimental Investigations.

The section which follows presents in a summary form significant features of selected experiments carried out by various investigators. The differentiation, based on approach which was readily available in the analytical section ceases to function when reviewing experimental work. It is usually found that there are definite groups of similar characteristics in all experimental investigations of the same field. These characteristics together with the particular aim of the experiment undertaken have been used as a basis of classification in this part of the review.

Overall Column Behaviour.

The common features of the following experimental investigations are summarised in this sub-section. Talbot and Moore (18); Howard and Buchanan (7); Reports of the Steel Structures Research Committee of the A.S.C.E. (17); Holt (6).

The lack of Integral Action: All the analyses quoted in the previous sections, assumed integral action about both or at least one axis of the column. Analyses such as Salmon's - one of the latter types - assume integral action when buckling perpendicular to the latticing and only consider lack of integrality if buckling takes place in the plane of latticing. All experimenters dealing with latticed columns make special mention of the fact that integral action is wholly lacking in columns with bolted or rivetted connections. This lack of integral action was deduced from various experimental observations such as

- (1) Considerable stress variation over the length of the specimens showing maximum stress values 1.4 to 1.5 times the average stress.
- (2) Irregular positioning of the fibre of maximum stress, sometimes occurring at the inside and other times at the outside of the column legs.
- (3) Considerable "local flexure" i.e. Action of components inconsistent with overall action of the column.

Modes of Failure of Test Columns: The mode of failure obtained by the various experimenters appears to depend to a large extent on the end conditions. The direction of the axis of the pin or roller end bearing used has considerable influence.

In general it appears that failure will occur by local buckling if the "local" slenderness ratio is greater than that for the column as a whole. If however the column acts as a unit, buckling takes place about the axis of least radius of gyration subject to any end condition imposed. It is relevant to point out here that experimenters seemed to classify any failure which was not a failure of the complete column as "local" collapse. This is ambiguous as it may mean buckling of the column panel element or buckling of one of the column legs as a component part.

Holt, in one of his tests noticed twisting of the angles of the column legs which he ascribed to eccentricity of loading. This effect could equally well have been a twisting action set up due to relative deflections of the column legs as indicated in the analyses of Section III.

The Effect of the Bracing: One of the most typical features of latticed column behaviour is the relative deflection of the column legs resulting in a "barelling" or "waisting" action. This action has been noted by many investigators, Howard and Buchanan giving the value of the ratio $\frac{\text{Lateral Expansion}}{\text{Longitudinal Contraction}} = \frac{1}{3.5}$

Their measurements are somewhat complicated by the use of diaphragm plates (battens) which restrict lateral expansion very considerably.

The "barelling" action is to some extent the effect of the latticing. This has been pointed out by the A.S.C.E. Steel Column Research Committee who state that when the legs shorten rotation of the lacing bars "force" the column shafts apart. They further indicate that the latticing has a stiffening effect under eccentric loading, this more than counteracting the transverse shear effect.

Many experiments have been made to determine the best types of bracing but none have met with any great success. The characteristic of all results in this field is their irregularity and inconclusiveness.

Imperfections in Columns and their Estimation.

Eccentricity of Load - Actual and Equivalent: The considerable effect of a small eccentricity on the strength of a column has been noted by all experimenters since Christie (13) but Ayrton and Perry (1) were the first to point out that assuming imperfections to exist in all columns a slight extra eccentricity would have little effect. Consequently small errors in the estimation of the load eccentricity are not important.

Actual eccentricity of load may be obtained either from actual measurements or by calculation from test results. It has become the general practice to express such probable load eccentricity in terms of the length or of the slenderness ratio. The "probable" load eccentricity has been derived by Smith (13) using probability methods as $\frac{7}{1000}$ of the total estimated eccentricity and is given for example by Salmon (13)

$$\text{as } \frac{\text{Length}}{1000}$$

The 1926 report of the A.S.C.E. (17) states that the eccentricities encountered never exceeded $L/1500$.

"Equivalent" load eccentricities have been introduced to cater for non homogeneity of material (i.e. variation in Young's Modulus E) and also to allow for rolling margins resulting in differences of flange areas.

The probable equivalent eccentricity due to the variation of E obtained from experimental results is given by various authorities as follows - (the assumptions being that E varies uniformly across each flange and that it is a constant longitudinally)

<u>Fidler</u> (5)	<u>Neville</u> (13)	<u>Salmon</u> (13)
$\frac{\text{Width}}{36}$	$\frac{\text{Width}}{36}$	$\frac{\text{Width}}{40}$

For flanges with equal areas the figures quoted correspond to an E variation of $\pm 10\%$. In view of the fact that the A.S.C.E. Research Committee (17) observed a total variation of $\pm 2\frac{1}{2}\%$ only, the quoted eccentricities may be considered exaggerated.

The equivalent eccentricity corresponding to area variation is given by Salmon (13) as $\frac{\text{Width}}{80}$ for a rolling margin of $2\frac{1}{2}\%$.

18

The total probable load eccentricity corresponding to the factors quoted is the sum of the actual and equivalent values. As an example values proposed by Salmon (13) are

$$E = \left\{ \begin{array}{l} \frac{\text{Length}}{1000} + \frac{\text{Width}}{40} + \frac{\text{Width}}{160} \\ \text{actual} \qquad \qquad \text{due to E} \qquad \qquad \text{due to flange} \\ \qquad \qquad \qquad \text{variati} \qquad \qquad \text{are difference.} \end{array} \right\}$$

Initial Curvature - Actual and Equivalent: All experimenters are agreed that a perfectly straight column does not exist. Ayrton and Perry (1) propose that for solid columns the effect of an initial curvature is equivalent to that of a load eccentricity of magnitude equal to the central deflection.

Robertson (12) after extensive investigations proposed a combined eccentricity and initial curvature factor of 0.003 L/K for solid columns. Pippard(11) suggests for use with batten plate columns the factor of 0.0015 L/K.

Salmon's (13) suggested equivalent eccentricity to allow for initial curvature is 0.0023 L/K or $\frac{\text{L}}{750}$. This approximates to

the A.S.C.E.'s (17) 1926 report which indicates that eccentricities equivalent to initial curvature encountered in the experiments undertaken have never exceeded $\frac{L}{750}$.

Reduction in Strength - The Effect of Past History of the Material: Manufacturing processes affect considerably the characteristics of the material. Baker (13) has shown that overstrain in tension while increasing the yield stress in tension reduces it in compression and vice versa. Consider Christie and Lilly (13) demonstrated the effect of cold work in raising the yield point. Howard (7) showed that the most suitable steels for columns are those rolled at the lowest temperatures.

Howard and Buchanan (7) in their tests on lattice columns ascribe the non linearity of the column compression encountered to the presence of small local permanent sets. These in turn are explained as being due to manufacturing processes such as cold straightening, punching, drifting, and rivet contraction.

The unanimous recommendation of all investigators is to allow for this reduction in strength by the use of reduced working stresses.

(d) Empirical Formulae.

Straight Line Formulae.

These forms are commonly used for strength prediction provided integral action obtains. The range of slenderness ratio for which this type of equation is applicable is limited, but the values of the constants can be so chosen that in combination with the Euler column formulae the full practical range may be covered. As an example Holt (6) quotes the form

$$\frac{P}{A} = S_0 - C \frac{L}{K} \quad \text{where}$$

So = crushing strength of the material. He proposes this formula for use with built up columns made of aluminium alloy when the column fails by sidewise bending.

Various values of the constants S₀ and C can be found in Ref. (6).

Parabolic Formulae.

Rather popular forms, in wide use for representation of experimental results, because of their simplicity, are the parabolic types. These are usually associated with either a straight line or the Euler variation to cover the full practical range of slenderness ratios and always have a stated limit of application.

For latticed columns Voss (13) proposed the allowable stress as

$$p = 14,200 \left(1 - 0.0005 \left(\frac{L}{K} \right)^2 \right) \text{ lb/in}^2$$

for length up to 78 K. Above this value the Euler critical stress with a factor of safety of 5 is suggested. The value of the constants is based on the series of tests carried out at the Watertown Arsenal (21).

Rankine - Gordon Type Formulae.

The earliest form introducing the influence of the direct compressive stress in addition to the Euler effect and utilising empirically determined constants is the Rankine - Gordon formula. While originally developed for solid columns it has been adapted, with its constants based on the Watertown Arsenal Tests Results, to Latticed braced columns.

Cooper (13) suggests the critical stress

$$\frac{P_c}{A} = \frac{34000}{1 + \frac{1}{12000} \left(\frac{L}{K} - 60 \right)^2} \text{ lb/in}^2$$

Schneider (13) proposes the allowable working stress as

$$\frac{P}{A} = \frac{15000}{1 + \frac{1}{13500} \left(\frac{L}{K} \right)^2} \text{ lb/in}^2 \text{ "soft" steels}$$

$$\frac{P}{A} = \frac{6 \cdot 17000}{1 + \frac{1}{11,000} \left(\frac{L}{K} \right)^2} \text{ lb/in}^2 \text{ "medium" steels}$$

Hutt (8) modifies the form to include the effect of shear force and suggests

$$\frac{P}{A} = \frac{f}{1 + \frac{L^2 B (1 + p/13)}{19000 K^3}}$$

- f = crushing stress of the material.
p = stress in the bracing tons/in².
B = extreme fibre distance.

(e) Discussion.

Contrast of the Analytical Developments.

The analyses presented in the review have all been based on either the idea of integral action or on the conception of force actions in latticed columns regarded as a structure. In both of these cases it was always assumed that the column will fail as a whole. Failure of say a panel element was either specifically excluded in the assumptions or treated as an incidental - not a fundamental - matter.

It is felt that such an approach to the problem is overly narrow. Any built up structure should be regarded as a connected system, each component of that system being capable of individual collapse, depending on its ultimate strength relative to the

20.
ultimate strength of the other components. Thus in the case of built up columns a minimum of four strength criteria should be considered simultaneously. These are:-

- (I) The strength of the column as a whole - assuming integral action as in a solid column.
- (II) The strength of one of the column legs as a whole - under its portion of the load and subjected to the force actions imposed by the bracing.
- (III) The strength of a panel element - under its end load and momental end restraint due to continuity.
- (IV) The strength of the lattice bars - under the loads imposed on them as columns.

In an ideal case the four strength values would be the same - while in a practical case they will differ. In view of the above, any treatment based on only one or other of these criteria becomes inapplicable, if the actual behaviour is controlled by the strength of a component not regarded as critical in the analysis. From such a point of view the analyses quoted, appear incomplete if taken singly, and the treatment of a practical case would require a synthesis of these.

Reclassification of the analyses on the basis of component strength criteria indicates that -

- (I) The overall column strength assuming integral action has been exhaustively covered.
- (II) The component strength of the column legs as a whole has been evaluated for batten plate columns (Pippard)(II) only.
- (III) The strength of a panel element has been obtained on the basis of maximum stress consideration (Salmon) (13). Analyses regarding the panel element as analogous to a hinged end column from the point of view of stability over simplify matters by neglecting the momental restraint due to continuity. The strength of the component is consequently underestimated.
- (IV) The ultimate strength of lattice bars as columns is fully analogous to integral solid column action and as such has been satisfactorily treated. The analysis of the actual force actions in the lattice bars as components of a built up column has largely been bypassed. The consequent uncertainty is manifested at the present time by the design of over heavy web systems.

General Features of the Experiments.

One of the most significant characteristics of all experimental work on built up columns is a demonstration of the lack of integral action. This is manifested firstly by features such as stress distributions inconsistent with "solid" column behaviour and secondly by the variety of overall and "local" failures obtained.

In this connection - keeping in mind the four strength criteria enumerated in the previous section - it is seen that "local" failure may mean failure of one of the column legs or failure of a panel element. Differentiation would be difficult particularly if the experimenter is not looking for it specifically. Thus it is necessary to associate a certain degree of ambiguity with a failure recorded as "local".

27.

The experimental investigation of built up columns concerned themselves mainly with load carrying capacity and strain measurement, recording lateral deflection values at isolated points only. No record of complete column distortion data - given in terms of lateral deflections - has been found.

Experimenters who measured the distance between the column legs during loading have reported "barrelling" actions. It is felt that insufficient attention has been given to this feature, which should be accepted as a fundamental characteristic of built up column behaviour.

The effect of column imperfections have been exhaustively investigated for solid columns. It is significant to realise that the findings of these investigations can only be applied to built up columns if the overall column strength is the failure criteria. If however, one of the component strengths is the critical feature, both the value and the effect of the particular imperfection will be different from the solid column case. As an illustration of the reasoning - initial curvature is equivalent to an eccentricity for the column as a whole, but can amount to oblique loading for a panel element. Further, eccentricity of loading for the column as a whole means unequal but concentric loads on the column legs. Therefore in the Perry-Robertson formula the values of the imperfection coefficient and that of the "ideal" critical stress p_c will depend on the type of failure assumed.

Summary and Outline of the Research Programme.

It was brought out in the review that there are two definite gaps in built up column study namely -

- (1) Component strength analysis and
- (2) Experimental data on column distortion.

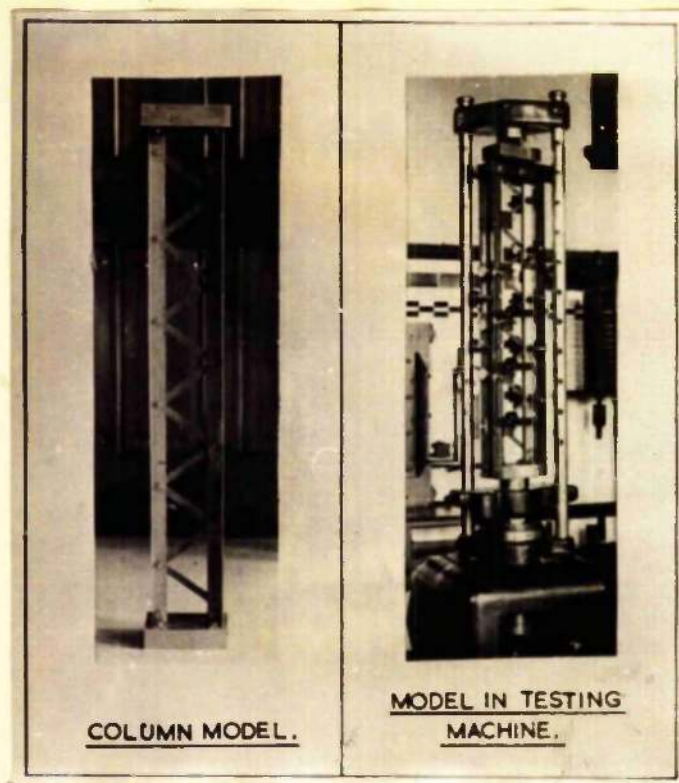
The work undertaken was directed towards filling these gaps. Model experiments were carried out in which the lateral deflections were recorded at 18 points along the length of each leg thus giving complete distortion data. The results of these are presented in Section II.

Using the results of these experiments as a qualitative guide a Lattice Column Analysis based on the consideration of component strength was developed and is put forward in Section III.

SECTION II.

EXPERIMENTAL WORK ON A MODEL COLUMN.

	<u>Page.</u>
(a) <u>Experimental Appliances.</u>	<u>23.</u>
Description of Model.	
Apparatus.	
Measuring Devices.	
Method of Testing.	
(b) <u>Experimental Results.</u>	<u>23.</u>
Deflected form of Column Legs.	
Relative Deflection of Column Legs.	
Panel Point Deflection v. Column Load.	
Centre of Panel Deflections v. Column Load.	
Centre of Panel Deflections relative to line of Panel Points v. Column Load.	
Distribution of Δ = $\left\{ \frac{\text{Leg Deflection}}{\text{Column Load}} \right\}$ along Column Legs.	
(c) <u>Discussion of Experimental Results.</u>	<u>24.</u>
Distorted form of Column Legs.	<u>24.</u>
Overall and Panel Unit Shape.	
Relative Movement between Column Legs - "Barrelling", "Contraction".	<u>25.</u>
Local Bending of Panel Elements.	<u>26.</u>
Variation of " Δ " with Load.	<u>29.</u>
"Active" and "Passive" Column Legs.	
(d) <u>Column Model Behaviour.</u>	<u>30.</u>
The Column as a Unit.	
The Individual Column Legs.	
The Panel Element.	
The Lattice System.	



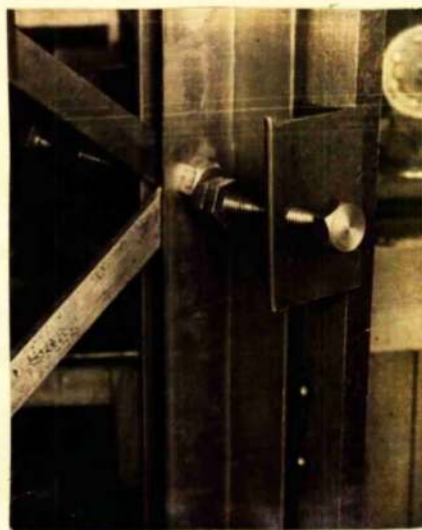
(a.)

(b.)

Fig. 2.



(a)



(b)

Fig. 3.

(a) Experimental Appliances.

The model of the latticed column is shown in Fig. 2a. The relevant dimensions were as follows:-

Total height of column legs	36 ins.
Panel Distance	6 ins.
Column Leg spacing	4 ins.

Each leg consisted of two 1" x 1" x $\frac{1}{16}$ " angles bolted together back to back.

The lattice members were $\frac{1}{2}$ " x $\frac{3}{8}$ " flats connected by means of single $\frac{1}{4}$ " bolts to the legs.

The testing machine was a 10 tons capacity Avery electro-hydraulic press (Fig. 2b). The smallest division directly readable on the load recording dial was 0.05 tons.

The model was supported in the machine as shown in Figs. 2b and 3a by means of ball and socket bearings at both ends. Centering of the column could be taken as accurate to 0.01 in.

Deflections of the column legs were measured relative to a rigid frame attached to the lower platen supporting the specimen. This frame was free at the top and it was provided at the top with a dial gauge capable of recording sway to 0.0001 in. to check for frame movement relative to the top platen. The column model was laterally braced at each panel point by means of bolts and cleats attached to the frame, preventing movement perpendicular to the plane of the latticing (Fig. 3b). The contact points of the lateral braces were greased to minimise friction, thus ensuring that the effect of the bracing on the recorded deflections was negligible. This was demonstrated during the trial load runs, when the screwing up and unscrewing of individual and groups of bracing bolts caused no measurable change in the observed deflections.

Deflection measurements were taken at every 2 in. along the length of the column for every 0.5 ton load increment by means of dials reading to 0.0001 in. A number of reloadings were necessary to obtain deflections at all points. To check that the column repeatedly distorted in the same manner the deflection measurements were arranged to overlap so that one set of deflection measurements were always repeated on each successive series of loadings.

(b) Experimental Results.

The experimental readings obtained and presented in graphical form in the discussion Figs. 4 to 13 are as follows:-

Deflected form of column loads at increasing loads
Relative deflection of column legs
Variation of panel point deflections with load
Variation of centre of panel deflection with load - relative to the ends of the column legs and relative to the adjacent panel points.

Distribution of $\Delta = \frac{\{\text{Leg Deflection}\}}{\{\text{Column Load}\}}$ along column legs

The graphs incorporated in the text are reproduced in a conveniently small size for ready reference.

It should be noted that some of the figures - because of the unavoidable choice of widely different length and deflection scales - are highly distorted images.

When the column model was tested to destruction failure occurred in the second panel from the top of the right leg at a load of 4.60 by sudden twisting of one of the two angles forming the leg.

(c) Discussion of Experimental Results.

Deflected Form of Column Legs. -- Figs. 4 and 5.

Considering the deflected form of the individual column legs it is apparent that each leg buckles as a whole with a simultaneous manifestation of secondary buckling effects between the panel points. The shape of the column legs buckling as a whole, as indicated by the panel points, appears to be a complete sine wave. The shape taken up by the portions between the panel points appears to vary according to the relative movements of adjacent panel points. This is illustrated for example by the *bent* form of portion C, D, of the left leg, the initial form of which may be taken as one-half of a sine wave, changing to three-half sine waves as the load is increased.

It appears, therefore, that the portions between adjacent panel points behave as columns with an unknown degree of fixity at the panel points and are subjected to end thrusts whose eccentricity varies continuously depending on the relative deflections of adjacent panel points.

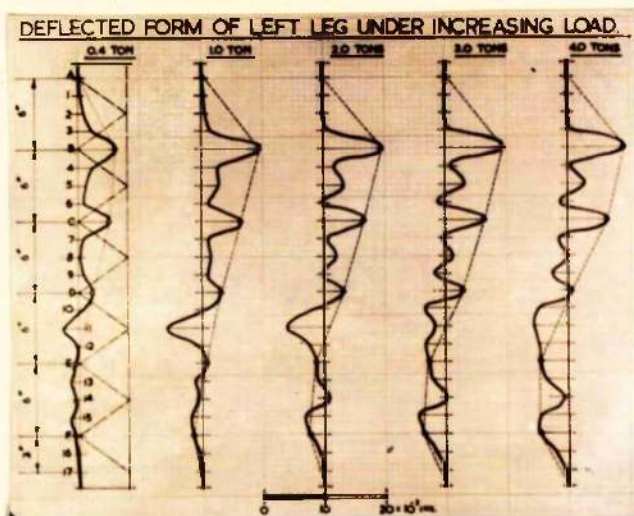


Fig. 4.

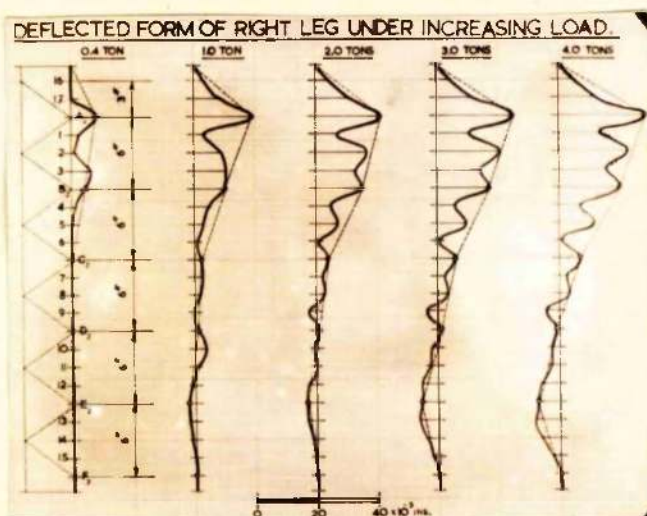


Fig. 5.

Relative Deflections of Column Legs. -- Fig. 6. This shows the deflected form of legs $A_1 F_1$ and $A_2 F_2$ at a load of 4 tons together with the deflected form of leg $A_2 F_2$ relative to $A_1 F_1$. The latter indicates the distortion of the latticing.

These graphs clearly indicate that the column does not behave as a unit, the legs deflecting relative to each other. The movements of the upper portion of the column amount to an expansion, with a corresponding contraction in the lower regions. This action is not a pure "barrelling" type since it is accompanied by deflection of both column legs to the same side of the centre line, the column tending to take up the configuration indicated in the sketch at the bottom of Fig. 6.

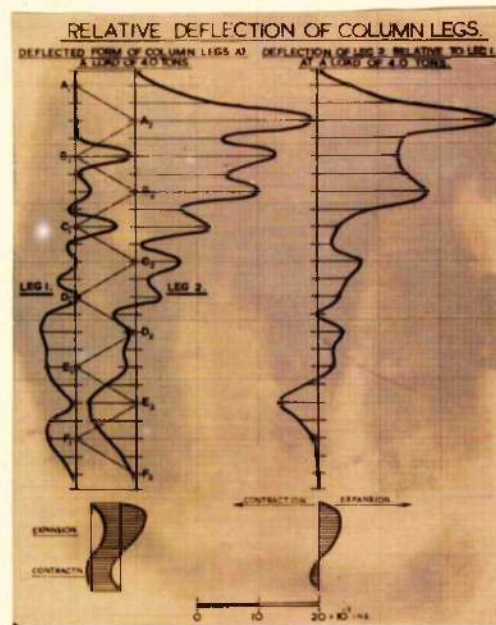


Fig. 6.

Panel Point Deflection Against Column Load. Figs. 7, and 8.

Left Leg. Deflection of points B, C, & D, are characterised by rapid increase in deflection during the initial stages of loading up to about 1 ton then a definite stiffening action and hence an apparent tendency to rapid decrease of the deflection resulting in the case of D, provided loading would have been continued, in a deflection opposite to the initial deflection.

Deflections of points E, & F, appear to show a roughly uniform rate of increase with a definite stiffening action towards the last stages of the loading.

Right Leg. Points A₂ ; B₂ ; C₂ ; E₂ ; show a gradually decreasing rate of deflection with a stiffening up tendency towards the latter stages of loading.

Point D₂ is similar in its behaviour to point D, of the left leg showing a tendency to deflect at an increasing rate during the last stages of loading, in a direction opposite to the initial deflection.

Summing up points A₂ B₂ C₂ E₂ of the right leg show characteristics similar to points E, and F, of the left leg while points B, C, D, of the left leg appear to behave in a manner similar to that of point D₂ of the right leg.

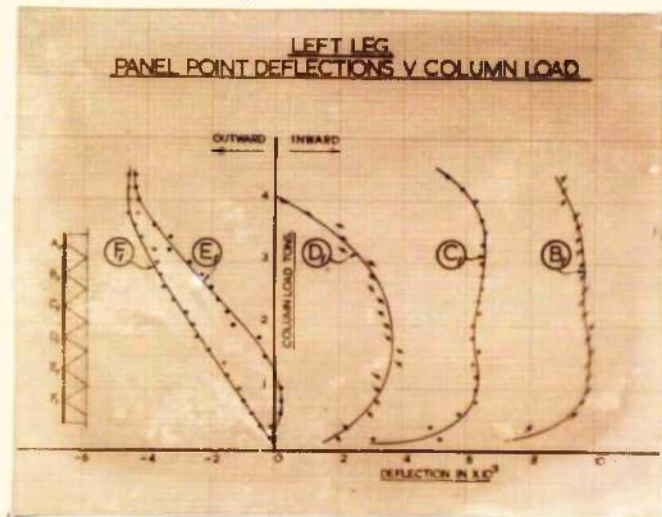


Fig. 7.

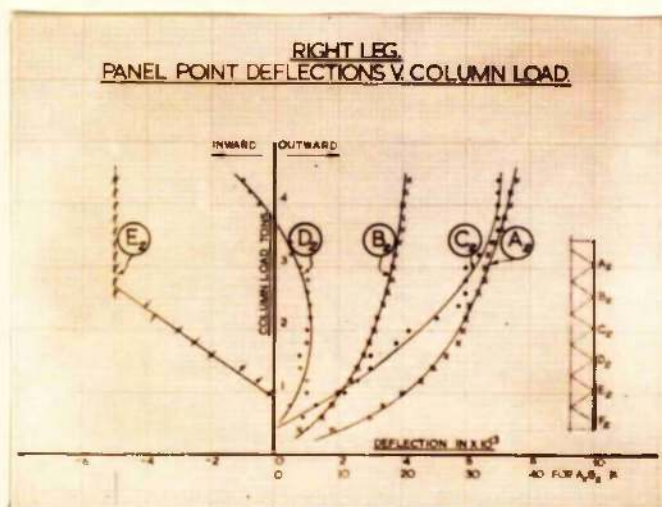


Fig. 8.

Centre of Panel Deflection against Column Load. Figs. 9 and 10.
 These curves have no great significance in themselves relative to latticed column behaviour since they show the combined effect of panel point deflections and local bending between the panel points and give, in most cases a deceptive idea of actual conditions. They, however, do show the characteristics of the variations of the deflection of columns (a) where the ends have movement relative to each other, (b) where in virtue of (a) the eccentricity of the thrust is changing continuously, and (c) where the ends are afforded varying degrees of fixity.

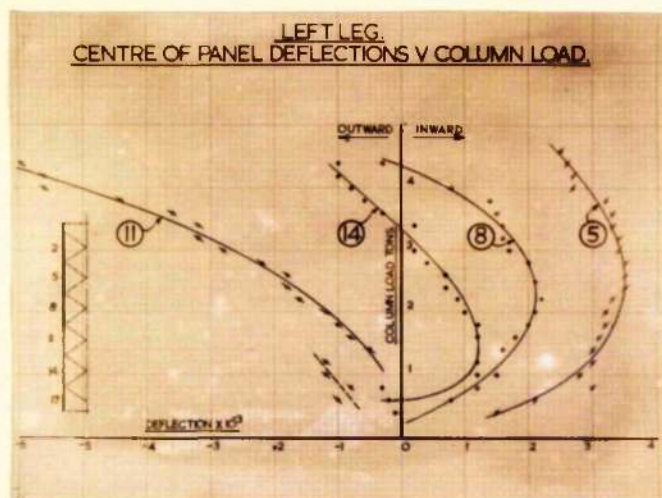


Fig. 9.

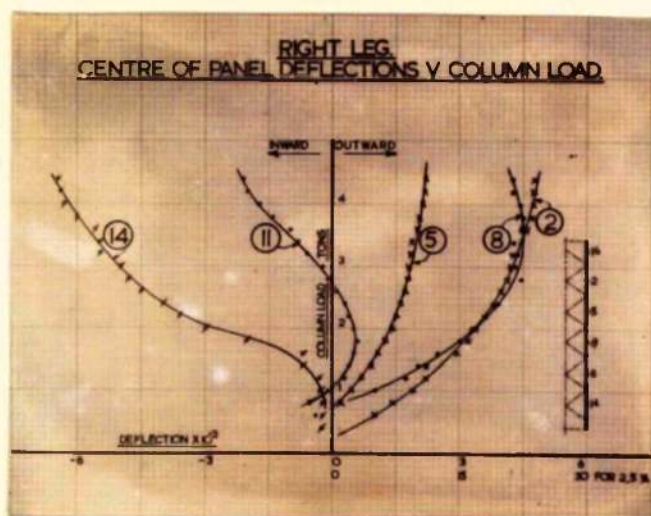


Fig. 10.

Centre of Panel Deflections relative to line of Panel Points against Column Load. Figs. 11 and 12. The curves shown support the view already obtained from the consideration of the deflected forms of the legs that the portions between the panel points buckle individually.

No direct connection appears to exist between these curves and the curves of panel deflection.

Considering the *left* leg it is interesting to note that these curves show to a certain extent regular variation for points such as point 14 lying on a portion whose initial *bent* form is not appreciably changed during loading.

Points such as 8 and 11 which are part of portions changing their initial deflected form as loading progresses show the irregularity which one would expect.

Similar observations apply to the points on the *right* column leg.

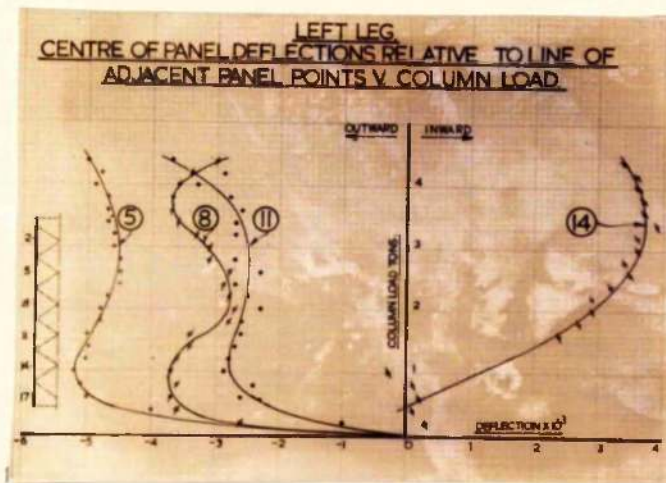


Fig. 11.

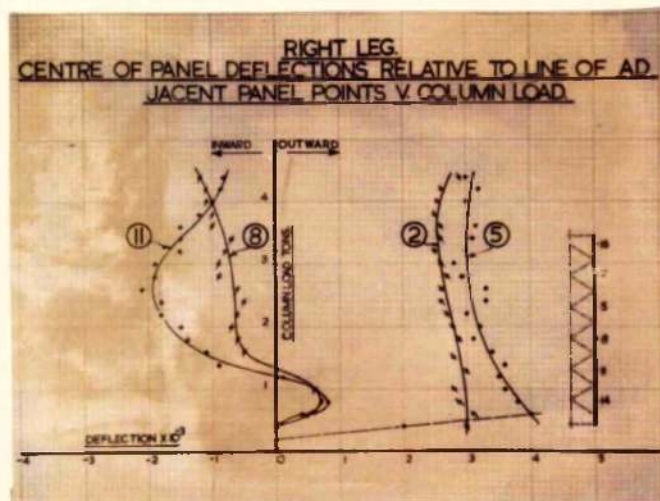


Fig. 12.

Distribution of $\Delta = \left\{ \frac{\text{Leg Deflection}}{\text{Column Load}} \right\}$ along Column Legs. Fig. 13.

The graphs shown give the rate of change of deflection of the panel points with load, obtained by evaluating the ratio (change in deflection) : (corresponding change in column load) for the different load ranges indicated.

It appears to be clear that with the exception of point D_1 of the left leg, the rate of increase of deflections for points of the right leg is greater.

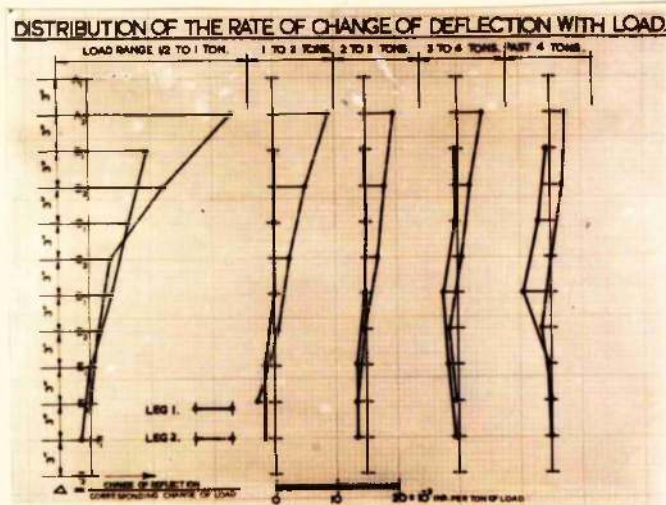


Fig. 13.

Considering column model behaviour in the various load ranges the following observations are relevant:-

Load range 0 to 1 ton -- the right leg $A_2 F_2$ is the "active" component -- indicated by its higher deflection rate -- deflecting due to load actions and, by means of the latticing, transmitting a forcing action to the left Leg $A_1 F_1$. This action the "passive" left leg has followed in a reluctant manner as indicated by its lower deflection rate.

Load range 1 ton to 2 tons -- The restraining or "dragging" action of leg $A_1 F_1$ in the upper portions appears to become effective, as indicated by the decreased deflection rate of leg $A_2 F_2$. The lower portion of leg $A_2 F_2$ is, however still transmitting a forcing action at E_2 , increasing the deflection rate of leg $A_1 F_1$ in this region.

Load ranges 2 tons to 4 tons and beyond -- The same process appears to continue, but a gradual increase in the deflection rate at D_1 showing a "running away" phenomenon indicates that this leg has now taken over the "active" part and is now transmitting a forcing action to leg $A_2 F_2$.

The characteristics shown up by these curves indicate the fact that one, or part of one, of the column legs plays the "active" part and the other the "passive" part in building up the deflected form of the column. It would also appear that a leg which is "active" during a certain range of loading may become "passive" during another range.

Column behaviour on this basis may be visualised as follows:-

The "active" leg is deflecting at a high rate -- due to external causes -- and transmits a forcing action by the agency of the bracing to the "passive" column leg which exerts a retarding influence.

Depending on the elastic characteristics of the structure as a whole, this retardation may be successful in checking the "active" column leg in which case equilibrium conditions will be reached. It is conceivable, however, that the "passive" leg due partly to weakness, to initial irregularity and to the type of bracing, at some points is not able to counteract the active influence, in which case local conditions may reach a critical stage culminating in local collapse.

(d) Column Model Behaviour.

1. The column as a Unit. - The column does not buckle as a unit, the column legs deflecting relative to each other. In the model tested the normal distance between the column legs increased between certain points with a simultaneous decrease between other points.
2. The individual column legs. - The deflected shapes of the column legs are similar. In the model tested both column legs buckled into approximately one full sine wave.
3. The panel element. -- Concurrently with the deformation of the column legs as a whole, there is a manifestation of secondary buckling effects between adjacent panel points.

The deformed shape of a part between adjacent panel points of any one leg appears to vary according to the initial irregularity of the part; according to the relative deflection of adjacent panel points (including continuous variation in the eccentricity of the thrust); and according to the degree of fixity afforded at the end of the part considered by virtue of continuity.

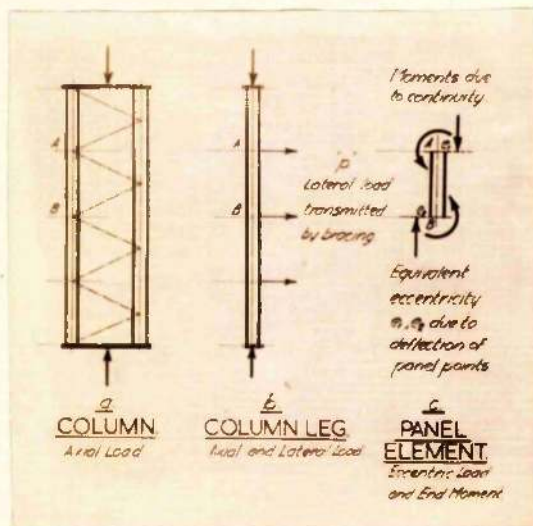


Fig. 14.

Contrast of 1, 2 and 3. - The force actions governing the deformation of a latticed structural member, as indicated by the experiments, are shown in Fig. 14. This contrasts the force actions on the column as a whole, on an individual column leg, and on a column panel element. It is apparent that the loading conditions are basically different in the three cases. Consequently

the conventional estimate for design purposes of the strength of the column and that of a column panel element for similar loading conditions is wholly untenable.

All the experimental results point to the fact that the critical behaviour criterion is that given by the individual column leg (Fig. 14b) subjected to axial and lateral loads, the latter depending on the relative deflection between the column legs.

4. The Lattice System. The single lattice bracing as used in the tests served as an agency for transmitting forcing action of one column to the other and did not contribute to the load resisting action of the column as a whole. That is the forces in the lattice bars are dependent on the relative movement of the column legs only.

SECTION III. - LATTICED COLUMN ANALYSIS AND APPLICATIONS.

1. ANALYSIS.

	<u>Page.</u>
Notation.	<u>33.</u>
General Assumptions.	<u>33.</u>
(a) <u>Eccentric Loading - Buckling in the Plane of the Latticing.</u>	<u>34.</u>
Equivalent Column.	
Derivation of the Equations.	<u>34.</u>
Hyperbolic Buckling Load Relation.	<u>35.</u>
Buckling with Legs Deflecting to the Same Side.	
Buckling with Legs Deflecting to Opposite Sides.	
Limiting Buckling Load Value at "full" eccentricity.	<u>37</u>
Variation with the factors " $\bar{\beta}$ " and " n^2 ".	
Buckling Load Variation with Eccentricity.	<u>37.</u>
(b) <u>Eccentric Loading - Buckling Perpendicular to the Plane of Latticing.</u>	<u>38.</u>
Assumptions.	
Force Actions on Column Legs.	
Second Order Quantities.	
Buckling Load Formulae.	
(c) <u>Concentric Loading.</u>	<u>38.</u>
Reduction of the Eccentric Load Equation.	
Alternative Modes of Buckling.	<u>38.</u>
Minimum Buckling Load Value.	
Variation with the factors " $\bar{\beta}$ " and " n^2 ".	<u>39.</u>
(d) <u>Calculation of the Equivalent Web Constant.</u>	<u>39.</u>
In the Plane of the Latticing.	<u>39.</u>
Perpendicular to the Plane of the Latticing.	<u>41.</u>
(e) <u>Summary.</u>	<u>42.</u>
The Perry-Robertson formula and the value of " P_e "	
The overall column strength.	
The column leg component strength.	
The Panel element strength.	

The review - presented in Section I - of publications on latticed columns indicated that the ultimate column load based on overall "solid" column strength and on panel element strength has been exhaustively investigated.

No analytical or experimental investigation was found however respecting the strength and stability of the individual column legs of a latticed column. The loading on the column legs is their share of the axial load combined with any lateral force actions transmitted by the bracing.

The experimental work presented in Section II confirmed the existence, and established the distribution of, the relative lateral movement between the column legs.

These two features - the lack of a satisfactory analysis of column leg strength, together with the experimentally established existence of a mode of behaviour not considered by previous investigators defined the aims and scope of this section as:-
(1) The theoretical evaluation of the "ideal column" buckling load for a latticed column, based on the stability of the individual column legs. Both eccentric and concentric loading is considered buckling of the column legs assumed to take place in the plane or perpendicular to the plane of the latticing.
(11) The extension of the Perry-Robertson formula to latticed struts, " p_e " (the "ideal column" critical stress) being based in general on the strength of the weakest column component. The case, when the weakest column component is the column leg (p_e being given by the theoretical treatment presented) is considered in detail, and is tested against experimental results on a wide range.

The following notation is used throughout:-

- I = Moment of Inertia of one of the column legs about an axis perpendicular to the plane in which buckling is considered.
- I_L = Moment of Inertia of one lattice bar about an axis in the plane of the latticing.
- E = Modulus of Elasticity in tension and compression.
- L = Total length of one column leg.
- d = Distance between the column legs.
- b = Distance between adjacent panel points.
- ℓ = Length of one lattice bar.
- β = Elastic constant of the latticing in the plane of buckling.
- θ = Angle of inclination of lattice bars to the horizontal.
- A = Area of one column leg.
- a = Area of one lattice bar.
- P_c = Critical or buckling load.
- P_e = Euler Buckling Load for hinged ends $\pi^2 EI/L^2$
- y = Deflection of column legs.

The following general assumptions are used throughout:-

- (1) The column legs are initially straight and homogeneous and E is a constant throughout.
- (2) The column legs are hinged at the ends.
- (3) The latticing is pinjointed in the plane of the bracing, but gives the effect of fixture perpendicular to the plane of bracing.
- (4) Buckling is uniplanar.

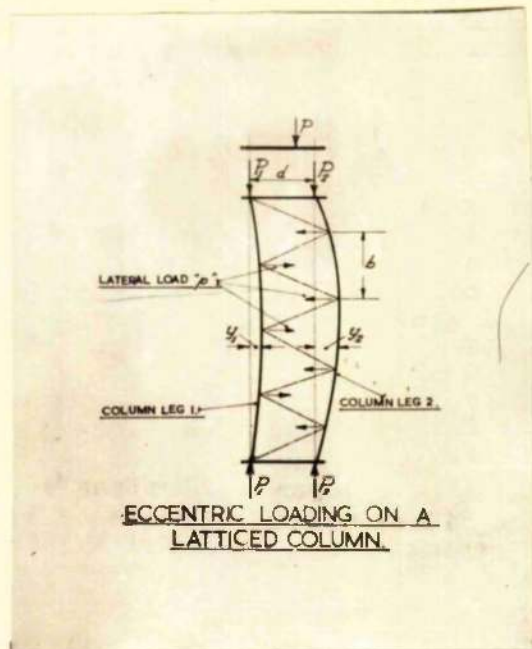


Fig. 15.

In considering latticed strut behaviour from the point of view of stability, the general case of an eccentric load on the column as a whole will be considered first since the actions involved are comparatively simple to visualise. The case of a concentric load can then be obtained by simplification of the equations.

(a) Elastic Stability under Eccentric Loading - Buckling in the Plane of the Latticing.

An eccentric load P , say on the column becomes equivalent to the loads P_1 and P_2 on the individual column legs as shown in Fig. 15. Considering the case when $P_2 > P_1$, the deflections y_2 of Leg 2 will tend to be greater than that of Leg 1, when the system is externally disturbed. Because of the difference in deflections the lattice system will be distorted giving rise to lateral force actions proportional to the relative deflection $y_2 - y_1$ of the column legs. The lateral force actions for the case shown will enhance the flexural effect in the case of Leg 1 opposing the same effect for Leg 2.

For purposes of analysis it has been considered approximately correct to use instead of a series of concentrated loads, a distributed lateral load proportioned to the difference in deflection of the column legs. This approximation is tantamount to assuming the flanges connected by a continuous elastic medium, the lateral force exerted by which, at any section, is proportional to the relative deflection of the column legs at that section. Further this elastic medium is assumed to be incapable of transmitting forces along the axis of the column. Let the elastic constant of this equivalent web be β per unit length per unit relative deflection.

The differential equation applicable to cases of columns subject to axial thrust P and lateral loads of magnitude p per unit length is -

$$EI \frac{d^4 y}{dx^4} + P \frac{d^2 y}{dx^2} = p$$

Applying this to the case of column leg 1. where the lateral actions enhance the flexural actions and column leg 2. where the lateral actions oppose the flexural action, the following equations are obtained:-

$$EI \frac{d^4 y_1}{dx^4} + P_1 \frac{d^2 y_1}{dx^2} - \beta(y_2 - y_1) = 0 \dots\dots\dots (1)$$

$$EI \frac{d^4 y_2}{dx^4} + P_2 \frac{d^2 y_2}{dx^2} + \beta(y_2 - y_1) = 0 \dots\dots\dots (2)$$

The boundary conditions are

$$\begin{array}{lcl} \text{at } x=0 & y_1 = y_2 = 0 & \text{and } \frac{d^2 y_1}{dx^2} = \frac{d^2 y_2}{dx^2} = 0 \\ x=L & y_1 = y_2 = 0 & \text{and } \frac{d^2 y_1}{dx^2} = \frac{d^2 y_2}{dx^2} = 0 \end{array}$$

Using the Fourier Sine transformation

$$Y(n) = \int_0^L y \sin \frac{n\pi x}{L} dx = \int_0^L f(x) \sin \frac{n\pi x}{L} dx$$

the equations reduce to (see Appendix No. 1)

$$\left[P_1 \frac{n^2 \pi^2}{L^2} - EI \frac{n^4 \pi^4}{L^4} - \beta \right] Y_1(n) + \beta Y_2(n) = 0 \dots\dots\dots (3)$$

$$\beta Y_1(n) + \left[P_2 \frac{n^2 \pi^2}{L^2} - EI \frac{n^4 \pi^4}{L^4} - \beta \right] Y_2(n) = 0 \dots\dots\dots (4)$$

Equations (3) and (4) will only give solutions other than

$$Y_1(n) = Y_2(n) = 0 \quad \text{if}$$

$$\begin{vmatrix} P_1 \frac{n^2 \pi^2}{L^2} - EI \frac{n^4 \pi^4}{L^4} - \beta & \beta \\ \beta & P_2 \frac{n^2 \pi^2}{L^2} - EI \frac{n^4 \pi^4}{L^4} - \beta \end{vmatrix} = 0$$

that is

$$(P_1 \frac{n^2 \pi^2}{L^2} - EI \frac{n^4 \pi^4}{L^4} - \beta)(P_2 \frac{n^2 \pi^2}{L^2} - EI \frac{n^4 \pi^4}{L^4} - \beta) = \beta^2 \dots\dots\dots (5)$$

A hyperbolic relation between P_1 and P_2 the buckling loads of Leg 1 and 2 respectively, for any given value of β - (the equivalent web elasticity) - and n (the number of half waves the column leg buckles into).

The Fourier Sine series corresponding to the function $y=f(x)$ converges to the function

$$y = f(x) = \frac{2}{L} \sum_{n=1}^{\infty} \sin \frac{n\pi x}{L} \int_0^L y \sin \frac{n\pi x}{L} dx$$

but $\int_0^L y \sin \frac{n\pi x}{L} dx =$ Fourier Sine transformation

$$Y(n) \text{ i.e. } y = f(x) = \frac{2}{L} \sum_{n=1}^{\infty} Y(n) \sin \frac{n\pi x}{L}$$

consequently

$$y_1 = \frac{2}{L} \sum_{n=1}^{\infty} Y_1(n) \sin \frac{n\pi x}{L}$$

$$y_2 = \frac{2}{L} \sum_{n=1}^{\infty} Y_2(n) \sin \frac{n\pi x}{L}$$

For a given set of values of P_1 ; P_2 and β equation (5) will have at most one integral solution for n . Hence all the Fourier coefficients will be zero but for the one corresponding to the integral value of n .

Therefore

$$y_1 = \frac{2}{L} Y_1(n) \sin \frac{n\pi x}{L}$$

$$y_2 = \frac{2}{L} Y_2(n) \sin \frac{n\pi x}{L}$$

and hence

$$\frac{y_1}{y_2} = \frac{Y_1(n)}{Y_2(n)}$$

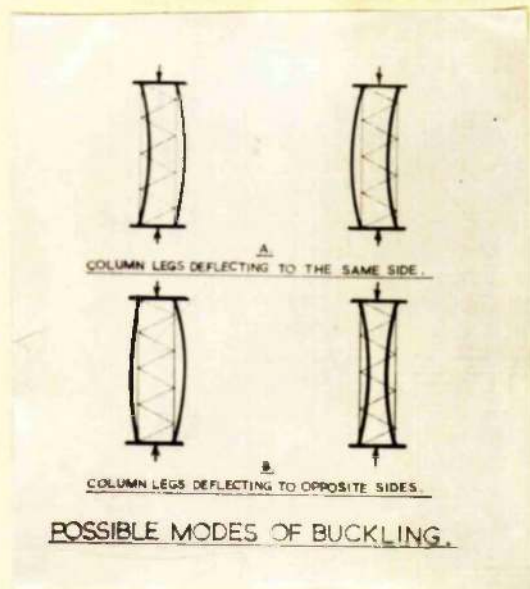


Fig. 16.

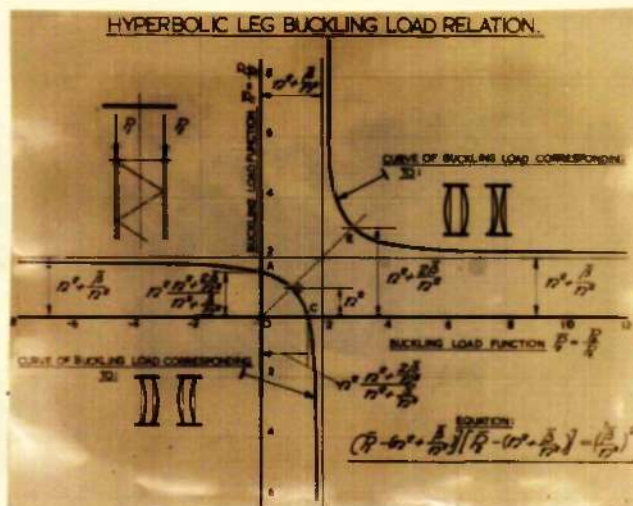


Fig. 17.

From equations (3) and (4)

$$\frac{y_1}{y_2} = \frac{y_1(n)}{y_2(n)} = \frac{-\beta}{(P_1 \frac{n^2 \pi^2}{L^2} - EI \frac{n^4 \pi^4}{L^4} - \beta)} = \frac{(P_2 \frac{n^2 \pi^2}{L^2} - EI \frac{n^4 \pi^4}{L^4} - \beta)}{-\beta}$$

In equation (5) the left hand side must be +ve since the right hand side is a square. Consequently the two factors forming the left hand side must both be +ve or -ve

If both are negative $\frac{y_1}{y_2}$ is positive (β is always positive) that is y_1 and y_2 are both of the same sign and the column legs deflect to the same side.

(Fig 16A.)

If both are positive $\frac{y_1}{y_2}$ is negative that is y_1 is of opposite sign to y_2 and the column legs deflect to opposite sides (Fig.16B)

Before representing graphically the buckling load variation corresponding to these two cases, it is convenient to rewrite equation (5) in the following non dimensional form.

$$(P_1/P_c - n^2 - \frac{\beta EI}{n^2 P_c^2})(P_2/P_c - n^2 - \frac{\beta EI}{n^2 P_c^2}) = (\frac{\beta EI}{n^2 P_c^2})^2$$

Denoting

$$\frac{\beta EI}{P_c^2} \text{ as } \bar{\beta}$$

$$P_1/P_c \text{ as } \bar{P}_1$$

$$P_2/P_c \text{ as } \bar{P}_2$$

the equation reduces to

$$(\bar{P}_1 - (n^2 + \frac{\bar{\beta}}{n^2}))(\bar{P}_2 - (n^2 + \frac{\bar{\beta}}{n^2})) = (\frac{\bar{\beta}}{n^2})^2 \dots\dots\dots (6)$$

For any given value of n and $\bar{\beta}$ equation (6) represents a hyperbolic variation between \bar{P}_1 and \bar{P}_2 as shown in Fig.(17)

Fig. 17. opposite.

$$\bar{P}_1 = \bar{P}_2$$

This indicates two load levels. With the exception of the case where both of these are possible, the lower one only is relevant. From equation (6) the lower value of the Buckling Load for the column based on the stability of the legs at "full" eccentricity (load applied in line with one of the legs) is obtained by putting say $\bar{P}_2 = 0$ yielding

$$\bar{P}_1 = n^2 \frac{n^2 + \frac{2\bar{\beta}}{n^2}}{n^2 + \frac{\bar{\beta}}{n^2}} \dots\dots\dots (6a)$$

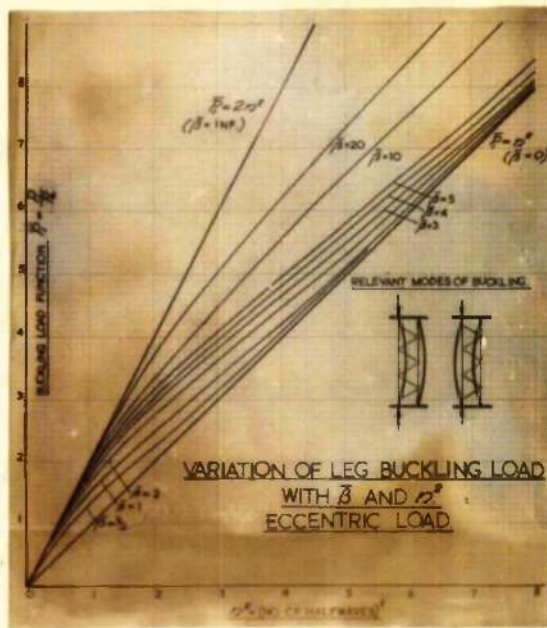


Fig. 18.

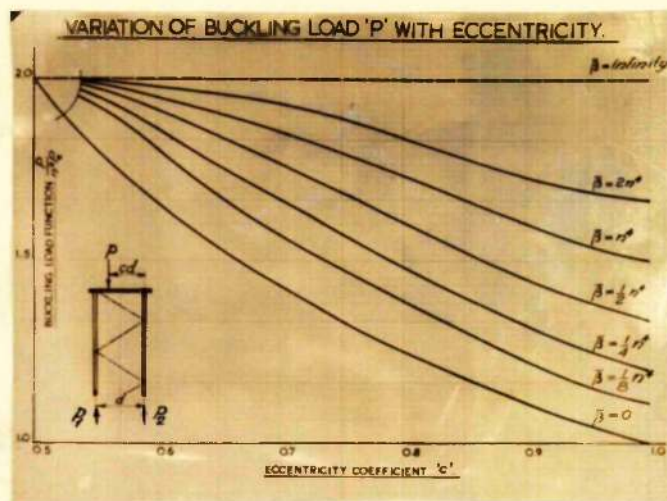


Fig. 19.

57.

$$\text{or total column load} = P = P_1 = n^2 P_e = \frac{n^2 + \frac{2\beta EI}{n^2 R^2}}{n^2 + \beta EI/n^2 R^2} \dots (66)$$

Plotting \bar{P} against n^2 from equation (6a), yields the family of curves shown in Fig. 18. It is interesting to note that all the curves lie within the field defined by the straight lines $\bar{P} = 2n^2$ and $\bar{P} = n^2$ approaching the former at low values of n^2 and the latter at higher values of n^2 .

A significant point of inflection is situated at a value of $n^2 = \sqrt{\beta}$ giving a value of $\bar{P} = 1.25n^2$. This implies that in columns having an equivalent web elasticity such that $\beta EI/P_e^2 = \frac{1}{3}n^4$ the buckling load is $1\frac{1}{4}$ times the Euler value, corresponding to the particular buckled form.

Any eccentric load condition may be expressed by the inequality of the column leg loads P_1 and P_2 (Fig. 19)

The total load on ^{the} column, P in terms of the load on the left leg is obtained by moments as $P = P_1 \cdot \frac{1}{c}$; the load on the right leg being $P_2 = \frac{1-c}{c} P$ where $\frac{1}{2} < c < 1$. Substituting for $\bar{P}_2 = \frac{1-c}{c} \bar{P}$ in equation (6) reduces to

$$\bar{P}_1^2 - \frac{1}{1-c} \bar{P}_1 (n^2 + \frac{\beta}{n^2}) + \frac{c}{1-c} n^4 (1 + \frac{2\beta}{n^4}) = 0$$

Considering the lower load level relevant to eccentric loading the following values of the total buckling load are of interest

$\beta = n^4 b$	$\frac{\bar{P}}{n^2} = \frac{1}{c} \frac{\bar{P}_1}{n^2} = \frac{1}{2c(1-c)} \{ (1+b) - \sqrt{(1+b)^2 - 4c(1-c)(1+2b)} \}$
0	$\frac{1}{2c(1-c)} \{ 1 - \sqrt{1 - 4c(1-c)} \} = \frac{1}{c}$
$\frac{n^4}{8}$	$\frac{1}{2c(1-c)} \{ 1.125 - \sqrt{1.265 - 5c(1-c)} \}$
$\frac{n^4}{4}$	$\frac{1}{2c(1-c)} \{ 1.25 - \sqrt{1.56 - 6c(1-c)} \}$
$\frac{n^4}{2}$	$\frac{1}{2c(1-c)} \{ 1.50 - \sqrt{2.25 - 8c(1-c)} \}$
n^4	$\frac{1}{2c(1-c)} \{ 2.0 - \sqrt{4 - 12c(1-c)} \}$
$2n^4$	$\frac{1}{2c(1-c)} \{ 3.0 - \sqrt{9 - 20c(1-c)} \}$
Infinity	2

Fig. (19) shows the variation of the total Buckling load for latticed columns, with eccentricity, for various values of the web elasticity β . It can be seen that considerable variation is shown particularly at low values of β where reductions up to 100% may take place as the load shifts from concentricity to full eccentricity.

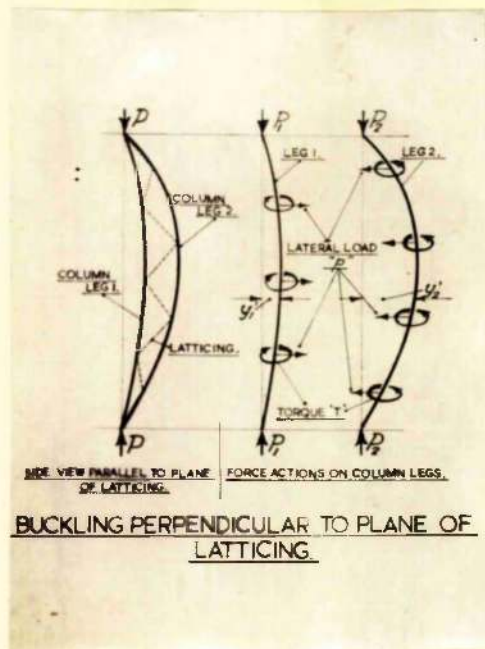


Fig. 20.

(b) Eccentric Loading - Buckling perpendicular to the plane of the latticing.

Referring to Fig. 20 it is readily apparent that the force actions to which the individual column legs are subjected are similar to that in (a) with an additional distributed torque by virtue of the latticing acting as a series of cantilevers. Consequently the continuous elastic medium connecting the flanges is assumed to exert lateral forces perpendicular to the plane of the latticing and proportional to the relative deflection of the column legs in that direction. In this particular case the deflected form of the column leg would be a space curve.

Assuming the projections of the deflections of Leg 1, on two perpendicular planes to be y_1' and y_1'' respectively (plane)' being the plane in which the lateral loads act; the magnitude of the torque at any section is $T = \text{constant} \times \beta d (y_2' - y_1')$ while the bending moment in (plane)' due to torque would be $M_T' = \text{constant} \times \beta \alpha (y_2' - y_1') \times \text{slope of leg in (plane)''}$. But the slope on (plane)'' is proportional to the deflection hence -

$$\text{for leg 1 (say), } M_T' = \text{constant} \times \beta d (y_2' - y_1') y_1'' \quad \text{for leg 1.}$$

Comparing this expression with the bending moments due to elastic lateral load $M_{Ls} = \text{Constant} \times \beta (y_2' - y_1')$ and end thrust $M_p = \text{Constant} \times P y_1'$ respectively in (plane)' it is seen that M_T' is negligible as of the second order. Therefore the load system reduces to one identical with the case of buckling in the plane of the latticing, yielding the same form for the critical loads and interpretation as in the former case, viz:

$$(\bar{P} - (n^2 + \frac{\bar{\beta}}{n^2})) [\bar{P} - (n^2 + \frac{\bar{\beta}}{n^2})] = (\frac{\bar{\beta}}{n^2})^2$$

$\bar{\beta}$ being the equivalent web constant in a plane perpendicular to the plane of the latticing.

(c) Concentric Loading.

The mode of distortion given in Subsection (a) will hold for the concentric case also but \bar{P}_1 will now become equal to \bar{P}_2 .

If $\bar{P} = \bar{P}_2$ equation (6) becomes

$$\bar{P} - (n^2 + \frac{\bar{\beta}}{n^2}) = \pm \frac{\bar{\beta}}{n^2}$$

If the column legs deflect to the same side the factors of equation (6) are of negative sign hence

$$\bar{P} = n^2 \quad \text{or} \quad P_1 = n^2 P_2 \dots \dots \dots (6c)$$

The column legs behave therefore as if there would be no latticing and the total load on the column is determined by the Euler buckling load of the individual legs. This load corresponds to the lower value shown in Fig. 17. It should be noted however that each panel point is a potential point of contraflexure and therefore n (the number of half waves) may be greater than one.

If the column legs deflect the opposite sides the factors of equation (6) are of positive sign hence

$$\bar{P} = n^2 + 2 \frac{\bar{\beta}}{n^2} \quad \text{or} \quad P_1 = n^2 P_2 + 2 \frac{\beta EI}{n^2 R} \dots \dots \dots (6d)$$

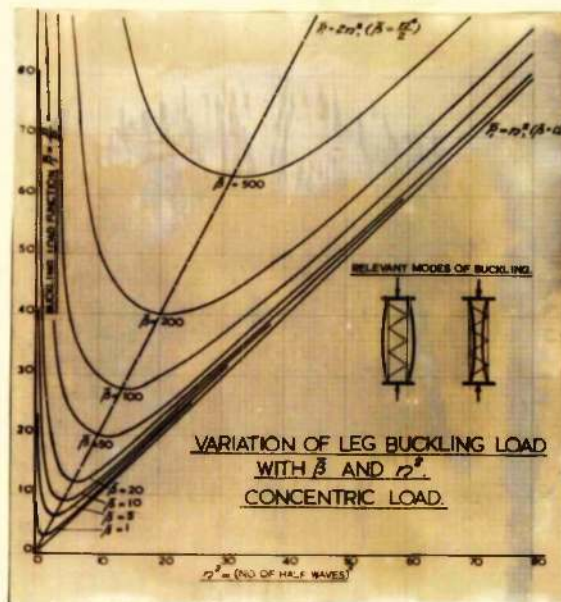


Fig. 21.

The column behaviour is now characterised by "barelling" or "waisting" action, the legs are elastically supported and the critical load is given by the higher load value of Fig. 17.

In this case the minimum value of \bar{P} obtains when

$$\frac{d\bar{P}}{dn} = 0 = 2n - \frac{4\beta}{n^3} \quad \text{i.e.} \quad n^4 = 2\beta$$

$$\text{giving} \quad \bar{P} = 2n^2 \quad \text{or} \quad P = 2n^2 R$$

That is in columns having an equivalent web elasticity such that $\beta EI/R^2 = n^4/2$ the buckling load of the column leg is twice the Euler value corresponding to the particular buckled form. The variation of the higher buckling load value with n^2 and β is shown in Fig. 21.

As indicated by the experiments quoted in Section I - the Review - of the paper and also by the model experiments carried out, this latter mode of buckling appears to be characteristic of latticed bar forms. In what follows a method of assessing the elastic constant of the equivalent continuous web used in the theoretical investigation, is put forward, for the case of column buckling, with the column legs deflecting to opposite sides.

(d) Calculation of the Equivalent Web Constant - Concentric Loading.

Applying the laterally loaded column equations to describe the conditions existing in column legs 1 and 2 under concentric loading the following simultaneous equations are obtained:

$$\text{Leg 1.} \quad EI \frac{d^4 y_1}{dx^4} + P \frac{d^2 y_1}{dx^2} - \beta(y_2 - y_1) = 0 \quad \dots\dots (7.)$$

$$\text{Leg 2.} \quad EI \frac{d^4 y_2}{dx^4} + P \frac{d^2 y_2}{dx^2} + \beta(y_2 - y_1) = 0 \quad \dots\dots (8.)$$

$$\text{adding, these reduce to} \quad \frac{d^4(y_2 + y_1)}{dx^4} + U^2 \frac{d^2(y_2 + y_1)}{dx^2} = 0; \quad U^2 = \frac{P}{EI}$$

$$\text{and subtracting} \quad \frac{d^4(y_2 - y_1)}{dx^4} + U^2 \frac{d^2(y_2 - y_1)}{dx^2} + 2V^2(y_2 - y_1) = 0; \quad V^2 = \frac{\beta}{EI}$$

The general solutions of the reduced equations are

$$y_1 + y_2 = Ax + B + C \cos Ux + D \sin Ux \quad \dots\dots (9.)$$

$$y_2 - y_1 = E \cosh \lambda_1 x + F \sinh \lambda_1 x + G \cos \lambda_2 x + H \sin \lambda_2 x \quad \dots\dots (10.)$$

$$\text{where } 2\lambda_1^2 = \sqrt{U^4 - 8V^2} - U^2 \quad \text{and} \quad 2\lambda_2^2 = \sqrt{U^4 - 8V^2} + U^2$$

Considering barelling or waisting action $y_1 = -y_2 = y$; $y_1 + y_2$ becomes zero and $y_2 - y_1 = 2y$

that is from 10. $2y = E \cosh \lambda_1 x + F \sinh \lambda_1 x + G \cos \lambda_2 x + H \sin \lambda_2 x$

Using the boundary conditions

$$x=0, y=0 \quad \dots\dots (i) \quad x=0, \frac{d^2 y}{dx^2} = 0 \quad \dots\dots (iii)$$

$$x=L, y=0 \quad \dots\dots (ii) \quad x=L, \frac{d^2 y}{dx^2} = 0 \quad \dots\dots (iv)$$

and assuming a deflection $2y = 2e$ at the centre when the system is disturbed there laterally, that is at $x = \frac{L}{2}$, $2y = 2e \dots\dots (v)$ gives

$$E = G = 0 \quad \text{from (i) and (ii)}$$

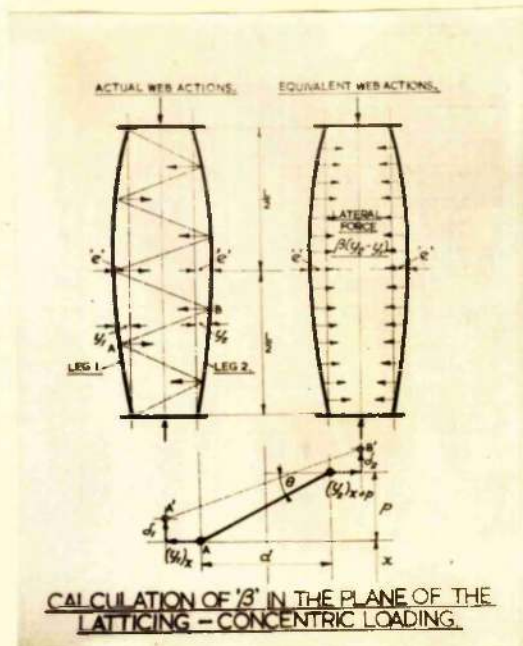


Fig. 22.

$$F = -H \frac{\sinh \lambda_2 L}{\sinh \lambda_1 L} = - \frac{2e \sin \lambda_2 L / \sinh \lambda_1 L}{(\sin \lambda_2 \frac{L}{2} - \frac{\sinh \lambda_2 L}{\sinh \lambda_1 L} \sinh \lambda_1 \frac{L}{2})} \quad \text{from (iii) and (v)}$$

$$H = \frac{2e}{\sin \lambda_2 \frac{L}{2} - \frac{\sinh \lambda_2 L}{\sinh \lambda_1 L} \sinh \lambda_1 \frac{L}{2}} \quad , \text{ substituting in (iv)}$$

$$0 = - \frac{(2e \sin \lambda_2 L) \lambda_1^2}{\sin \lambda_2 \frac{L}{2} - \frac{\sinh \lambda_2 L}{\sinh \lambda_1 L} \sinh \lambda_1 \frac{L}{2}} - \frac{2e \lambda_2^2 \sin \lambda_2 L}{\sin \lambda_2 \frac{L}{2} - \frac{\sinh \lambda_2 L}{\sinh \lambda_1 L} \sinh \lambda_1 \frac{L}{2}}$$

For this to be satisfied for any value of "e" $\sin \lambda_2 L = 0$ i.e. $\lambda_2 L = n\pi$, substituting this value in F and H gives $F = 0$, $H = 2e$

that is $2y = y_2 - y_1 = 2e \sin \frac{n\pi x}{L}$

or $y = e \sin \frac{n\pi x}{L} \dots \dots \dots (11)$

Value of the equivalent web elasticity β in the plane of the latticing.

Due to relative deflection of the column legs laterally (barelling or waisting) and shortening of the legs due to bending, the ends of any latticed bar A.B. move to the positions A' B' as indicated in Fig.22.

$$\text{Change in length of A.B.} = [(y_1)_x + (y_2)_{x+p}] \cos \theta + (\delta_2 - \delta_1) \sin \theta$$

Shortening of a column leg due to bending, δ is the difference between the arc length and the chord length. That is

$$\text{say } \delta_2 = \int_{x+p}^{L/2} (ds - dx) dx = \int_{x+p}^{L/2} \left(\frac{dy_2}{dx} \right)^2 dx$$

or since $y_2 = e \sin \frac{n\pi x}{L}$

$$\delta_2 = \int_{x+p}^{L/2} \frac{n^2 \pi^2}{L^2} e^2 \cos^2 \frac{n\pi x}{L} dx$$

Hence change in length of A.B. (substituting for y 's and δ 's) =

$$= e \cos \theta \left[\sin \frac{n\pi(x+p)}{L} + \sin \frac{n\pi x}{L} \right] + \sin \theta \left[\int_{x+p}^{L/2} \frac{n^2 \pi^2}{L^2} e^2 \cos^2 \frac{n\pi x}{L} dx - \int_x^{L/2} \frac{n^2 \pi^2}{L^2} e^2 \cos^2 \frac{n\pi x}{L} dx \right]$$

The terms forming the coefficient of $\sin \theta$ depend on the (deflection)² and as such are second order quantities in comparison with the cosine terms and can be neglected.

Therefore change in length of A.B. = $e \cos \theta \left[\sin \frac{n\pi(x+p)}{L} + \sin \frac{n\pi x}{L} \right]$

Assuming that the lattice bar is elastic and Hooke's law holds the change in length = $W e / \sigma E$ where W is the force in the lattice bar.

hence $\frac{W e}{\sigma E} = e \cos \theta \left[\sin \frac{n\pi(x+p)}{L} + \sin \frac{n\pi x}{L} \right]$

Expressing the horizontal component of this force as $W \cos \theta$ and noting that $e = d / \cos \theta$

$$W \cos \theta = \frac{\sigma E}{d} e \cos^3 \theta \left[\sin \frac{n\pi(x+p)}{L} + \sin \frac{n\pi x}{L} \right]$$

Thence the total lateral force transmitted by the latticing for half the length of the column leg becomes

$$\sum_{x=0}^{x=\frac{L}{2}} W \cos \theta = \frac{0E}{d} e \cos^3 \theta \sum_{x=0}^{x=\frac{L}{2}} \left(\sin \frac{n\pi(x+p)}{L} + \sin \frac{n\pi x}{L} \right)$$

The lateral force exerted per unit column length by the equivalent web of elasticity $\beta = \beta(y_2 - y_1) dx = 2\beta e \sin \frac{n\pi x}{L} dx$

that is the total lateral force for a half column leg length

$$= \int_0^{\frac{L}{2}} 2\beta e \sin \frac{n\pi x}{L} dx$$

For equivalence the values given by the actual latticing and the continuous elastic web must be equal, hence

$$\frac{0E}{d} e \cos^3 \theta \sum_{x=0}^{x=\frac{L}{2}} \left(\sin \frac{n\pi(x+p)}{L} + \sin \frac{n\pi x}{L} \right) = \int_0^{\frac{L}{2}} 2\beta e \sin \frac{n\pi x}{L} dx$$

$$\text{or } \frac{0E}{d} \cos^3 \theta \sum_{x=0}^{x=\frac{L}{2}} \left(\sin \frac{n\pi(x+p)}{L} + \sin \frac{n\pi x}{L} \right) = 2\beta \int_0^{\frac{L}{2}} \sin \frac{n\pi x}{L} dx \dots (12.)$$

Equation (12) gives the value of β for any particular lattice arrangement. If the value of β corresponding to minimum buckling load conditions is substituted the equation can be further simplified.

That is if $2\bar{\beta} = n^4$ or $2\beta = \frac{n^4 R_e^2}{EI}$ (refer to p. 39)

equation (12) becomes

$$\frac{0E^2 I}{d R_e^2} \cos^3 \theta \sum_{x=0}^{x=\frac{L}{2}} \left(\sin \frac{n\pi(x+p)}{L} + \sin \frac{n\pi x}{L} \right) = n^4 \int_0^{\frac{L}{2}} \sin \frac{n\pi x}{L} dx \dots (13.)$$

Equation (13) can be solved by any method of successive approximation for single or double bracing in any given case, yielding a value for n (the number of half waves the leg tends to buckle into). The corresponding column buckling load then becomes

$$\bar{P} = 2\bar{P}_1 = 2(n^2 + 2\frac{\bar{\beta}}{n^2}) \text{ or } P = 4n^2 R_e \dots (14.)$$

It should be noted that the equivalent web column theory was developed on the assumption that n is an integer. Hence if the value of n obtained from (13) is not an integral value, equation (14) gives two loads within which the actual buckling load will lie. These will be the values corresponding to the nearest lower and higher integers within which n lies.

Value of the equivalent web elasticity β perpendicular to the plane of the latticing.

Using exactly similar reasoning and noting that the lattice bars act as a series of cantilevers of moment of Inertia I_b the lateral load exerted by any lattice bar

$$W = \frac{3EI_b}{e^3} e \left[\sin \frac{n\pi(x+p)}{L} + \sin \frac{n\pi x}{L} \right]$$

also the total lateral load for half the column leg length becomes

$$\frac{3EI_L}{L^3} e \sum_{x=0}^{x=L/2} \left(\sin \frac{n\pi(x+L)}{L} + \sin \frac{n\pi x}{L} \right)$$

or in terms of the equivalent web $\int_0^{L/2} 2\beta e \sin \frac{n\pi x}{L} dx$

The equivalent condition then is

$$\frac{3EI_L}{L^3} \cos^3 \theta \sum_{x=0}^{x=L/2} \left(\sin \frac{n\pi(x+L)}{L} + \sin \frac{n\pi x}{L} \right) = 2\beta \int_0^{L/2} \sin \frac{n\pi x}{L} dx \quad \dots (15)$$

Substituting as before $2\beta = n^4$ or $2\beta = n^4 R^2 / EI$

gives
$$\frac{3E^2 I_L}{L^3 R^2} \cos^3 \theta \sum_{x=0}^{x=L/2} \left(\sin \frac{n\pi(x+L)}{L} + \sin \frac{n\pi x}{L} \right) = n^4 \int_0^{L/2} \sin \frac{n\pi x}{L} dx \quad \dots (16)$$

and the corresponding buckling load as before

$$P = 4n^2 R^2 \quad \dots (17)$$

(e) Summary.

Latticed columns may fail in a number of ways depending on the relative strength of the column as an integral whole, of the column leg component and of the panel elements. The most satisfactory formula developed to date is the Perry Robertson formula which forms the basis of design in Great Britain. This is of the form

$$p_c = \frac{p_y + (\eta + 1)p_e}{2} - \sqrt{\left[\frac{p_y + (\eta + 1)p_e}{2} \right]^2 - p_y p_e}$$

where

- p_c = critical stress of column
- p_y = yield stress of material.
- p_e = Relevant "ideal" column buckling stress.
- η = Eccentricity factor.

The value of " p_e " - the theoretical stress to produce neutral elastic stability may be given by

(1) The overall column strength -

If the column is of such a construction that integral action obtains, the column would be treated as "solid" p_e being the Euler stress corresponding to the end conditions. All experimental investigations indicate that this is unlikely.

(11) The Column Leg component strength.

The buckling load of a latticed column based on the leg component strength may be obtained - as indicated in the foregoing theory - from the hyperbolic buckling load relation. Its value is affected considerably in the concentric case by the distorted form under load varying from the Euler load $n^2 P_e$ per leg (if the leg deflections are to the same side) to the critical load of an elastically supported column $n^2 P_e + \frac{2\beta EI}{n^2 R^2}$ per leg (if the leg deflections are such as to induce barreling or waisting).

In the eccentrically loaded case only one mode of buckling is practicable (provided the column legs are not preset in any way) corresponding to the legs deflecting to the same side. The buckling load is considerably affected by the equivalent elasticity of the bracing and the eccentricity, and is given by

$$n^2 P_e \frac{n^2 + 2\beta EI / n^2 R^2}{n^2 + \beta EI / n^2 R^2}$$

43

The value of the web elasticity can be calculated corresponding to any given lattice system from equations (12) and (15).

(111) The Panel Element Strength.

The column elements between panel points may serve as the basis of estimating p_c , if on comparison with the overall and leg component strengths their critical stress appears to be the lowest. In the absence of more satisfactory analyses respecting the effect on the Buckling Strength of oblique eccentricity of loading, the Euler "solid" column formulae may be used to evaluate this critical stress.

SECTION III. - LATTICED COLUMN ANALYSIS AND APPLICATIONS.

2. APPLICATIONS.

	<u>Page.</u>
(a) <u>Analysis of Collected Experimental Results.</u>	<u>45.</u>
Method of Calculation of Theoretical Failure Stress.	<u>45.</u>
The Evaluation of " p_e " based on the Theory of Section III (1).	<u>45.</u>
The use of the Perry-Robertson Formula.	<u>47.</u>
The Equivalent Slenderness Ratio and Allowance for Imperfections.	<u>47.</u>
Table of Test Specimens' Particulars and Discussion	<u>47.</u>
Table of Experimental and Calculated Results and Discussion.	<u>47.</u>
(b) <u>Summary.</u>	<u>49.</u>
Overall and Column Component Strength.	
Selection of the Relevant " p_c " Value.	
Allowance for Imperfections in Built Up Columns.	
The Applicability of the Perry-Robertson Formula.	

(a) Analyses of Collected Experimental Results.

Method of Calculation of Theoretical Failure Stress.

As has been pointed out in the Summary of Section III (1) the number of ways any column may fail corresponds to the number of its components. The critical strength of the column will always be defined by the strength of its weakest component.

Consequently p_e the "ideal column" critical stress is the smallest of (i) the overall column strength (integral action) (ii) the column leg strength and (iii) the panel element strength. If the panel element itself consists of two or more components the analysis is to include the examination of the strengths of these also. This is the case with the model tests quoted - this will be discussed in greater detail further on.

Given the particulars of any column, the analysis is as follows:-

The overall column strength - Assuming integral action - is obtained from

$$p_e = \mu \frac{\pi^2 E}{(4k)^2} \quad \text{the Euler}$$

column formula, where

$$\begin{aligned} \mu &= \text{Constant defining end conditions.} \\ E &= \text{Young's Modulus.} \\ 4k &= \text{Slenderness ratio as a whole on the full length.} \end{aligned}$$

The Column Leg Component Strength - Assuming lack of integral action - is obtained from

$$p_e = 4n^2 \frac{\pi^2 E}{(4k)^2} \quad - \text{ from}$$

Equation (14) of Section III (1) where

$$4k = \text{Slenderness ratio for column leg section on the full length.}$$

n is the number of half waves the column legs tend to buckle into and is given by





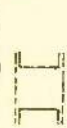
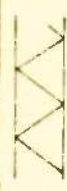


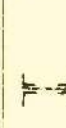

$$\frac{dE^2 I}{d^3 p_e^2} \cos^3 \theta \sum_{x=0}^{x=\frac{L}{2}} \left(\sin \frac{n\pi(x+p)}{L} + \sin \frac{n\pi x}{L} \right) = n^4 \int_0^{\frac{L}{2}} \sin \frac{n\pi x}{L} dx$$

from Equation (13) of Section III (1) or

$$\frac{3E^2 I L}{d^3 p_e^2} \sum_{x=0}^{x=\frac{L}{2}} \left(\sin \frac{n\pi(x+p)}{L} + \sin \frac{n\pi x}{L} \right) = n^4 \int_0^{\frac{L}{2}} \sin \frac{n\pi x}{L} dx$$

from Equation (16) of Section III (1) depending whether buckling takes place in the plane or perpendicular to the plane of the latticing.

TABLE 1.
DESCRIPTION OF TEST SPECIMENS.

Number	Type of Section Nominal Dimensions	Type of Latticing Nominal Dimensions	Area in. ²			Length ft.-in.			Slenderness Ratio			Material	Yield Stress T ₉₀	Young's Modulus T ₉₀	Reference Number in Bibliography with date
			Column	Leg	Lattice Bar	Column	Panel Element	Lattice Bar	Column	Leg	Panel Element				
1.	 Plates 20" x 2" spaced 2" apart	 Single - staggered at 6 3/4" to 8 1/2"	18.76	9.38	0.546	21-0	1'-4	1-5 1/2	37 1/8	593	37 1/8	Steel	19,30	12,500	Talbot and Moore (18) 1910.
2.	 0" channe's	 Single at 4 1/2" to 5 1/2"	17.64	8.82	0.938	15-10	1-3 3/8	1-9 5/8	43 5/8	400	33 7/8	Wrought iron	13,70	11,600	Talbot and Moore (18) 1910. - Four identical columns.
3.	 7" x 2" channe's	 Single 5 1/2" to 6 1/2"	7.17	3.585	0.302	9-04	9-04	0-8 5/8	41 7/8	202	15 1/8	Aluminum Alloy 253	Ultimate Stress 18,40	4,600	Holt (6). 1938.
4.	 7" x 2" channe's	 Single of 5 1/2" to 6 1/2"	—	do.	—	—	do.	—	—	do.	—	Steel	18,20	12,910	Holt (6). 1938.
5.	 7" x 2" channe's	 Single at 5 1/2" to 6 1/2"	0.4046	0.2424	0.0623	3-0	3-0	0-6	18	37	29	Steel	14,0	11,000	Model Test reported in Section I. Column brace perpendicular to latching.

* based on results of tensile tests presented in Appendix No. 3.

The Panel Element strength is obtained from

$$p_e = \frac{\pi^2 E}{(b/k)^2} \quad \text{the Euler column formula}$$

for hinged ends where

$$b/k = \text{slenderness ratio of column leg section on panel length.}$$

This form is approximate in that it neglects the effects of both continuity and eccentricity on the panel element. It would appear however that in the majority of cases it represents a safe underestimate of strength. If the panel element itself may lack integral action the strength of its components is to be computed by the relevant formula.

The actual failure stress is calculated by the Perry-Robertson formula.

$$p_e = \frac{p_y + (\eta + 1)p_e}{2} - \sqrt{\left(\frac{p_y + (\eta + 1)p_e}{2}\right)^2 - p_y p_e}$$

This introduces the limitation of the yield stress of the material and an allowance for imperfections by means of the coefficient η . The "ideal column" critical stress p_e is the stress determined as outlined above.

The value of the imperfection coefficient η is taken as $0.0015 \frac{L}{K}$.

Further, when component strength is the critical factor, the slenderness ratio to be used in conjunction with η is taken as $\frac{L}{K_e}$, L being the overall length of column and

$$K_e = K_1 \sqrt{\frac{P}{2P_1}}$$

P_1 and K_1 are critical load and radius of gyration of the component considered and P is the column strength calculated on the basis of the particular component strength. This method of imperfection assessment is due to Pippard (11).

Appendix (N°2) gives a sample calculation in detail.

Table I - Description of Test Specimens. The table presents the particulars of 8 built up columns tested to destruction. These include tests carried out by Talbot and Moore on steel and wrought iron columns, tests by Holt on Aluminium Alloy and steel columns and the Model tests on steel column reported in Section II.

The test specimens represent a variation of overall length from 21' - 0" to 31' - 0" and in slenderness ratio of column leg component from 593 to 37.

The type of sections included are (i) fully built up from angles and plates and (ii) are channel sections laced together.

The type of latticing introduces single; staggered single and double lacing.

The values given in the Table are the quantities which have been used in drawing up Table 2.

Table 2 - Comparison of Experimental and Calculated Values. In general good agreement is indicated between the calculated and experimental results.

It may be noted that the calculated stress values are given in the form of a stress range. This results from the fact that

TABLE 2.
COMPARISON OF EXPERIMENTAL AND CALCULATED VALUES.

Number	Overall Length of Column ft.	Calculated Strength based on Theory of Section II (1).		Collected Experimental Results		Reference Number in Bibliography with date.
		Critical Stress T_{lin}^2	Type of Failure.	Critical Stress T_{lin}^2	Type of Failure	
1.	21'00	9'60 to 13'06	leg Buckling in Plane of Latticing	10'5	Leg Buckling in Plane of Latticing.	Talbot and Moore 18, 1910 Test No 17.
2.	15'83	11'37 to 12'20	do.	11'80	End Failed	do. Test No 6.
3.	15'83	11'37 to 12'20	do.	12'20	do.	do. Test No 7.
4.	15'83	11'37 to 12'20	do.	11'45	do.	do. Test No 8.
5.	15'83	11'37 to 12'20	do.	12'40	Boared perpendicular to lacing.	do. Test No 9.
6.	9'04	8'24 to 14'70	do.	14'60	Buckling in Plane of Latticing.	Holt (6) 1938, Specimen 2C1.
7.	9'04	14'56 to 16'55	do.	17'10	do.	do. Specimen 2C3.
8.	3'00	9'95 (based on torsional instability, Thomas (32))	Twisting of panel/element.	9'52	Twisting of panel/element.	Model experiment reported in Section II.

"n" the number of half waves was assumed to be an integer in the theory. Consequently if Equation (13) or (16) of Section III (I) gives a non integral value of n the actual failure stress will be between the stresses corresponding to the nearest lower and higher integral values of n.

In the case of columns No.6 and No.7 the end conditions during the test were somewhat indeterminate, and it is possible that some degree of fixity obtained. The calculated values are based on the assumption of hinged ends.

The type of failure for columns No. 2 to 5 was inconclusive. To quote from Talbot and Moore: " For all the tests of the wrought iron bridge posts -- the failures were very gradual. Final failure occurred near the middle or at the end. In the former case, high stresses in one channel had been shown, --- at working loads". This implies some irregularity of construction or local weakness, primarily responsible for the bowing perpendicular to the plane of the latticing, as calculations indicate failure to take place by buckling in the plane of the latticing.

During the tests of the 3 ft. steel column model the distorted form of the legs indicated that bowing of the column legs was taking place. The immediate cause of failure however was the buckling of one of the angles forming the right column leg, due to torsional instability. This is in agreement with the analysis, indicating the torsional buckling strength of a single angle of a panel element as the weakest component strength of the column.

(b) Summary.

From the foregoing theory and experiment the following conclusions are put forward:-

- (1) The strength of the column as a whole is defined by the strength of the weakest component.
- (II) The Perry Robertson formula is applicable to built up columns provided the value of " p_e " is taken as the critical stress of the weakest component.
- (III) The analysis put forward in Section (III) (1) for the determination of the column leg strength appears to give results in good agreement with the experiments.
- (IV) The values of the factor η allowing for imperfections appears to be reasonable at 0.0015; although it is felt that further investigation of this is necessary. This factor will in all probability be different depending on which is the controlling component.
- (V) The method given by Pippard of determining K_e the equivalent radius of gyration for the column as a whole in cases when component strength is the limiting factor appears to give results in good agreement with the experiments.

P A R T II.

THIN WALLED COLUMNS.

37.

SECTION I.

THE COMPOSITE BEHAVIOUR OF THIN WALLED COLUMNS.

	<u>Page.</u>
(a) <u>Overall Column Stability under Concentric End Load.</u>	<u>52.</u>
Flexural Instability - Euler.	<u>52.</u>
Torsional Instability - Lundquist, Fligg, Thomas.	<u>52.</u>
(b) <u>Plate Component Stability under Lengthwise Compression.</u>	<u>53.</u>
Flexural Instability - Bryan, Timoshenko.	<u>53.</u>
The Effect of Edge Conditions.	
Contrast of the Elastic Critical Load and the Ultimate Load - v Karman.	<u>53.</u>
The Effective Width - Winter.	
(c) <u>Optimum Conditions - Equal Overall and Component Strength.</u>	<u>54.</u>
"Column" v "Plate" Failure.	
The Combined Column - Plate Failure Curve.	<u>54.</u>
The Dimension Ratios L/r and b/t .	
The Relation $b/t = \text{Constant} \times L/r$ for Maximum Strength.	<u>55.</u>
Structures of Maximum Strength and Minimum Weight - Cox and Smith.	<u>55.</u>
The Use of the Perry-Robertson Formula.	<u>55.</u>

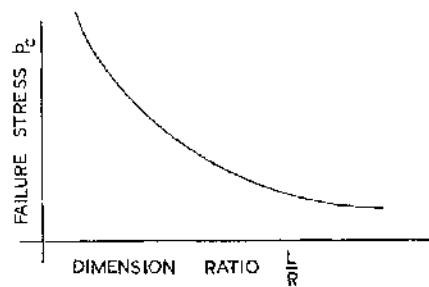


Fig. 23.

Thin walled columns may fail in a variety of ways. The column as a whole may collapse due to flexural or torsional instability; or some of its plate components may buckle, culminating in complete failure of the column. Theories and formulae abound - all with varying degrees of experimental substantiation. The survey presented in this section summarises the main features of the theories in use at present.

(a) Overall Column Stability under Concentric End Load.

The axial stress causing flexural instability for a long column is given by the classic Euler (19) theory and may be stated as

$$p_c = K_1 \frac{E}{(L/r)^2}$$

where K_1 = Constant depending on end conditions (π^2 for hinged ends).
 E = Young's Modulus for the material.
 r = Radius of Gyration of the cross section.
 L = Length of Column.

The critical stress p_c plotted against the slenderness ratio L/r gives the well known Euler curve shown in Fig. 23.

The axial stress causing torsional instability is given by Lundquist and Fligg (30) as

$$p_c = \frac{1}{I_p} (GJ + \frac{\pi^2}{L^2} EC)$$

where I_p = Polar Moment of Inertia of the Cross Section about the axis of rotation.
 GJ = Torsional rigidity of section.
 L = Effective length of column.
 C = The torsion - bending constant dependent on the location of the axis of rotation and the dimensions of the section.

The evaluation of C may be of some complexity depending on the section considered.

Thomas (32) using the strain energy method obtains for angle sections

$$p_c = \left\{ k \frac{\pi^2}{1-\sigma^2} \frac{r^2}{L^2} + \frac{1}{2(1+\sigma)} \right\} E \left(\frac{t}{b} \right)^2$$

where k = Constant depending on end conditions, values as follows:-

Lower End	Position } Fixed direction }	Position Fixed	Position } Fixed direction }	Position } Fixed direction }
Upper End	Free	do.	Position Fixed	do.
k	$\frac{1}{2}$	2	4.1	8

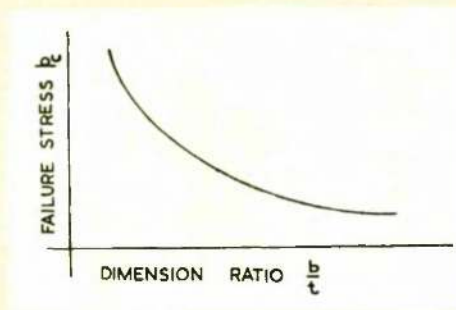


Fig. 24.

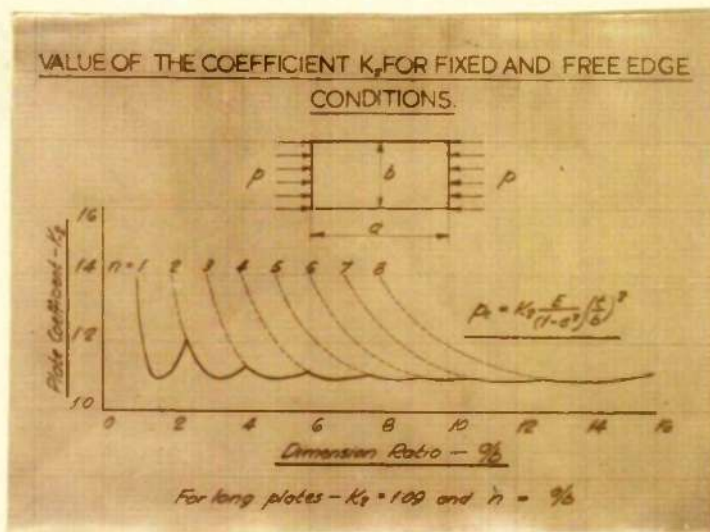


Fig. 25.

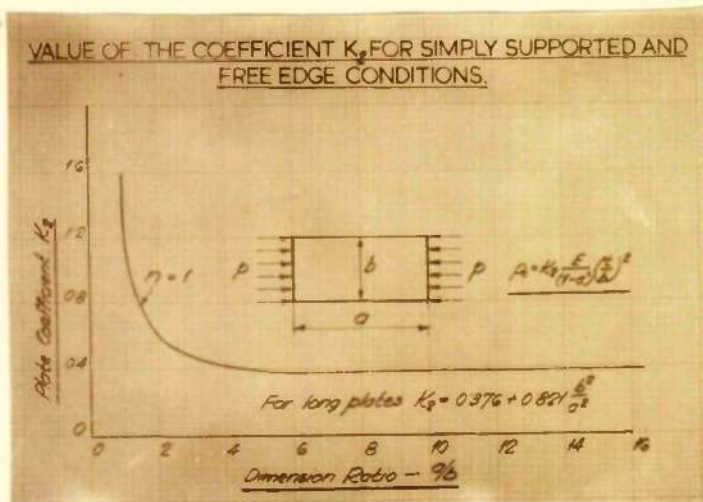


Fig. 26.

- σ = Poisson's Ratio
- L = Length
- r = Radius of Gyration
- b = Width of leg of angle
- t = Thickness of angle
- E as before.

(b) Plate Component Stability Under Lengthwise Compression.

The stress corresponding to flexural instability for a plate with simply supported edges was first obtained by Bryan (24).

Timoshenko (19) gives the general form applicable to plates simply supported along edges perpendicular to the line of compression, with various edge conditions along the edges parallel to the line of compression as

$$p_c = K_2 \frac{E}{(1-\sigma^2)} \left(\frac{t}{b}\right)^2 \dots\dots\dots (18)$$

- where
- K_2 = Constant depending on edge conditions parallel to the line of compression.
 - b = Width of plate.
 - t = Thickness of plate.
 - E and σ as before.

The graph of p_c plotted on the basis of ^{the} b/t dimension ratio is of the general K_2 form shown in Fig. 24.

The influence of the edge conditions is represented by various values of K_2 depending on the overall dimensions and edge conditions of the plate considered. Figs. 25 and 26 give the variation of K_2 for fixed and free and simply supported and free edges respectively. These are the cases relevant to the matter treated in the paper, and the figures give in addition to K_2 , n the number of half waves the plate buckles into.

It is necessary at this stage to differentiate between the critical load causing buckling, and the ultimate load a plate may be capable of supporting. It has been demonstrated that in some cases thin plates supported along both edges can carry, without failure, a load many times larger than the critical load at which buckling begins. The plate buckling form, which gives the stress causing buckling becomes inapplicable in these cases, as it is based on the assumption of small plate deflections.

An exact mathematical treatment of plates in compression on the basis of large deflections is extremely complex. Attempts at a solution have failed to give results of practical applicability. To overcome this difficulty v. Karman (27) suggested the assumption that the middle strip of the buckled plate supported along the edges be disregarded from the point of view of load carrying capacity. The total load is assumed to be taken by two strips next to the edge supports, across which the stress is regarded as uniform.

The equivalent width b_e of these strips for plates simply supported along both edges is given by Winter (34) correlating the experimental results of Sechler and others as

$$b_e = 1.9t \sqrt{\frac{E}{p}} \left[1 - 0.574 \left(\frac{t}{b}\right) \sqrt{\frac{E}{p}} \right]$$

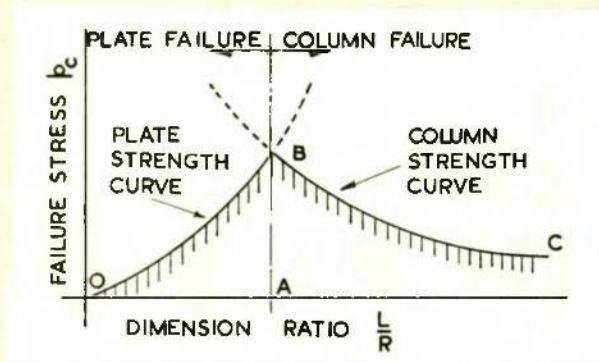


Fig. 27.

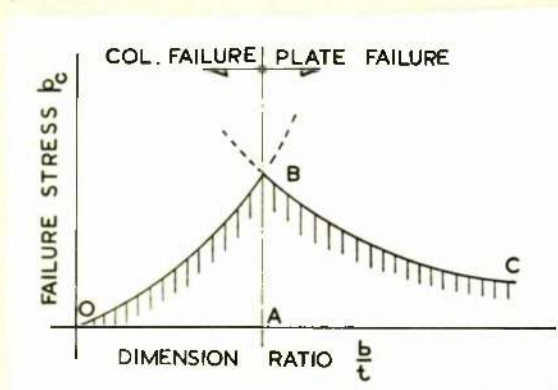


Fig. 28.

The ultimate load is given by

$$P = p_r b_e t$$

or

$$P = 1.9 t^2 \sqrt{E p_r} \left[1 - 0.574 \left(\frac{t}{b} \right) \sqrt{\frac{E}{p_r}} \right]$$

where

p_r = yield stress
 E , t and b as before

Attempts have been made to extend the semi empirical approach of the "effective width" method to plates supported along one edge only. Winter (34) gives the effective width in such a case as

$$b_e = 0.8 t \sqrt{\frac{E}{p_r}} \left(1 - 0.202 \left(\frac{t}{b} \right) \sqrt{\frac{E}{p_r}} \right)$$

valid to about

$$\frac{t}{b} \sqrt{\frac{E}{p_r}} = 1.75$$

He suggests the use of the following semi empirical buckling stress form for b/t ratios ranging from 12 to 30

$$p_c = p_r - \frac{p_r - 15,050}{18} \left(\frac{b}{t} - 12 \right)$$

where

p_c = critical stress, p_r as before.

For b/t ratios above 30 he proposes to use the elastic plate buckling formula as given by equation 18, with $K_2 = 0.41$.

(c) Optimum Conditions - Equal Overall and Component Strength.

From the point of view of structural efficiency a section is said to possess maximum strength if it is designed for the maximum load to weight ratio. That such maximum strength corresponds to equal overall and component strength in the case of thin walled columns can be shown by the following simple qualitative reasoning.

Failure in a simple structural section - such as a channel - may take place in a variety of ways. The column may fail by integral action as a whole or it may fail due to failure of the flange or of the web.

Considering for example the case when the strength* of the weaker of the plate components - the flange - and the strength* of the column as a whole are the criteria of the failure, the behaviour over the whole range of the L/r and b/t ratios is shown by Figs. 27 and 28 for any selected thickness t . These are obtained by superposing Figs. 23 and 24 the basis of plotting being the L/r and b/t ratios in turn.

Considering Fig. 27 if the slenderness ratio lies between 0 and A the channel will fail due to failure of the flange as a plate, at a stress less than that represented by AB. If the slenderness ratio lies between A and C the channel will fail as a column, again at a stress less than that represented by AB. Consequently, only if the slenderness ratio is at A, that is flange and column failure occur simultaneously, will the maximum possible stress AB be reached.

The same reasoning applies to Fig. 28 also, the only difference being that OA is now the range of the column failure, AC being the range of the plate failure.

*flexural.

The position of the ordinate AB is defined by the equality of the integral column strength and the plate component strength. Using the forms relevant to flexural instability, quoted in subsections (a) and (b), give

$$K_1 \frac{E}{(L/r)^2} = K_2 \frac{E}{(1-\sigma^2)} \left(\frac{t}{b}\right)^2$$

$$\text{or } \frac{b}{t} = \left\{ \sqrt{\frac{K_2}{K_1(1-\sigma^2)}} \right\} \frac{L}{r} \dots\dots\dots (19)$$

This yields a linear relationship between the slenderness ratio and the relevant plate dimension ratio for equal overall and component strength.

Relations of this type (not necessarily linear) can be obtained by equating the strengths corresponding to all the possible modes of failure. Such relations combined with a dimensional condition for minimum weight allows the development of design criteria to give structures of Maximum Strength and of Minimum Weight.

Cox and Smith (26) show that the minimum weight corresponding to maximum possible strength under a given set of conditions depends (1) on the characteristics of the materials of construction; (11) on the "structure loading coefficient" P/ρ^2 where P is the typical load and ℓ the typical linear dimension and (111) on the factors of safety provided against failure in the several possible modes of failure. With reference to struts it is shown that the weight per unit length is a decreasing function of the structure loading coefficient and in general it is proportional to

$$\rho E^{-m} \left(\frac{P}{\rho^2} \right)^{m-1}$$

where ρ = Density of Material
 E = Young's Modulus
 m = Numerical coefficient.
 P/ρ^2 = Structure loading coefficient.

The forms giving the critical stress quoted in this brief summary are based - with the exception of Winter's semi empirical form-on the assumption of elastic behaviour and are valid therefore only within certain limits of the characteristic dimension ratios L/r and b/t . The introduction of the effect of material failure, through the inclusion of the yield stress in the relevant formulae, may be effected by using ^{the} Perry-Robertson column form. As indicated in the Latticed Column part of the thesis, the Perry-Robertson formula is of general validity provided that ^{the} "Ideal column" critical stress p_e corresponds to the mode of failure of the structural element considered.

36.

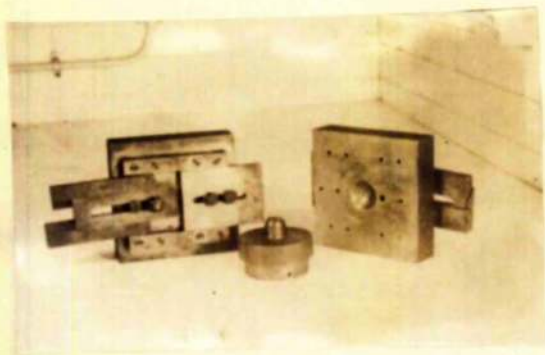
SECTION II.

EXPERIMENTAL WORK AND ANALYSIS

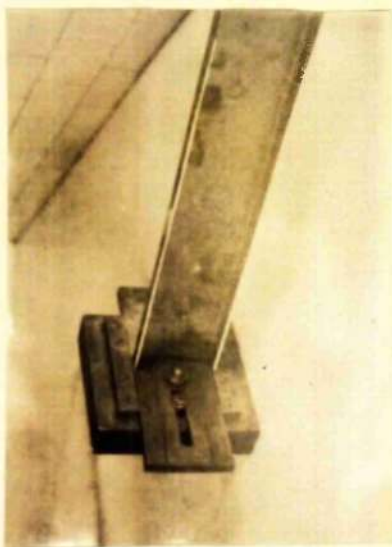
OF RESULTS.

1. MODEL SCALE INVESTIGATION.

	<u>Page.</u>
(a) <u>Experimental Appliances.</u>	<u>57</u>
Description of Specimens and Range.	
Apparatus.	
Method of Testing.	
(b) <u>Experimental Results.</u>	<u>57</u>
Typical Modes of Failure.	
Table of Typical Results.	
Graph of Experimental Failure Stress Against the Slenderness Ratio L/r .	
Graph of Experimental Failure Stress Against the Plate ratio b/t .	
(c) <u>Analysis and Discussion of Results.</u>	<u>59</u>
Variation of the Experimental Failure Stress with L/r and b/t .	<u>59</u>
Relative Scatter of Column v. plate Failure Results.	
The "Optimum" Range - Simultaneous Column and Plate Component Collapse.	<u>60</u>
Logarithmic Interpolation of "Peak" Values.	<u>60</u>
Comparison of the Experimental and Theoretical Straight Line Variation of b/t with L/r for Optimum Conditions.	<u>62</u>
Flange Plate Edge Support under Optimum Conditions.	
Column Behaviour in the Plate Component Failure Range.	<u>63</u>
Comparison of the Experimental Average Stress Curve with the Theoretical Plate Stress Curves.	
The variation of the Edge Fixity Coefficient K_2 .	<u>63</u>
The Value of the Perry Robertson Imperfection Coefficient n for Plate Failure.	<u>64</u>
Comparison of the Perry-Robertson Stress form with the Lower Scatter Boundary of the Experimental Failure Stress Curve.	<u>64</u>
(d) <u>Summary.</u>	<u>65</u>
Maximum Strength and Simultaneous Integral Column and Plate Component Collapse.	
Plate Component Edge Support Corresponding to Simultaneous Collapse.	
Plate Component Edge Fixity Variation with the b/t Ratio.	
The Application of the Perry-Robertson Formula to Plate Component Failure.	



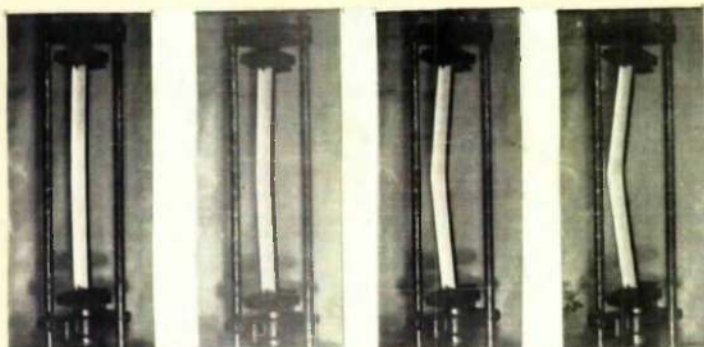
(a)



(b)

Fig. 29.

(a)



(b)

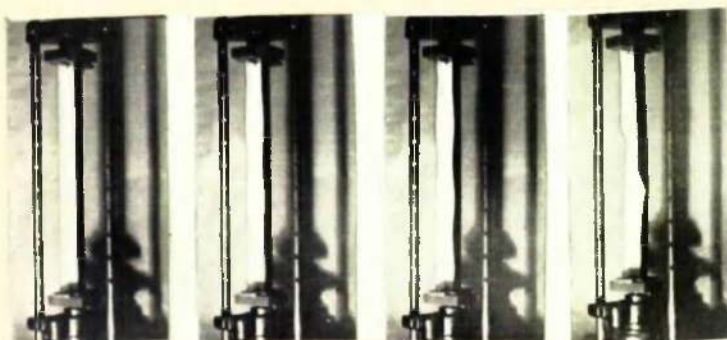


Fig. 30.

37

(a) Experimental Appliances.

The results presented were obtained from tests carried out on pressed plain channel sections, having a constant outside web dimension of 3". Sets of 8 to 10 specimens for each thickness, with nominal flange dimensions varying from $\frac{1}{4}$ in. to $2\frac{1}{2}$ ins. were tested to destruction. The nominal thicknesses investigated were 12, 14, 16, 17, 18, 19 and 20 gauge.

The specimens were compressed in a 10 ton Avery Universal Testing Machine with hemispherical end platens transmitting the load to the specimen through bearing plates with hemispherical cups, producing hinged end conditions, - Fig. 29a. The end bearing plates of the specimens were adjustable - Fig. 29b. to ensure that the load was applied at the centre of gravity of the section. Positioning could be taken as accurate to within $\frac{1}{100}$ in. of an inch.

The load was applied at a uniform rate of approximately 0.2 Ton per minute. Failure occurred either by buckling of the column as a whole Fig. 30a. or by crinkling of the flange plates - Fig. 30b. The buckling load was taken as the maximum load recorded on the automatic load recording dial of the machine. The critical stress was then obtained by dividing this load by the sectional area. No readings other than the maximum load were taken.

(b) Experimental Results.

The results collected were the mode of failure and the value of the buckling load of some 70 test specimens.

Two typical modes of failure were encountered. The first (Fig. 30a) - termed "column" failure - took the form of a sudden bowing of the specimen with practically instantaneous collapse. The second type (Fig. 30b) - termed flange or "plate component" failure was characterised by rapid development of crinkling or waving in the flange, the web remaining perfectly plane and straight. The waving was demonstrated to be elastic, as on removal of the load it disappeared, the flange resuming its previous straightness. Collapse occurred due to sudden excessive development of the waving at one peak point in each flange symmetrically opposite each other, all other waves completely disappearing. In the majority of cases the wave peak in one of the flanges suddenly gave way with a consequent twist of the whole column. The final appearance of the failed specimen was as shown in the last photograph of Fig. 30b.

The load corresponding to the full development of the elastic waving and the collapse load differed at the maximum by about 5% only. In view of this and also because of its more explicit nature the collapse load was recorded as the experimental failure load.

Table 3 shows a typical set of experimental results (overleaf).

The experimental failure stress values are plotted in Figs. 31 and 32, against the slenderness ratio L/r and the plate dimension ratio b/t in turn. These figures are incorporated in the Discussion section which follows, for convenient reference.

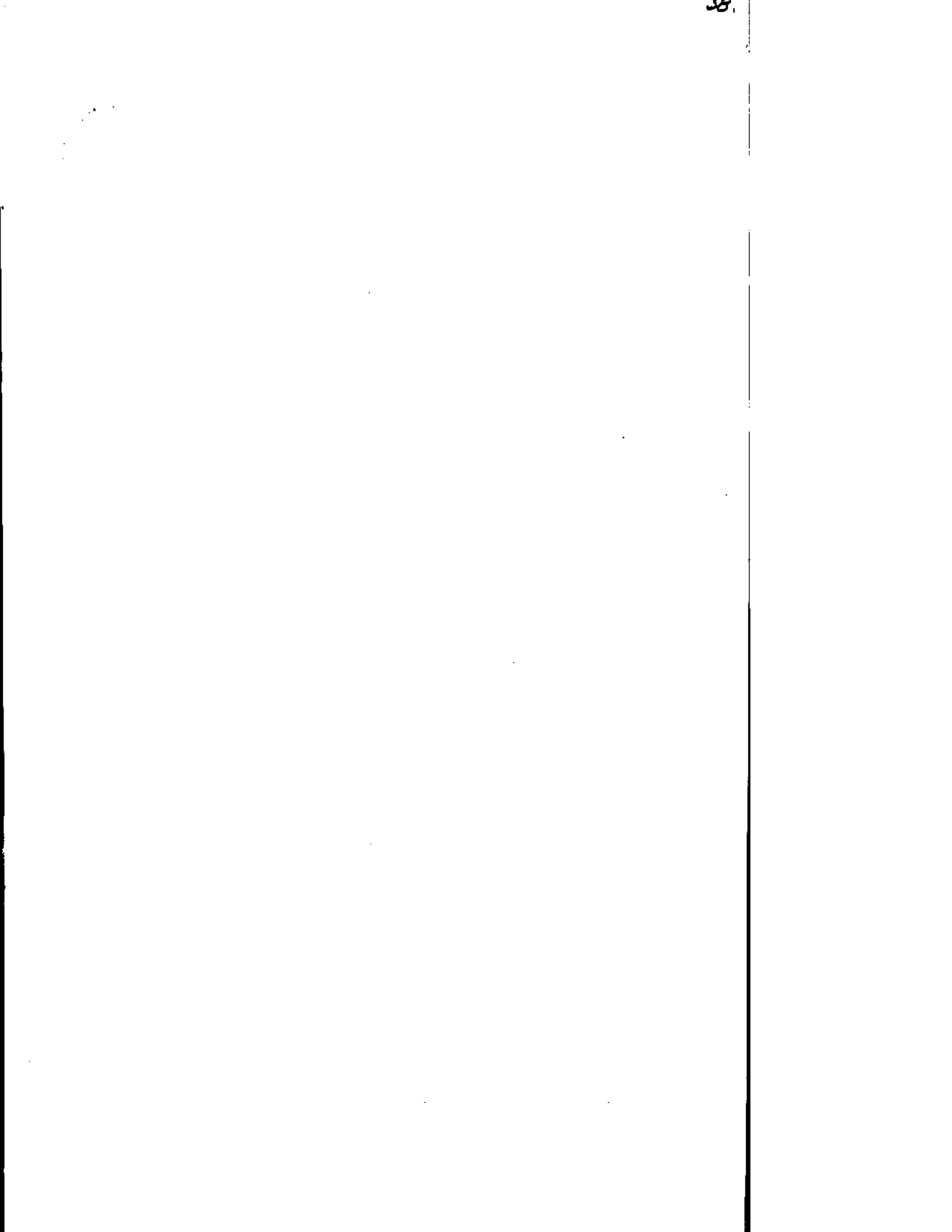


TABLE 3. TYPICAL EXPERIMENTAL RESULTS 18G.

Column Length $L = 36$ ins.; Width of Web = 3 ins.; Thickness 18G.

Column Ends hinged.

Flange Width b ins.	Sectional Area A in ²	Minimum r ins.	Stentness Ratio L/r	Plate Ratio b/t	Failure Load Tons.	Failure Stress Ton/in ²	Mode of Failure
0.40	0.1614	0.0897	402	8.3	0.20	1.25	Column
0.64	0.1865	0.1717	210	13.3	1.02	5.47	Column
0.78	0.1970	0.2208	163	16.3	1.48	7.52	Column
0.97	0.2139	0.2892	124	20.2	2.66	12.44	Column and Plate
1.19	0.2615	0.3658	99	24.8	3.14	12.00	Column and Plate
1.64	0.3035	0.5264	68	33.2	2.78	9.16	Plate
2.05	0.3508	0.6692	54	42.8	2.60	7.41	Plate
2.53	0.3800	0.8340	43	52.6	2.10	5.53	Plate

(c) Analysis and Discussion of Results.

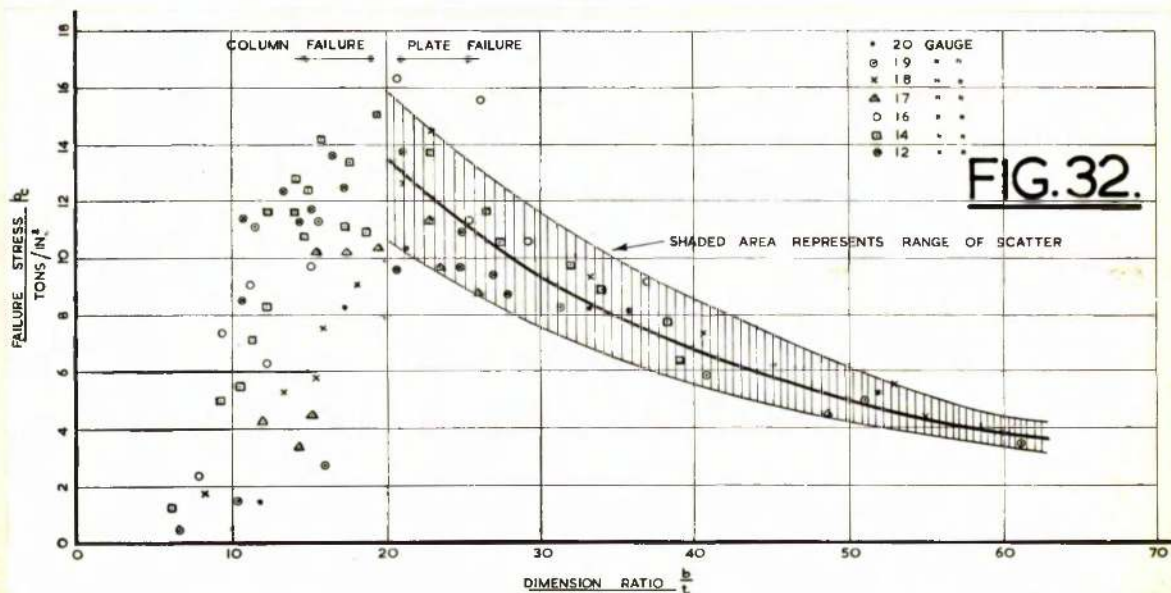
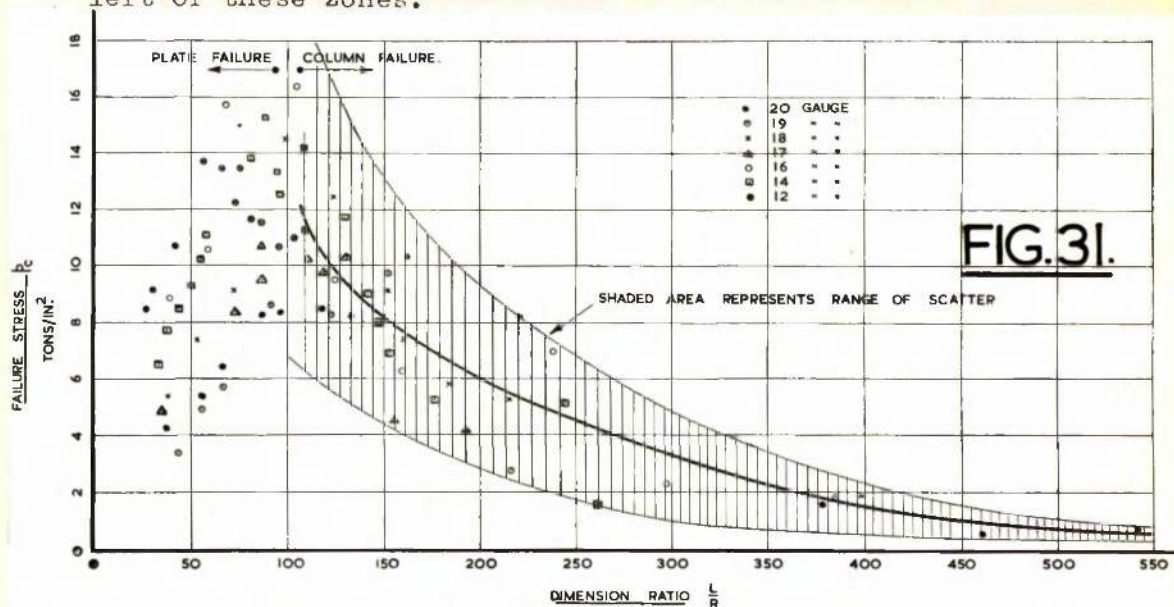
The following material characteristics are used in the calculations - based on the results of the tensile tests recorded in Appendix No. 3.

$$\begin{aligned}\text{Young's Modulus } E &= 11000 \text{ tons / in}^2 \\ \text{Yield Stress } p_y &= 14 \text{ tons / in}^2\end{aligned}$$

In computing the theoretical elastic buckling stress of the plate components the edges perpendicular to the line of compression were assumed to be simply supported in every case.

Variation of the Experimental Failure Stress with the Characteristic Dimension Ratios - Figs. 31 and 32. - The general distribution of the points and the type of curves obtained show good correspondence with the theoretically predicted form.

When considering scatter it should be noted that (i) points in the shaded zones of the Figures should fall on a single curve irrespective of the plate thickness of the specimens tested but (ii) points to the left of the shaded zones map out a field consisting of a series of curves one for each plate thickness. Thus consideration of scatter is relevant to these shaded zones but is meaningless when applied to points to the left of these zones.



The scatter shown by the results corresponding to column failure - Fig. 31 is considerably greater, than that indicated by the results when the flange failed as a plate component - Fig. 32. As all the test specimens were manufactured as a batch, were tested with the same equipment and by the same operator, it is reasonable to assume that the type and order of irregularities were similar for all the specimens. It would therefore appear that the column type failure is affected to a relatively greater extent by the presence of initial irregularities than the plate component type of failure.

Characteristics of the "Optimum" range - simultaneous column and plate component collapse. Figs. 33 and 34. - As indicated in the theory (Figs. 27 and 28 Page 54.) the peak value AB of the combined column and plate buckling curve is obtained by equating the column and flange plate strength, namely

$$p_c = K_1 \frac{E}{(\frac{L}{r})^2} = K_2 \frac{E}{1-\sigma^2} (\frac{t}{b})^2 \dots\dots\dots (20)$$

The position of this "Optimum" peak is extremely difficult to obtain by direct experimentation, and would have involved a practically impossible trial and error method accompanied by considerable wastage of material. This experimental difficulty was overcome by the development of a logarithmic interpolation method, which involving straight line plotting only, gives the position of this peak value with good accuracy, provided a sufficient number of ^{equations} ~~equations~~ ^{20.} these ^{available to each} side of the peak value.

Taking logarithms ⁱⁿ ~~equations~~ ^{20.} these reduce to

$$\log p_c = -2 \log(\frac{L}{r}) + \log K_1 E$$

for the column strength and to

$$\log p_c = -2 \log(\frac{b}{t}) + \log K_2 \frac{E}{1-\sigma^2}$$

for the plate strength.

In both of these $\log p_c$ varies linearly with the logarithm of the dimension ratios L/r and b/t respectively.

Further, the *slenderness* ratio in the case of channel elements of flange width b , web width w , and length L can be expressed as

$$\frac{L}{r} = \frac{1}{(\frac{b}{t})^{\frac{1}{3}}} \cdot t^{\frac{1}{3}} b^{\frac{1}{3}} \left\{ \frac{\frac{w}{b} + 2}{(2\frac{w}{b} + 1)^{\frac{1}{2}}} \right\} \sqrt{3} L$$

provided the wall thickness is small in comparison with the cross section dimensions.

The specimens of any one set were of constant length web width and thickness. The term

$$b^{\frac{1}{3}} \frac{\frac{w}{b} + 2}{(2\frac{w}{b} + 1)^{\frac{1}{2}}}$$

is for all practical purposes a constant for the range of values of the flange width b encountered in the experiments, as its total variation does not exceed $\pm 5\%$ of its mean value.

Consequently taking logarithms gives linear relationships between L/r and b/t for any given set of the one thickness, of the type

$$\log\left(\frac{L}{r}\right) = -\frac{6}{5} \log\left(\frac{b}{t}\right) + \log(\text{Constant})$$

The three linear logarithmic variations involving the critical stress p_c , the slenderness ratio L/r and the flange plate ratio b/t given by these equations can be combined in the manner shown in Fig. 33. This gives the results of such a logarithmic plot for the 18 gauge thick set of specimens.

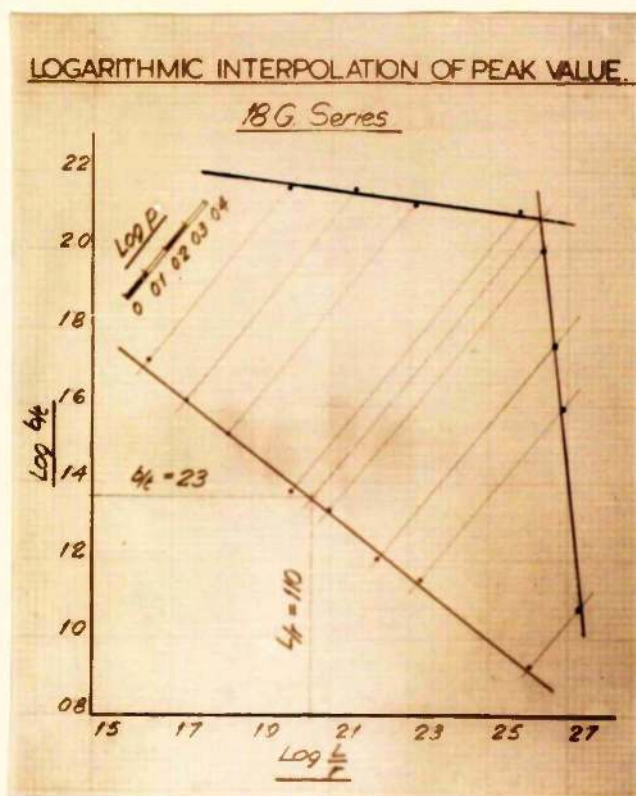


Fig. 33.

The optimum point - corresponding to equal column and plate strength - is given by the intersections of the straight lines defined by the plate failure points (to the left of the peak) and the column failure points (to the right of the peak). Once this optimum point is located the corresponding values of the slenderness ratio L/r and the flange plate ratio b/t can either be read off directly (if the diagram is accurately drawn to a reasonably large scale) or calculated from the geometry of the figure.

One particular value of L/r and b/t will be obtained in this manner for each set of specimens of the one thickness. These correspond to the position of the single peak point B of the curve characterising combined behaviour (Figs. 27 and 28).

Plotting *the* L/r and b/t ratios corresponding to simultaneous column and plate component collapse the variation shown in Fig. 34. is obtained.

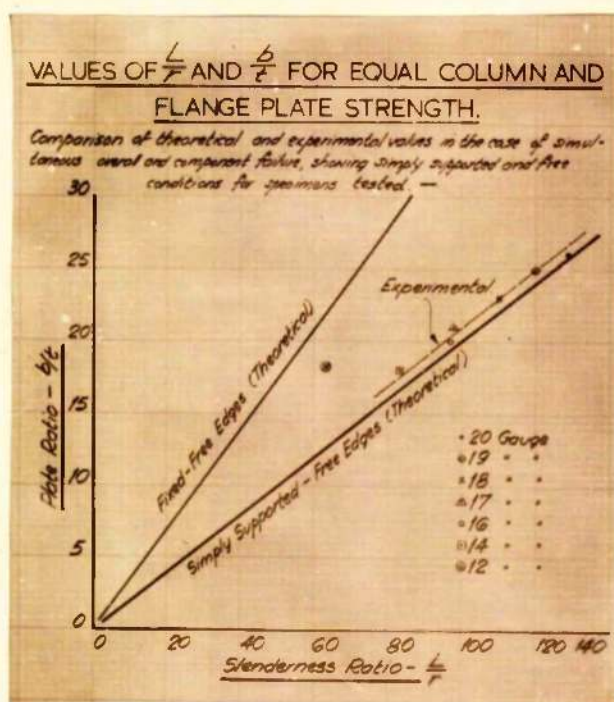


Fig. 34.

Two features are of significance:

(i) The points with the exception of the one corresponding to the 12 gauge thickness define a straight line, thus showing good agreement with the theoretically predicted linear relationship of equation 19, p. 55.

The divergence of the point representing the 12 gauge thickness is due to the fact that, because of its comparatively heavy section all the specimens of this set were grouped rather close to the peak value. Thus the determination of the peak point by the interpolation method described became somewhat uncertain, the "spread" of the values to either side of the peak being insufficient for accurate definition of the straight line portions.

(ii) The straight line defined by the interpolated points is parallel and lies very close to the theoretical line computed on the basis of simply supported and free edges for the flange plate.

It would appear therefore that when overall and component collapse is simultaneous the support given by the column to its plate component is a minimum consistent with the existing boundary conditions.

Column Behaviour in the "Plate Component" Failure Range. Figs. 35 and 36. - The curves shown in Fig. 35 compare the experimental mean curve of the plate failure range from Fig. 32 with theoretical curves computed using equation No. 18 (p. 59) on the basis of fixed - free ($K_2 = 109$) and simply supported - free ($K_2 = 0.376$) edge conditions for the flange.

It can be seen that the support given to the flange at its edge adjoining the web varies from complete fixture to simple support, as the failure stress of the plate component approaches the critical stress of the column as an integral whole.

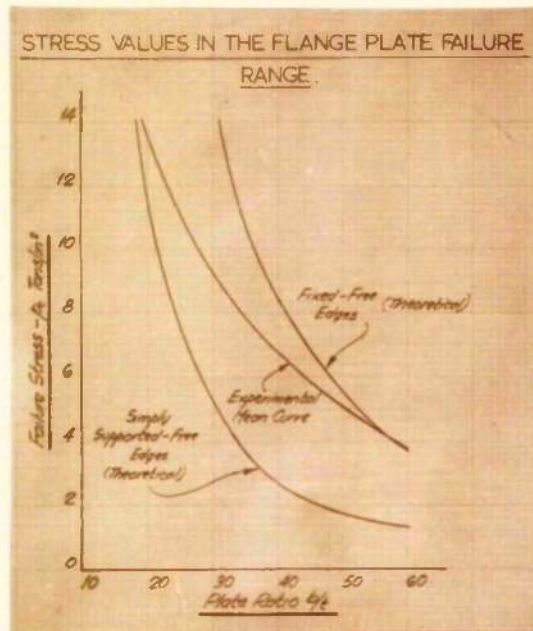


Fig. 35.

The edge fixity coefficient K_2 in the plate equation (Equation No. 18) corresponding to the experimental mean curve can be expressed as

$$K_2 = \frac{b/t}{46 + 0.15 \frac{b}{t}}$$

On substitution equation No. 18 becomes

$$p_c = \frac{\frac{b}{t}}{46 + 0.15 \frac{b}{t}} \frac{E}{1 - \sigma^2} \left(\frac{t}{b} \right)^2$$

$$\text{or } p_c = \frac{E}{(1 - \sigma^2)} \frac{t/b}{(46 + 0.15 \frac{b}{t})} \dots \dots \dots (21)$$

This expression is valid for values of the plate dimension ratio b/t lying within the limits of $b/t = 20$ and $b/t = 60$, and $\frac{L}{r} \neq 100$.

The use of an experimental average curve is justifiable when comparison with theoretical values is made. When however, it comes

to the determination of a possible design basis, the lower boundary limit of the field of scatter is the relevant basis of comparison. Using this line of reasoning, the value of the imperfection coefficient η in the Perry-Robertson (12) formula

$$p_c = \frac{p_r + (\eta + 1)p_e}{2} - \sqrt{\left(\frac{p_r + (\eta + 1)p_e}{2}\right)^2 - p_r p_e}$$

was determined to suit the lower scatter limit of Fig. 32. A suitable value was found to be

$$\eta = 0.0025 \frac{b}{t}$$

The "ideal column" stress p_e in the formula was taken as the critical stress of the flange given by equation (21), using the values of K_2 corresponding to the experimental mean curve stated above.

Fig. 36 shows the experimental average curve with its scatter boundaries; the Perry-Robertson curve derived as indicated above, and the allowable stress curve proposed by Winter (34) P. 54. This latter curve consists of two parts - (i) a straight line portion over the range from $b/t = 12$ to $b/t = 30$, the stress value varying from the yield stress of the material to a stress given by the plate strength equation (18) with a K_2 value of 0.41 and (ii) a curve portion for values of b/t above 30 representing the plate strength equation with the K_2 value of 0.41.

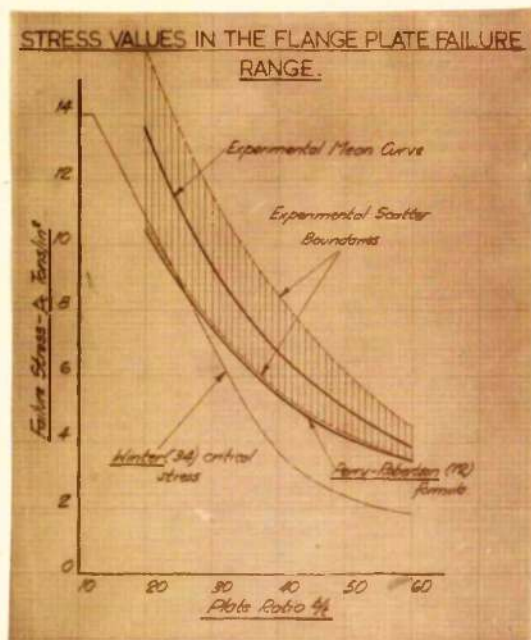


Fig. 36.

It can be seen that the agreement between the Perry-Robertson form and the lower scatter boundary is excellent, the two curves practically coinciding for the range tested. This indicates that the conception of the effect of imperfections represented by the formula is not restricted to integral column action only, but can be extended also to cover plate component collapse as the criteria of overall strength.

The critical stress variation as proposed by Winter indicates some correspondence of values - in the range of $b/t = 20$ to $b/t = 30$ - but shows deviation of form. On the whole in the region of the larger b/t ratios it appreciably underestimates the actual strength of thin compression flanges even if based on the full actual width, and not, as proposed, on a reduced effective width (See also discussion of collapse load in Appendix No. 4.)

(d) Summary.

The main findings of the Model Scale Investigation may be summarised as follows:-

(i) Thin walled struts proportioned for simultaneous column and plate component collapse possess maximum strength.

(ii) If column and plate component collapse are simultaneous the critical stress of the weakest plate component corresponds to the minimum possible edge support. For the flanges tested this was equivalent to simply supported and free edges.

(iii) The equivalent edge support obtained by the flange plate increases with the dimension ratio b/t reaching fixed free edges at a b/t ratio of about 60, *for columns with $\frac{t}{r}$ values of less than 100.*

(iv) In the transition from the equivalent simply supported to fixed edge conditions (i.e. from about $b/t = 20$ to $b/t = 60$) the critical stress corresponding to the experimental results is given by

$$p_c = \frac{E}{(1-\sigma^2)} \frac{t/b}{(46 + 0.15 \frac{b}{t})}$$

(v) The Perry-Robertson formula gives good agreement both in form and values with the lower scatter boundary of the plate failure range provided the imperfection factor $\eta = 0.0025 b/t$ and the "ideal column" critical stress p_e is taken as p_c quoted under (iv) above.

SECTION II.

EXPERIMENTAL WORK AND ANALYSIS
OF RESULTS.

2. FULL SCALE INVESTIGATION.

	<u>Page.</u>
(a) <u>Experimental Appliances.</u>	<u>67.</u>
Descriptions of Specimens and Range.	
Apparatus.	
Measuring Devices.	
Method of Testing.	
(b) <u>Experimental Results.</u>	<u>67</u>
Mode of Distortion and Failure.	<u>68.</u>
Deflected Form of the Flanges.	
Variation of the Flange Deflections with the Axial Load.	
Longitudinal and Transverse Stress Survey of Flanges (In Appendix No. 4).	<u>89.</u>
(c) <u>Analysis and Discussion of Results.</u>	<u>68.</u>
Deflected Form of the Flanges.	<u>69.</u>
Development of Form.	
Number of Half Waves.	
Magnitude of Deflections.	
Flange Deflection Variation with Axial Load at Particular Points.	<u>70.</u>
"Stationary" Tendency.	
Reversal of Deflection Direction.	
"Running Away" Tendency.	
Derivation of the Elastic Buckling Load from the Flange Deflections.	<u>70.</u>
The Southwell - Lundquist Straight Line Plot.	
Elastic Buckling Stress. Comparison: Full Scale v. Model Scale.	
(d) <u>Summary.</u>	<u>73.</u>
The Elastic Buckling Load to Collapse Load Margin.	
Application of the Southwell-Lundquist Plot to Plate Buckling Analysis.	
Comparison of Full Scale and Small Scale Behaviour.	
The Absence of Scale Effect in the Elastic Range.	

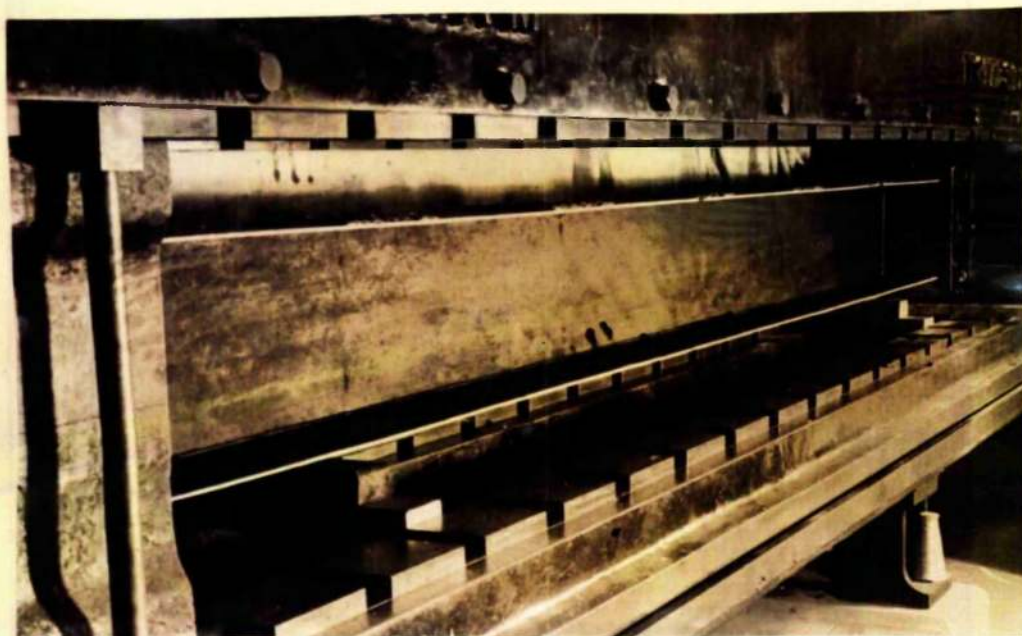


Fig. 37.

7 inch Flange Specimen in 100 tons
Testing Machine.

(a) Experimental Appliances.

The investigation described in this section was carried out on two 12 ft. long column specimens, built up of 7/32 inch thick plates welded to form channel sections. The web dimension was kept constant at 12 inches; the flange sizes at 7 inches and 12 inches respectively were selected to exclude integral column failure and to ensure collapse of the flange plate as the weakest component.

The column ends consisted of 1" thick bearing plates, welded and accurately squared off to ensure parallelism. The columns were tested in a horizontal, hydraulically operated Avery testing machine of 100 tons capacity. The features of the machine incorporate end platens with ball and socket type bearings. These platens may be locked in any position or can be left free to pivot, thus simulating hinged end conditions. X

In view of the fact that the columns were tested horizontally they were placed in the machine such that bending due to dead weight took place about the axis of maximum moment of inertia. While, these bending stresses are not significant - their uncompensated magnitude would not have amounted to more than about 0.07 tons/in² at a maximum or about 1 1/2 % of the elastic buckling stress - the line of the axial loading was offset from the centroid of the specimens, so as to reduce their value at the centre by 50%. This equivalent eccentricity was computed as for a short column since the overall slenderness ratios in the plane of bending did not exceed 30. The maximum offset values required were in the region of 0.03 ins.

Centering of the columns was effected by aligning lines scribed on the machine platens and on end plates welded to the specimens. A Chesterman height gauge reading to 1/1000th of an inch was used for setting out these lines. Centering can be taken as accurate to 1/100 th of an inch. To ensure uniform bearing over the platen surface a plaster of Paris pack was introduced between the platens and the column end plates. The platens were set to give hinged end conditions. Fig. 37 shows the 7 inch flange specimen in position. K

Flange deflections were measured at points spaced at one foot intervals along the length of the flanges. Measurements taken relative to the bed plate of the machine indicated that the flanges distorted in a completely symmetrical manner. Once this was established relative deflections of the flanges were measured only, using an internal micrometer reading to 1/1000th of an inch.

Longitudinal and transverse strains were measured at various points in the flanges, using electrical resistance strain gauges. Layout of the gauges and their general arrangement is given in Appendix No. 4.

Readings of both the flange deflections and the flange strains were taken at every 2 tons load increment.

(b) Experimental Results.

The results recorded were (i) The mode of distortion and failure (ii) The deflected form of the flanges and (iii) The longitudinal and transverse strain variations in the flanges.

Initial Load: 1^T



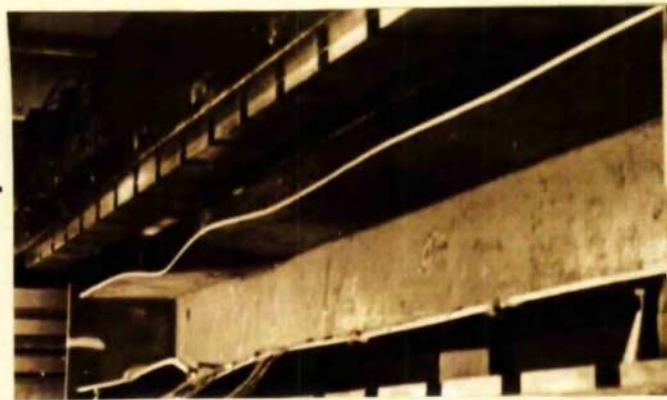
38^T



Fig. 38. 48^T



52^T



Failure Load:
52.9^T



The modes of failure corresponded to the type already described in the model scale investigation. The waving of the flanges developed in a gradual fashion due in all probability to the initial irregularities of the flange form.

One definite difference between the 3 ft. and the 12 ft. column tests was the increase in the load margin between the elastic buckling load and the collapse load. In the case of the 3 ft. specimens this margin did not exceed about 5% (at its maximum) of the elastic buckling load, while in the case of the 12 ft. columns of the same geometric proportions the collapse load was about 30% greater (at its maximum) than the elastic buckling load.

The development of the flange waving and the mode of failure is shown in the series of photographs of Fig. 38, for the 12 inch flange column. The excessive development of one set of peaks just prior to collapse together with the consequent "ironing out" of all the other elastic waves can be clearly seen.

The following table gives the relevant dimensions and collapse loads of the columns tested.

Width of web W ins	Width of Flange b ins	Thick- ness t ins	Sec ² Area A in ²	In plane of bending $\frac{1}{4}r$	Perpend- to plane of bending $\frac{1}{4}r$	b/t	Collapse Load Tons
1202	6.92	0.2137	5.52	29	64	32.4	56.0
1201	12.02	0.2205	7.95	26.8	35.7	54.6	52.9

The development of the deflected form of the flanges as the axial load increased is shown in Figs. 39 and 40. The variation of the flange deflection at particular points is shown in Fig. 41 and Appendix No. 6. All of these figures are incorporated in the subsection dealing with the analysis of the results for convenient reference.

Typical results of the stress investigation are given in Appendix No. 4 as their detail analysis is outwith the scope of the Thesis.

(c) Analysis and Discussion of Results.

The following values of the material characteristics were used in all the calculations, based on the tensile test results presented in Appendix No. 3.

$$\begin{aligned}\text{Young's Modulus } E &= 12,500 \text{ tons / in}^2 \\ \text{Yield Stress } p_y &= 18.5 \text{ tons / in}^2.\end{aligned}$$

Deflected Form of the Flanges under Increasing Loads - Figs. 39 and 40. - The figures show the deflected form of the 12 inch and 7 inch flanges respectively. As indicated previously the waving was completely symmetrical and only relative deflections of the flanges were measured. The method of representation shows (unavoidably to a very highly distorted scale) half of such relative deflections as contributed by each flange.

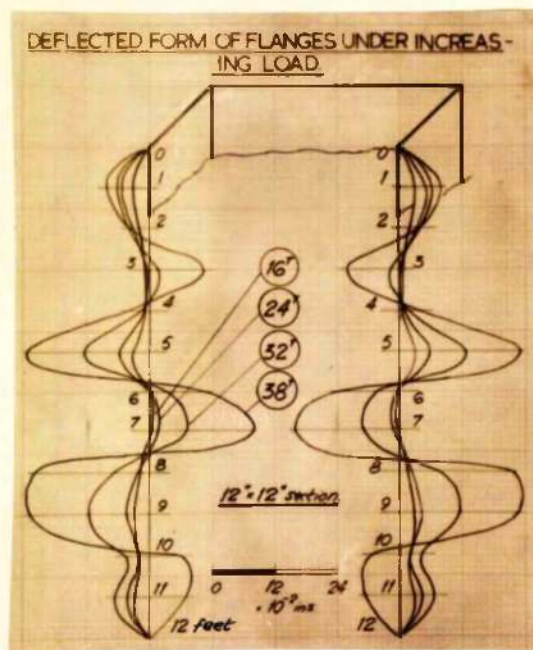


Fig. 39.

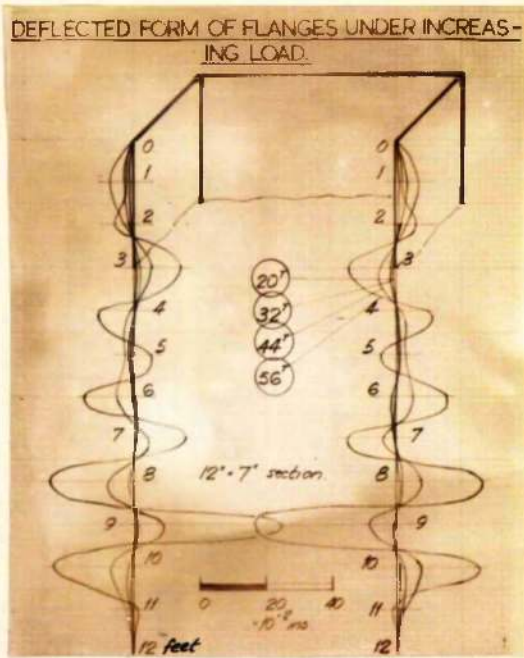


Fig. 40.

The development of the waving as the load increases, is gradual with stationary node points. The number of half waves in the case of the 12 inch flange is seven up to 32 tons, reducing to six as the deflection at point 11 reverses in direction with the increase in load. This value corresponds to the number of half waves given by the elastic theory - Fig. 25 - for a plate length to plate width ratio of 12 in the case of fixed free edge conditions parallel to the line of compression. The number of half waves developed by the 7 inch flange is nine - less than the theoretical value of 12, given by fixed free edge conditions for a plate length to width ratio of about 21. While this could be taken to indicate that the edge support along the web is no longer equivalent to fully fixed conditions, such evidence - in view of the initial irregularities present in the flanges - must be treated as inconclusive.

In the case of the 7 inch flange specimen, deflection readings were taken practically up to collapse. The start of the "excessive" development of a pair of wave peaks - previously referred to - can clearly be seen at point 9. The "ironing out" action shown in the photographs of Fig. 38 takes place during the actual process of collapse and is far too rapid to record by means other than photographic.

The actual values of the flange deflections were appreciable and reached values as much as half inch to either side.

Deflected Form of the Flanges under Increasing Loads - Figs. 39 and 40. - The figures show the deflected form of the 12 inch and 7 inch flanges respectively. As indicated previously the waving was completely symmetrical and only relative deflections of the flanges were measured. The method of representation shows (unavoidably to a very highly distorted scale) half of such relative deflections as contributed by each flange.

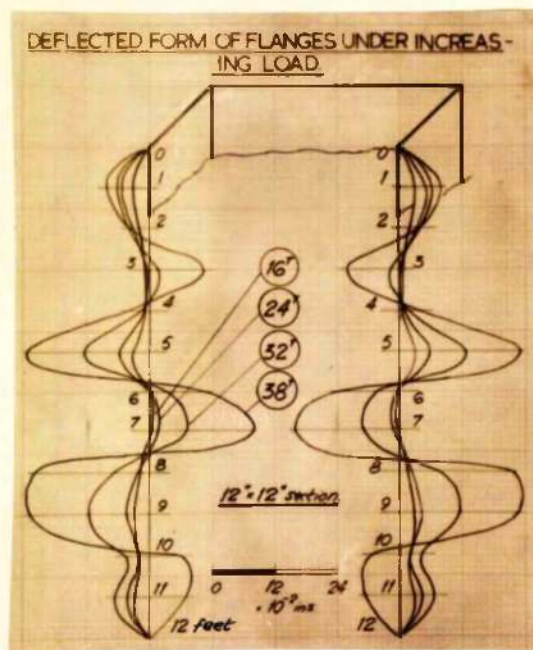


Fig. 39.

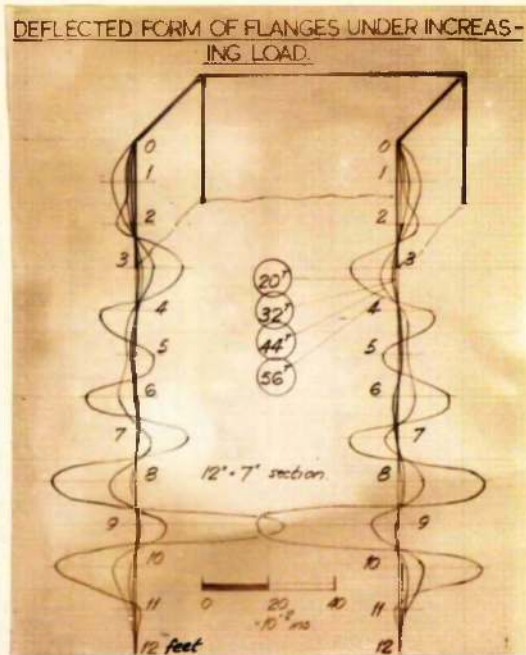


Fig. 40.

The development of the waving as the load increases, is gradual with stationary node points. The number of half waves in the case of the 12 inch flange is seven up to 32 tons, reducing to six as the deflection at point 11 reverses in direction with the increase in load. This value corresponds to the number of half waves given by the elastic theory - Fig. 25 - for a plate length to plate width ratio of 12 in the case of fixed free edge conditions parallel to the line of compression. The number of half waves developed by the 7 inch flange is nine - less than the theoretical value of 12, given by fixed free edge conditions for a plate length to width ratio of about 21. While this could be taken to indicate that the edge support along the web is no longer equivalent to fully fixed conditions, such evidence - in view of the initial irregularities present in the flanges - must be treated as inconclusive.

In the case of the 7 inch flange specimen, deflection readings were taken practically up to collapse. The start of the "excessive" development of a pair of wave peaks - previously referred to - can clearly be seen at point 9. The "ironing out" action shown in the photographs of Fig. 38 takes place during the actual process of collapse and is far too rapid to record by means other than photographic.

The actual values of the flange deflections were appreciable and reached values as much as half inch to either side.

Variation of the Flange Deflection with Load at Particular Points. - Fig. 41. - The deflection variation with axial load at peak points of the wave form for the 12 inch flange is shown in Fig. 41.

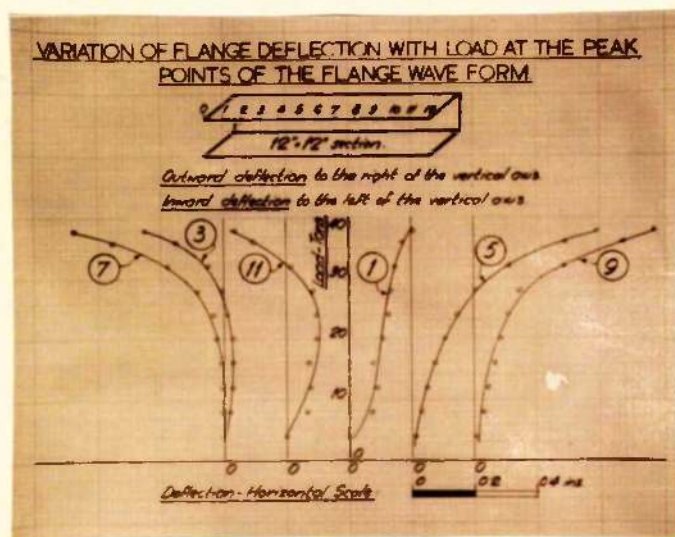


Fig. 41.

Three distinct types of curves are indicated:- (i) The type represented by point 1 indicating a stationary tendency after an initial deflection has taken place; (ii) The type represented by point 11 where reversal of direction of the flange deflection is indicated. The point shows outward deflections up to 32 tons and inward deflections past this load; (iii) The type represented by point 9 where the deflections develop at a gradually increasing rate, indicating a "running away" tendency as the critical load is approached.

As the characteristics exhibited by all other points in both of the test columns correspond to one or other of the types quoted only the typical selection shown has been incorporated in the text, the rest are presented in Appendix No. 6.

Derivation of the Elastic Buckling Load for the Flange Plates Using the Southwell - Lundquist Straight Line Plot.- Figs. 42 and 43. - In the analysis of distortion data obtained from stability experiments the method originally proposed by Southwell (15) is widely used. Southwell has shown that the variation of the central deflection δ of a slender column - additional to any existing initial irregularity - with the axial column load P is given by a rectangular hyperbola. Thus plotting δ against δ/P gives a straight line whose slope is the value of the first critical load for the column. Timoshenko (19) proved that this relation holds even when there is some eccentricity in applying the load.

The approach has been extended by Lundquist (35) who proved that the same method of plotting applies to any increase in deflection $\delta - \delta_1$ and its corresponding increase in load $P - P_1$ where δ_1 and P_1 are any initial readings of deflection and corresponding load respectively.

The method was originally proposed in connection with single column units. In the analysis of the results it is applied to the peak deflections of the flange wave form, as each half wave is analogous to such a single column unit.

Figs. 42 and 43 show $\delta - \delta_1$ plotted against $P - P_1$ for the specimens tested. The initial readings were taken at $P_1 = 1$ ton and $P_1 = 1\frac{1}{2}$ tons for the 12 inch and 7 inch flanges respectively.

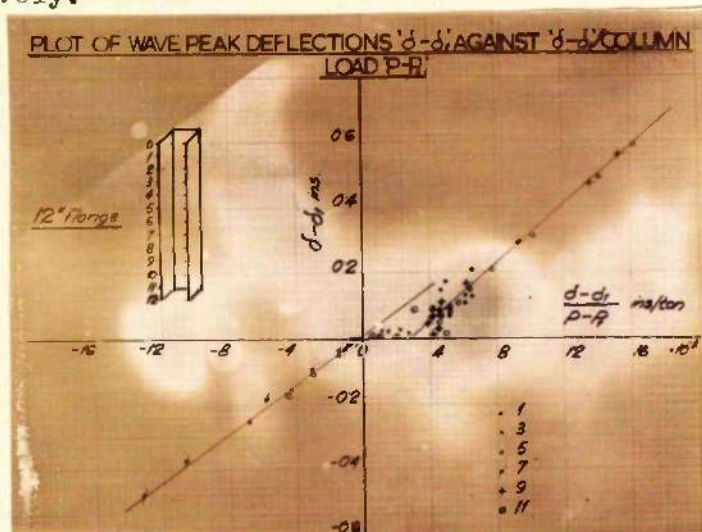


Fig. 42.

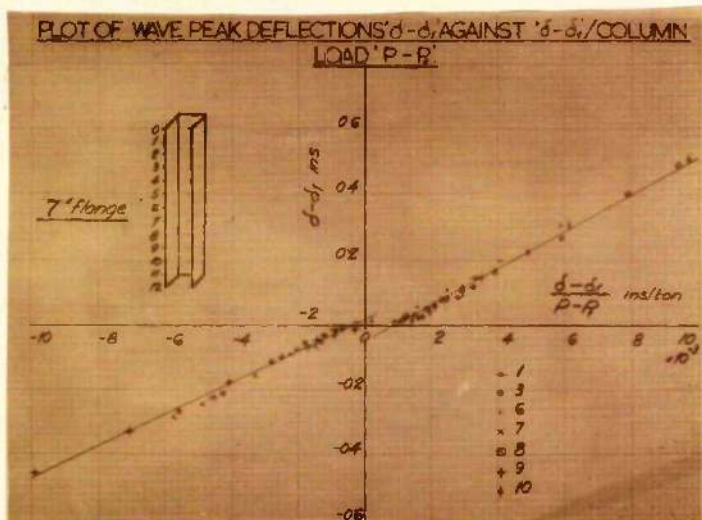


Fig. 43.

As can be seen, in both cases, two straight lines of slightly different slopes are obtained, one for the outward and one for inward peak deflections. That not a single straight line is obtained may be explained by the fact that the intercept on the vertical axis is influenced by the initial irregularity existing at the particular point considered. It is of some interest to note that all the outward deflections and all the inward deflections fall on the same straight line. This indicates that the amplitude of the first harmonic in the Fourier series expressing the unknown initial irregularity is sensibly the same for all points deflecting in the same direction.

The elastic buckling loads and the corresponding stresses as given by the mean slope of the two straight lines in each case are as follows:

Nominal Flange Width b	Plate ratio b/t	Sectional Area A	Elastic Buckling Load Tons.	Elastic Buckling Stress $-T/in^2$
12 ins.	54.6	7.95 in^2	41.0	5.16
7 ins.	32.4	5.52 in^2	53.9	9.75

To be able to compare these values with the experimental buckling stress variation of the 3 ft. specimens, allowance must be made for the difference in Young's Moduli 12,500 tons / in^2 for the full scale specimens and 11,000 tons / in^2 for the model scale. In the elastic range (assuming Poisson's ratio to be the same) the critical stress is directly proportional to E , consequently comparable values of the buckling stress can be obtained by reducing the full scale results in the ratio of 11 to 12.5. The comparable stress values then become 4.56 tons / in^2 and 8.59 tons / in^2 for the 12 inch and 7 inch flanges respectively. The corresponding b/t ratios are 54.6 and 32.4 respectively.

Fig. 44 shows the above values plotted on a copy of the 3 ft. specimen results given in Fig. 36.

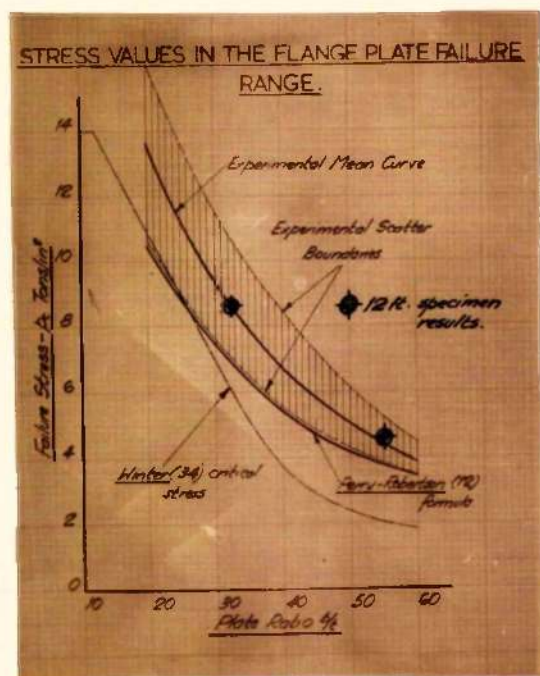


Fig. 44.

It is seen that good agreement is obtained, the same equivalent edge fixity variation being manifested as was encountered in the case of the model scale results. There is a complete absence of scale effect in the elastic range and

consequently all the conclusions of the model scale experiments are applicable to the full scale range also.

(d) Summary.

The following points have been brought out by this particular experimental range:-

(i) The load margin between the elastic buckling load and the collapse load increases for flanges of the same geometric proportions as the thickness increases.

(ii) The Southwell-Lundquist method of evaluating the elastic buckling load - based on hyperbolic variation of transverse deflection with axial column load - gives good results when applied to the wave peaks of the deflected form of the flange plates.

(iii) The full scale behaviour fully substantiates the observed model scale behaviour.

(iv) There is no difference between model and full scale behaviour in the elastic range.

BIBLIOGRAPHY.

Bibliography.

References to the Bibliography in the text of the thesis are given thus:-

Author's Name (No. in Bibliography)

1. Ayrton W.E. and Perry J. - "On struts", The Engineer (London) Dec. 1886.
2. British Standards Institution - Specifications No.153(1937) and 449 (1937).
3. Christensen N. - "Detail Design of Large Bridge Columns" Engineering News Record Vol. 95, No.14, Oct. 1925.
4. Dinnik A.N. - "Design of Columns of Varying Cross Section" Trans. A.S.M.E. Vol. 54, 1932.
5. Fidler C. - "The Practical Strength of Columns" Proc. A.S.C.E. 1900 also "Engineering" (London) June 1902.
6. Holt M. - "Tests on Built Up Columns of Structural Aluminium Alloys" Proc. A.S.C.E. Nov. 1938 also "Column Strength of Various Aluminium Alloys" Technical Paper No.1, Aluminium Research Laboratories, Aluminium Co. America 1938.
7. Howard J.E. and Buchanan C.P. - "Some Tests of Large Steel Columns" Trans. A.S.C.E. Vol. 73, 1911.
8. Hutt H.V. - "The Theoretical Principles of Strut Design" Engineering (London) Aug. 1912.
9. Karman T. and Biot M.A. - "Mathematical Methods in Engineering" McGraw-Hill 1940.
10. Osgood N. - "Column Curves and Stress Strain Diagrams" U.S. Bureau of Standards Research Paper No. 492.
11. Pippard A.J.S. - "The Critical Load of a Battened Column" the Philosophical Magazine. Vol.39. January, 1948.
12. Robertson A. - "The Strength of Struts" Inst. of C.E. Selected Paper No.28.
13. Salmon E.H. - "Columns" - Oxford Technical Publications 1921.
14. Shimkin B.M. - "Laboratory Tests on Arc Welded Latticed Steel Columns" Engineering News Record Vol. 120, No.22, May 1929.
15. Southwell R.V. - "On the Analysis of Experimental Observations in Problems of Elastic Stability" Proc. Royal Society (A) Vol. 135, 1932.
16. Southwell R.V. - "Theory of Elasticity" Oxford University Press 1941.
17. Special Committee on Steel Column Research - Progress Reports Proc. A.S.C.E. March 1926 and Feb. 1929.
18. Talbot A.N. and Moore H.F. - "An Investigation of Built Up Columns Under Load". University of Illinois Bulletin No.40, 1910 also Proc. A.S.C.E. 1908 and Trans. A.S.C.E. 1909.

19. Timoshenko S. - "Theory of Elastic Stability" - McGraw - Hill 1936.
20. U.S. Bureau of Standards - Tests on Large Built Up Columns Technologic Paper No.101.
21. Watertown Arsenal - "Report of the Test of Metals" Washington 1881/82/85; 1910/11/13.
22. Young G.R. - "The Lateral Strength of Columns Subject to Flexure", Engineering News Record Vol. 89. 1922.
23. Young D.H. - "Rational Design of Steel Columns" Proc. A.S.C.E. Vol.60. Dec. 1934.
24. Bryan G.H. - "On the stability of a Plane Plate Under Thrust in Its Own Plane". Proc. London Math. Soc. Vol.22, 1890.
25. Cox H.L. - "Summary of the Present State of Knowledge of Sheet Metal Construction" R. and M., No. 1553, British A.R.C. 1933.
26. Cox H.L. and Smith, H.E. - "Structures of Minimum Weight" R. and M. No. 1923, British A.R.C. 1943.
27. v. Karman Th., Sechler E.E. and Donnell L.H. - "The Strength of Thin Plates in Compression". Trans. A.S.M.E. Vol. 54, 1932.
28. Moir C.M. and Kenedi R.M. - "Factors Influencing the Design of Thin Walled Columns" Journal Inst. of Strut. E. Feb. 1948.
29. Niles A.S. and Newell J.S. - "Airplane Structures" John Wiley and Sons, Inc. New York 3 Ed. 1943.
30. Sechler E.E. and Dunn L.G. - "Airplane Structural Analysis and Design", John Wiley and Sons, Inc. New York 1942.
31. "Specification for the Design of Light Gauge Steel Structural Members" American Iron and Steel Institute, April 1946.
32. Thomas E.W. - "Torsional Instability of Thin Angle Section Struts", Journal Inst. of Strut. E. May 1941.
33. Timoshenko S. "Strength of Material" (Vol.1) Von Nostrand, New York, 1930.
34. Winter G. - "Strength of Thin Steel Compression Flanges". Proc. A.S.C.E. Feb. 1946 and June 1946.
35. Wang, Chi-Teh - "Inelastic Column Theories and an Analysis of Experimental Observations". Journal of the Aero. Sc. Vol. 15, May 1948. No.5.

ACKNOWLEDGEMENTS.

The experimental work presented in the thesis was carried out in the Laboratories of the Civil and Mechanical Engineering Department of the Royal Technical College, Glasgow.

The author wishes to record his sense of indebtedness to Professor William Kerr C.B.E., Ph.D., A.R.T.C., M.I. Mech. E., for his continued interest and encouragement.

78.

APPENDIX No. I

SOLUTION OF THE ECCENTRIC LOAD EQUATIONS
FOR LATTICED COLUMNS BY FOURIER SINE TRANSFORMATION.

Reference: "Modern Operational Mathematics in Engineering" R.V. Churchill, McGraw Hill 1944

The column equations are

$$\left. \begin{aligned} EI \frac{d^4 y_1}{dx^4} + P_1 \frac{d^2 y_1}{dx^2} - \beta(y_2 - y_1) &= 0 \\ EI \frac{d^4 y_2}{dx^4} + P_2 \frac{d^2 y_2}{dx^2} + \beta(y_2 - y_1) &= 0 \end{aligned} \right\} \text{Substituting } D = \frac{d}{dx}$$

equations become

$$EID^4 y_1 + P_1 D^2 y_1 - \beta(y_2 - y_1) = 0 \quad \text{--- 1.}$$

$$EID^4 y_2 + P_2 D^2 y_2 + \beta(y_2 - y_1) = 0 \quad \text{--- 2.}$$

The boundary conditions — assuming hinged ends for the column legs are $y_1 = y_2 = 0$ $\left\{ \begin{array}{l} \text{at } x=0 \text{ and } x=L \\ D^2 y_1 = D^2 y_2 = 0 \end{array} \right.$

Multiplying equations 1. and 2. by $\sin \frac{n\pi x}{L}$ where n is any integer and integrating from $x=0$ to $x=L$ gives

$$EI \int_0^L D^4 y_1 \sin \frac{n\pi x}{L} dx + P_1 \int_0^L D^2 y_1 \sin \frac{n\pi x}{L} dx - \beta \int_0^L y_2 \sin \frac{n\pi x}{L} dx + \beta \int_0^L y_1 \sin \frac{n\pi x}{L} dx = 0$$

$$EI \int_0^L D^4 y_2 \sin \frac{n\pi x}{L} dx + P_2 \int_0^L D^2 y_2 \sin \frac{n\pi x}{L} dx + \beta \int_0^L y_2 \sin \frac{n\pi x}{L} dx - \beta \int_0^L y_1 \sin \frac{n\pi x}{L} dx = 0$$

Let $Y(n) = \int_0^L y \sin \frac{n\pi x}{L} dx = \int_0^L f(x) \sin \frac{n\pi x}{L} dx$ when $y = f(x)$

Hence $\int_0^L y_1 \sin \frac{n\pi x}{L} dx = Y_1(n)$ and $\int_0^L y_2 \sin \frac{n\pi x}{L} dx = Y_2(n)$

$$\begin{aligned} \text{Also } \int_0^L D^2 y \sin \frac{n\pi x}{L} dx &= \int_0^L f''(x) \sin \frac{n\pi x}{L} dx = \left[f'(x) \sin \frac{n\pi x}{L} \right]_0^L + \frac{n\pi}{L} \int_0^L f'(x) \cos \frac{n\pi x}{L} dx \\ &= 0 + \frac{n\pi}{L} \left[f(x) \cos \frac{n\pi x}{L} \right]_0^L - \frac{n\pi}{L} \int_0^L f(x) \sin \frac{n\pi x}{L} dx \\ &= \frac{n\pi}{L} (-1)^n [f(L) - f(0)] - \frac{n^2 \pi^2}{L^2} Y(n) \end{aligned}$$

For the given boundary conditions in both y_1 and y_2
 $y=f(x)=0$ at $x=L$ and $x=0$, that is $f(L)=0$ and $f(0)=0$ hence

$$\int_0^L D^2 y_1 \sin \frac{n\pi x}{L} dx = -\frac{n^2 \pi^2}{L^2} Y_1(n); \int_0^L D^2 y_2 \sin \frac{n\pi x}{L} dx = -\frac{n^2 \pi^2}{L^2} Y_2(n)$$

$$\begin{aligned} \int_0^L D^4 y \sin \frac{n\pi x}{L} dx &= \int_0^L f^{(4)}(x) \sin \frac{n\pi x}{L} dx = [f'''(x) \sin \frac{n\pi x}{L}]_0^L + \\ &\quad + \frac{n\pi}{L} \int_0^L f'''(x) \cos \frac{n\pi x}{L} dx \\ &= 0 + \frac{n\pi}{L} \left\{ [f'''(x) \cos \frac{n\pi x}{L}]_0^L - \frac{n\pi}{L} \int_0^L f''(x) \sin \frac{n\pi x}{L} dx \right\} \\ &= \frac{n\pi}{L} (-1)^n [f'''(L) - f'''(0)] - \frac{n^3 \pi^3}{L^2} \left\{ [f'(x) \sin \frac{n\pi x}{L}]_0^L + \right. \\ &\quad \left. + \frac{n\pi}{L} \int_0^L f'(x) \cos \frac{n\pi x}{L} dx \right\} \\ &= \frac{n\pi}{L} (-1)^n [f'''(L) - f'''(0)] - 0 - \frac{n^3 \pi^3}{L^2} \left\{ [f(x) \cos \frac{n\pi x}{L}]_0^L - \right. \\ &\quad \left. - \frac{n\pi}{L} \int_0^L f(x) \sin \frac{n\pi x}{L} dx \right\} \\ &= \frac{n\pi}{L} (-1)^n [f'''(L) - f'''(0)] - \frac{n^3 \pi^3}{L^2} (-1)^n [f(L) - f(0)] + \frac{n^4 \pi^4}{L^3} Y(n) \end{aligned}$$

For the given boundary conditions in both y_1 and y_2
 $y=f(x)=0$ } at $x=L$ and $x=0$, that is $f(L)=0$; $f(0)=0$
 $D^2 y=f''(x)=0$ } $f''(L)=0$ and $f''(0)=0$ hence

$$\int_0^L D^4 y_1 \sin \frac{n\pi x}{L} dx = \frac{n^4 \pi^4}{L^4} Y_1(n); \int_0^L D^4 y_2 \sin \frac{n\pi x}{L} dx = \frac{n^4 \pi^4}{L^4} Y_2(n)$$

Substituting in the equations gives

$$EI \frac{n^4 \pi^4}{L^4} Y_1(n) - P_1 \frac{n^2 \pi^2}{L^2} Y_1(n) - \beta [Y_2(n) - Y_1(n)] = 0$$

$$EI \frac{n^4 \pi^4}{L^4} Y_2(n) - P_2 \frac{n^2 \pi^2}{L^2} Y_2(n) + \beta [Y_2(n) - Y_1(n)] = 0$$

rearranging, equations 3 and 4 (page 35) are obtained

$$[P_1 \frac{n^2 \pi^2}{L^2} - EI \frac{n^4 \pi^4}{L^4} - \beta] Y_1(n) + \beta Y_2(n) = 0 \quad \text{--- 3.}$$

$$\text{and } \beta Y_1(n) + [P_2 \frac{n^2 \pi^2}{L^2} - EI \frac{n^4 \pi^4}{L^4} - \beta] Y_2(n) = 0 \quad \text{--- 4.}$$

27

APPENDIX No. 2.

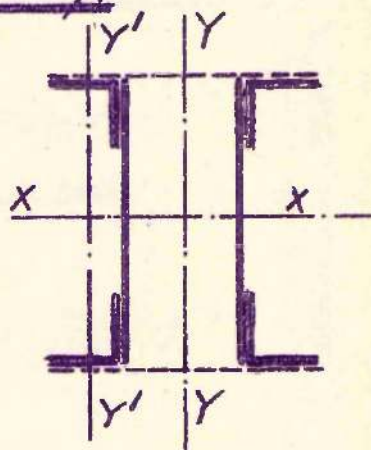
NUMERICAL EXAMPLE OF BUCKLING LOAD

ANALYSIS FOR A LATTICED COLUMN.

Calculation for Column No 1 - Talbot and
Moore (18), 1910 Test No 17.

The following data extracted
from Reference (18) was used
in the calculations.

Symbolism as in Section III (1).



Column ends hinged.

Item	L ft	d ins.	b ins.	Area in ²	I _x in ⁴	I _y in ⁴	I _{y'} in ⁴	θ°	E T/in ²	Yield stress T/in ²
Column	21.0	16.0	8.0	18.76	836	860	-	26.5	-	-
Column Leg	21.0	-	do.	9.38 (A)	418	-	1.70	do.	12,500	19,300
Panel Element	1.33	-	do.	9.38	418	-	1.70	do.	-	-
Lattice Bar	1.49	-	-	0.546 (a)	-	-	-	do.	-	-

The Latticing of the column was single and
staggered. There were 19 panels (at 8 inch spacing)
in the half length exclusive of end plates.

Calculation of the "ideal column" critical
stress.

(i) Overall Column strength

$$\text{Minimum about XX } P_e = \frac{\pi^2 \times 12,500 \times 836}{(21 \times 12)^2} = 1630^T$$

(ii) Column Leg Strength - in the plane of the latticing

Euler load for column leg on full length - minimum

$$\text{about YY } - P_e = \frac{\pi^2 \times 12,500 \times 1.70}{(21 \times 12)^2} = 3.31^T$$

To obtain the number of half waves n equation (13) is used viz:

$$\frac{a E^2 I_y}{d R^2} \cos^3 \theta \sum_{x=0}^{x=\frac{L}{2}} \left(\sin \frac{n \pi (x+p)}{L} + \sin \frac{n \pi x}{L} \right) = n^4 \int_0^{\frac{L}{2}} \sin \frac{n \pi x}{L} dx$$

For the given case $\frac{a E^2 I_y}{d R^2} \cos^3 \theta = \frac{0.576 (12,500)^2 \times 1.70}{16 \times (3.31)^2} \times (0.8952)^3$
 $= 5.98 \times 10^5 \text{ ins}$

$$\sum_{x=0}^{x=\frac{L}{2}} \left(\sin \frac{n \pi (x+p)}{L} + \sin \frac{n \pi x}{L} \right) = 4 \sum_{K=0}^{K=13} \sin n K \alpha \text{ where } \alpha = \frac{\pi \times \frac{L}{2}}{21 \times \frac{L}{T}} = 5.72^\circ$$

but $4 \sum_0^K \sin n K \alpha = 4 \sin n \frac{(K+1)}{2} \alpha \sin \frac{n K \alpha}{2} \times \frac{1}{\sin \frac{n \alpha}{2}}$ and
 substituting for $K=13$ and $\alpha = 5.72^\circ$, the sum of the series becomes $4 \sin 40.04 n \sin 34.2 n \cdot \operatorname{cosec} 2.86 n$

also $n^4 \int_0^{\frac{L}{2}} \sin \frac{n \pi x}{L} dx = n^3 \frac{L}{\pi} [1 - \cos n \frac{\pi}{2}] = 80.2 n^3 (1 - \cos \frac{n \pi}{2})$

Therefore Equation (13) reduces to on substitution

$$2.392 \times 10^6 \sin 40.04 n \sin 34.2 n \operatorname{cosec} 2.86 n = 80.2 n^3 (1 - \cos \frac{n \pi}{2})$$

The left hand side first becomes zero when $n \div 4.5$, while the right hand side is zero when $n = 4$.

In view of the relative magnitudes of the coefficients of the right and left hand sides, the value of n satisfying the equation will be near these zero values. Physically interpreted this indicates that the latticing is over stiff and the spacing of the bars and not their elasticity is the major factor in determining the value of n .

Solving the transcendental equation for n by means of the tabular method as follows:-

① n	② $\sin 40.04n$	③ $\sin 34.2n$	④ $\text{cosec } 2.86n$	⑤ $2.342 \times 10^6 \cdot \frac{1}{n^3}$	⑥ n^3	⑦ $1 - \cos \frac{n\pi}{2}$	⑧ $86.2 \cdot \frac{1}{n^3}$
4	0.3476	0.5150	5.06	2.24×10^6	64	0	0
4.25	0.1736	0.3446	4.78	.745	76.44	.6428	$.00045 \times 10^6$
4.50	0	—	—	0	91.13	.3929	.0029
4.75	-.01436	.0523	4.25	-.092	104.2	.6093	.00574
5.00	-.0342	-.01045	4.04	.346	125.0	1.00	.0100

By interpolation the two approximate values of n satisfying the equation are 4.50 and 4.80 respectively. As indicated in Section III(1), the theory is based on integral values of n — consequently the relevant solutions for n in this case are $n = 4$ or $n = 5$.

Hence the critical load values based on column strength are

$$P_c = P_e \times 2n^2 \times 2 = 3.31 \times 4 \times 16 = 212 \text{ Tons}$$

or $= 3.31 \times 4 \times 25 = 331 \text{ Tons.}$

(iii) Column Leg Strength — perpendicular to the plane of the latticing.

Euler load for column leg on full length — about

$$XX = P_e = \frac{\pi^2 \times 12,500 \times 418}{(21 \times 12)^2} = 815^T$$

At the minimum value of $n = 1$, the critical load, based on column leg strength in this plane is $P_c = 2n^2 P_e = 1630^T$. Obviously as far as

column leg strength is concerned, the value in the plane of the latticing limits and this case requires no further investigation.

(iv) Panel element strength

$$\text{Minimum value about } Y'Y' \text{ on } 16'' = \frac{8^3 \times 12,800 \times 1.40}{16^3} = 820^T$$

$$\text{hence } \underline{\text{total column load} = 1640^T}$$

Contrasting (i), (ii), (iii) and (iv) the calculations indicate that failure will take place in the plane of the latticing by buckling of one of the column legs. the "ideal column" buckling load corresponds to 4 or 5 half waves lying within the range of 212 to 331 Tons.

To obtain the actual failure stress the Perry - Robertson formula based on the "ideal column" load calculated above is used.

$$p_0 = \frac{p_y + (\eta + 1)p_e}{2} - \sqrt{\left[\frac{p_y + (\eta + 1)p_e}{2}\right]^2 - p_y p_e}$$

$$p_y = 19.30 \text{ T/in}^2 \quad p_e = \frac{212}{18.46} = 11.30 \text{ T/in}^2 \text{ or } \frac{331}{18.46} = 17.65 \text{ T/in}^2$$

$$K_e = \text{Equivalent radius of gyration} = K_r' \sqrt{\frac{p}{2R}}$$

(see Section III (2)).

$$\text{i.e. } K_e = \sqrt{\frac{1.40}{9.38}} \times \sqrt{\frac{212}{2 \times 331}} = 2.41 \text{ or } \sqrt{\frac{1.40}{9.38}} \times \sqrt{\frac{331}{2 \times 331}} = 3.01$$

$$\text{hence } \frac{1}{K_e} = \frac{21.52}{2.41} = 104.6 \text{ or } \frac{21.12}{3.01} = 83.6.$$

Using the coefficient given by Pippard (11) for batten plate columns $\eta = 0.0015 \times 104.6 = 0.154$ or

$$0.0015 \times 83.6 = 0.125.$$

Consequently

$$p_c = \frac{19.30 + 1.157 \times 11.30}{2} - \sqrt{16.15^2 - 19.30 \times 11.30} = 9.60 T_{in}$$

$$\text{or } p_c = \frac{19.30 + 1.125 \times 14.65}{2} - \sqrt{19.55^2 - 340} = 13.06 T_{in}$$

The failure stress of the column lies within the range $9.60 T_{in}$ to $13.06 T_{in}$.

Comparing the experimental results given by Talbot and Moore (18) - (Table 7, page 35 Column No 1 Test No 14 in the reference). namely a failure stress of $194/18.46 = 10.50 T_{in}$ with the above calculated values, it is seen that reasonable agreement is obtained.

The mode of failure forecast by the calculations was column leg failure, which experimentally, implies a failure usually described as "local". The failure recorded by Talbot and Moore was of this type.

The foregoing results together with other column test results are recorded in Tables 1 and 2 of Section III (2) of the thesis. All theoretical results have been calculated as indicated in this Appendix.

87.
APPENDIX No.3.

SUMMARY OF TENSILE TEST RESULTS ON
MATERIAL OF SPECIMENS USED IN THE EXPERIMENTAL WORK.

Summary of Tensile Tests.

Specimens cut from each flange and web of columns.
Width of specimens $\frac{1}{2}$ inch - Gauge Length 2 inches.

Column Length ft.	Nominal Thickness	Young's Mod. E Tons/in ²	Yield Stress p_y Tons/in ²	Ultimate Stress Tons/in ²
3 ft. column specimens and lattice column model.	18G	11,400	13.3	22.8
		11,800	15.4	24.0
		12,000	14.3	21.6
	17G	11,200	14.2	23.0
		11,000	14.0	22.1
		11,200	13.4	23.0
	16G	10,800	13.8	22.4
		11,300	14.2	22.0
		11,200	14.0	22.4
	14G	10,800	13.6	22.2
		10,900	13.3	21.8
		10,600	14.2	23.0
	12G	11,100	14.3	21.6
		11,100	13.6	21.9
		10,800	13.5	21.8
	Average	11,150	13.90	22.40
12 ft. columns.	$\frac{7}{32}$ in.	12,420	18.90	29.10
		12,450	18.50	28.80
		12,550	18.45	28.80
	Average	12,470	18.62	28.90

Values used in Calculations.

Column Length	E Tons/in ²	p_y Tons/in ²	p_{ult} Tons/in ²
3 ft columns and lattice model.	11,000	14.0	—
12 ft columns	12,500	18.50	—

Summary of Tensile Tests.

Specimens cut from each flange and web of columns.
Width of specimens $\frac{1}{2}$ inch - Gauge Length 2 inches.

Column Length ft.	Nominal Thickness	Young's Mod. E Tons/in ²	Yield Stress p_y Tons/in ²	Ultimate Stress Tons/in ²
3 ft. column specimens and lattice column model.	18G	11,400	13.3	22.8
		11,800	15.4	24.0
		12,000	14.3	21.6
	17G	11,200	14.2	23.0
		11,000	14.0	22.1
		11,200	13.4	23.0
	16G	10,800	13.8	22.4
		11,300	14.2	22.0
		11,200	14.0	22.4
	14G	10,800	13.6	22.2
		10,900	13.3	21.8
		10,600	14.2	23.0
	12G	11,100	14.3	21.6
		11,100	13.6	21.9
		10,800	13.5	21.8
	Average	11,150	13.90	22.40
12 ft. columns.	$\frac{7}{32}$ in.	12,420	18.90	29.10
		12,450	18.50	28.80
		12,550	18.45	28.80
	Average	12,470	18.62	28.90

Values used in Calculations.

Column Length	E Tons/in ²	p_y Tons/in ²	p_{ult} Tons/in ²
3 ft columns and lattice model.	11,000	14.0	—
12 ft columns	12,500	18.50	—

89.

APPENDIX No. 4.

I. STRESS SURVEY OF THE FLANGE OF A 12 FT. LONG THIN WALLED
COLUMN SPECIMEN.

Apparatus and Measuring Devices.

Experimental Stress Results and Discussion.

Stress Variation along length of Column.

Stress Variation with Column Load at Particular Points.

Summary of Stress Survey.

II. EXPERIMENTAL COLLAPSE LOAD RESULTS AND DISCUSSION.

Fig. 45.

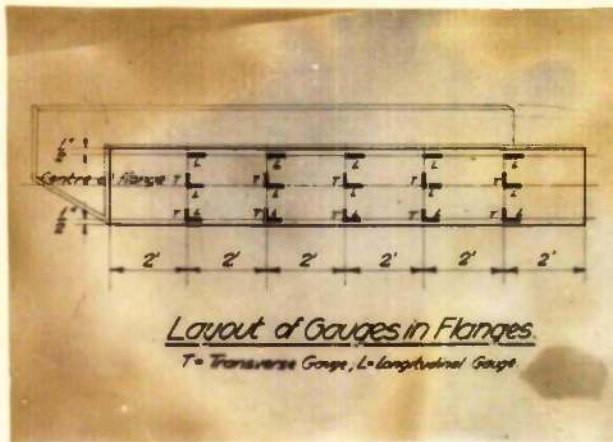


Fig. 46.



Free edge
of flange

Edge adjoining
web.

Fig. 47.

I. STRESS SURVEY OF FLANGES.

Apparatus and Measuring Devices.

The test specimens were set up in the 100 Tons Avery machine as described in Part II Section II of the Thesis.

Strain readings were obtained using Electrical Resistance Strain Gauges of approximately 200 ohms. resistance. The strain gauge bridge used - Fig. 45 - was capable of accommodating 50 gauges. The disposition of the 25 gauges used along and across the flanges is shown in Fig. 46. Along the free edge of the flange only longitudinal gauges were utilised, both longitudinal and transverse gauges being used however along the centre line of the flange and along the edge adjoining the web. A close up of one group of gauges incorporating transverse and longitudinal live gauges and temperature compensator dummy gauges is shown in Fig. 47.

In installing the gauges precautions such as thorough degreasing of surface, drying out of gauges, replacement of gauges with an insulation resistance of gauge to surface of less than 100 megohms etc. were strictly observed and led to satisfactory gauge response during the experiments.

The gauge factors of the gauges used with the 12 inch and the 7 inch flange were 2.17 and 1.99 respectively.

The gauge readings were reduced to stress readings using the value of Young's Modulus as 12,500 tons / in² and the value of Poisson's ratio as .3. (See appendix No.3)

Experimental Stress Results and Discussion.

The experimental results presented are those obtained for the 12 inch flange. The characteristics shown up by the 7 inch flange are exactly similar and are therefore not included.

Stress Variation Along Length of Column.

Note: The experimental points on the graphs are connected by straight lines, as it is felt that they are too few in number to define the true shape of the existing curvilinear distribution with accuracy.

Fig. 48 shows the longitudinal stress values as given by the gauge readings at axial loads of 8, 16, 24, 32 and 38 tons. The distributions are given along the free edge (line A), along the centre of the flange (line B) and along the edge adjoining the web (line C).

It should be noted that the stress values are a combination of the direct stresses due to the end load and the bending stresses due to the flange waving.

Fig. 49 gives the percentage deviation of the longitudinal stress from the average stress at the same loads and along the same lines. This figure in effect indicates the stresses existing in the flange due to its waving only.

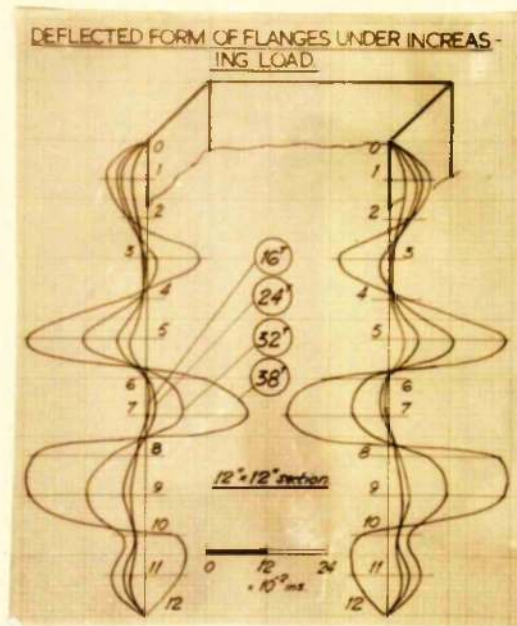


Fig. 39.

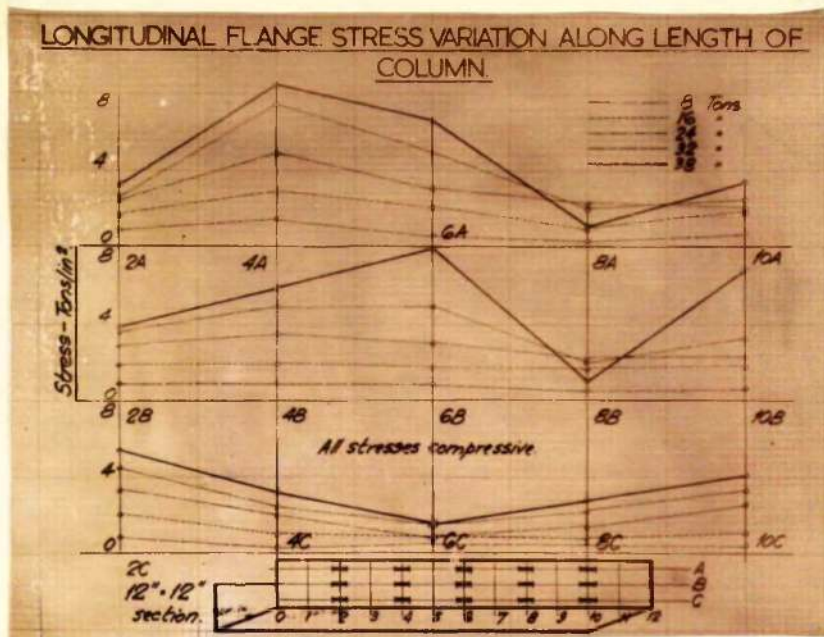


Fig. 48.

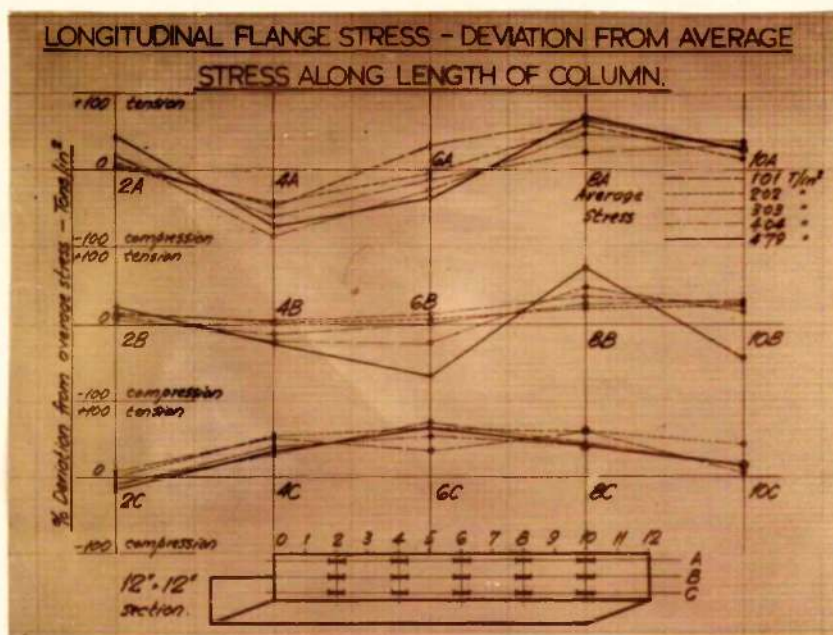


Fig. 49.

The main features are as follows:-

- (1) Considerable stress variations obtain longitudinally. For example at a load of 38 tons (average stress 4.79 tons /in²) the stress drops from about 8 tons / in² at 4A to about 0.8 tons / in² at 8A, that is a percentage deviation of about - 70% to + 70% from the average stress.

92.
(ii) The stress variations are similar in form along the free edge and the centre line but change completely along the edge adjoining the web.

Comparing the nature of the variations along the free edge with its deflected form - Fig. 39 reproduced opposite - it is seen that correlation is possible. For example at ^{point} 8A the gauge having been installed on the outer surface of the flange will measure the combination of tensile bending stresses and compressive direct stresses. In view of the considerable flange deflection at point 8A the tensile stresses due to bending are large (about 70% of the average stress at the load of 38 tons) giving the resultant stress of 0.8 tons / in². Similar correspondence obtains at points 2A and 10A.

At point 6A the flange deflections are such as to induce compression in the outer fibres thus giving the increase in the direct compressive stress indicated.

The correlation at point 4A is uncertain. Point 4 on the free edge lies very near to an apparent node point, consequently if the initial irregularity of the flange at that point is not appreciable the bending effect should be small. The stress readings indicate the existence of considerable compressive bending stresses. One possible explanation is that although the deflection at point 4 is small, the curvature of the plate at the point is large, thus accounting for the bending stresses indicated. The experimental data of the deflected flange form given in Fig. 39 is inconclusive in respect of curvature.

The stress variations along line B follow in general outline that of line A and consequently the deflected form of the flange surface along this line is probably similar to the free edge.

Line C gives a distribution of a different type. The presence of tensile bending stresses increasing towards the centre is indicated. It may be noted in this connection that these stresses are not overall bending effects due to deadweight as these were compressive on the gauge side, on the length 40 to 80. In any case their magnitude is of a negligible order.

A possible explanation may be found in the nature of the actions obtaining along the edge adjoining the web. Along this edge the flange is restrained from taking up a deflected form. The restraint will be given by distributed moments acting along this edge of the flange in the plane of the web. The initial form the flange tends to assume, will determine the type of distribution of these moments and the corresponding longitudinal bending stresses.

The distribution shown along line C could for example be visualised as corresponding to an initial tendency to deflect into a single half wave for the full length.

The stress values shown in Fig. 50 are due to the transverse bending effects set up by the distortion of the flange plate.

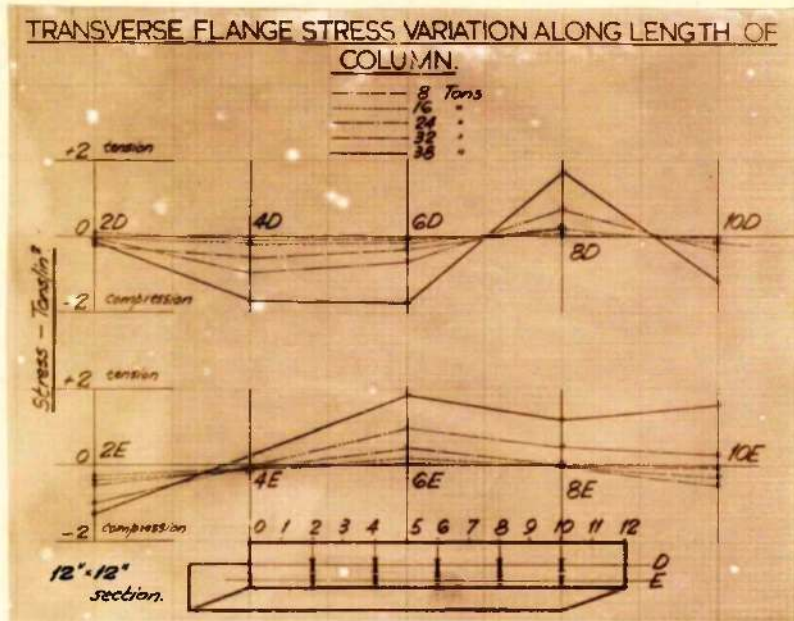


Fig. 50.

The distributions indicate variations both of magnitude and nature, along and across the flange plate.

The magnitudes are appreciable and for example amount to about 40% of the average longitudinal stress at a load of 38 tons.

The change from tension to compression at points such as 6 (6E to 6D) is particularly significant as it indicates a change in the transverse curvature of the flange. Consequently the deflected form of the flange across its width is one of double curvature at points 4, 6 and 10. It is probably of the same type at points 2 and 8 also.

Stress Variation with Column Load at Particular Points.

The longitudinal or axial flange stress variations are shown in Figs. 51 and 52. The graphs contrast the combined direct and bending stress against column load variation at points near the centre and near the end of the column length.

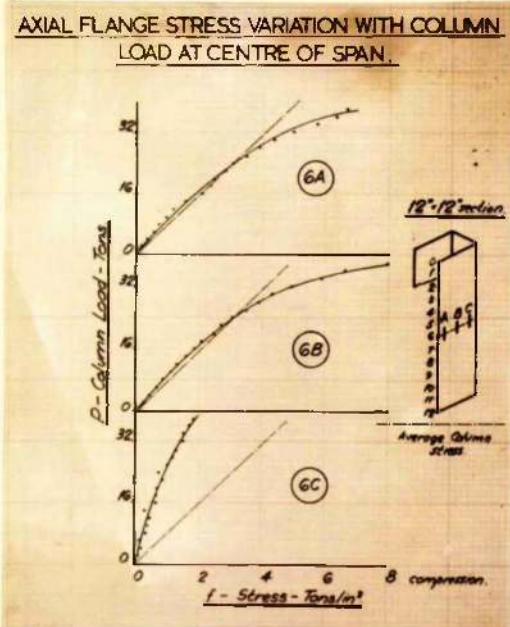


Fig. 51.

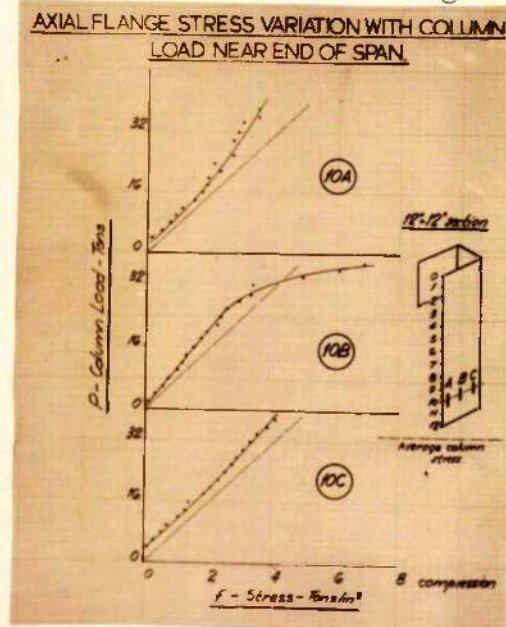


Fig. 52.

The graphs indicate by their deviation from the average stress the variation of the longitudinal stress along the length of the column. This has already been discussed.

Two main types are apparent:

- (i) Distributions of the type 10A, 10C and 6C exhibit a more or less uniform rate of increase of stress.
- (ii) Graphs such as 10B, 6A and 6B show a gradually increasing rate of stressing and cross the average stress line.

Comparing the stress variations from the point of view of position across the flange and along the flange the main difference is shown up by graphs 10C and 6C. These, while similar in form, differ considerably in their deviation from the average stress, 6C showing the effect of the longitudinal tensile bending stress.

The variation of the transverse bending stress with column load is shown in Figs. 53 and 54. These are all of the same non linear form.

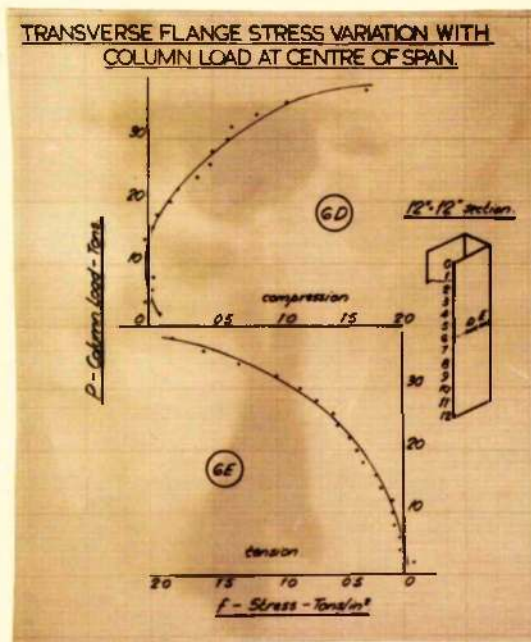


Fig. 53.

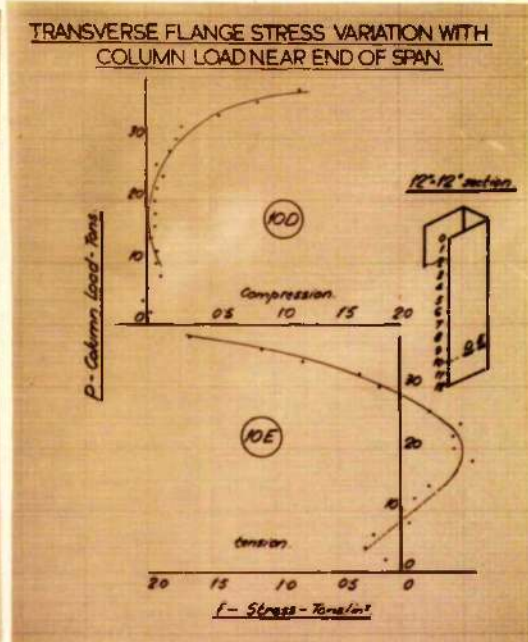


Fig. 54.

The stresses increase at a gradually increasing rate as the flange deflections increase. The significant feature is the change in tension to compression from the web edge to the free edge. In addition 10E exhibits a change from tension to compression and back to tension as the load increases. These features again confirm the complex nature of the deflected form of the flange surface.

Summary of Stress Survey.

The features brought out by the stress survey under elastic conditions may be summarised as follows:

- (i) The stress variations are on the whole non linear.
- (ii) Both longitudinal and transverse stresses exist in the flange plates due to the combined action of the column load and the flange distortion.
- (iii) The longitudinal and transverse stresses vary both lengthwise and crosswise. The maximum variation of the longitudinal stresses encountered in the experiment was approximately 75% of the average stress, obtained when the column load was approaching the elastic buckling value. The maximum value of the transverse stress was about 40% of the corresponding average longitudinal stress under the same conditions.
- (iv) The distorted form of the flange surface is more complex than it is indicated by the edge deflections alone, reversal of flange plate curvature obtaining in the transverse directions.

II. EXPERIMENTAL COLLAPSE LOAD RESULTS

AND DISCUSSION.

The computation of the collapse load of thin plates as distinct from their elastic buckling load is usually based on the "effective width" conception originally proposed by v.Karman (27) for plates supported along both edges.

As indicated in the brief survey of Part II Section I. Winter (34) has put forward the semi-empirical expression

$$b_e = 0.8t \sqrt{\frac{E}{p}} \left(1 - 0.202 \frac{t}{b} \sqrt{\frac{E}{p}} \right)$$

for the effective width which, it was claimed could be applied both to the computation of the elastic buckling load and the collapse load.

The experimental results presented in Part II Section II (Fig. 36 p. 64) clearly indicated that the elastic buckling stress proposed by Winter for use in conjunction with b_e seriously underestimates the actual elastic buckling strength past a b/t value of 30 even if based on the full plate width and not as proposed on a reduced effective width. Further the stress survey did not indicate any radical stress transference in the elastic range from the plate strip along the free edge to the plate strip adjoining the web. Thus the claim put forward by Winter that the effective width conception for flanges supported along one edge only applies in the elastic range is not in accord with experimental findings.

On the other hand utilising the expression for b_e in conjunction with the yield stress p_y of the material, in the computation of the collapse load, good agreement with experimental values is obtained.

The following table gives the experimental and calculated collapse load results for the 12 ft. specimens.

Width of Web w ins.	Width of Flange b ins.	Thickness of flange t ins.	Sectional Area of column A in ²	b/t	Tons. Collapse Load	
					Experi- mental	Calculated
12.02	6.92	0.2137	5.52	32.4	56.0	54.6
12.01	12.02	0.2205	7.95	54.6	52.9	50.6

The method of computation is as follows:
Considering the 12 inch (nominal) flange for example.

$$b_e = 0.8 \times 0.2205 \sqrt{\frac{12,500}{18.5}} \left(1 - 0.202 \frac{1}{54.6} \sqrt{\frac{12,500}{18.5}} \right)$$

$$\text{i.e. } b_e = 4.14 \text{ ins.}$$

Therefore the collapse load for the flange is

$$P = b_e t p_y = 4.14 \times 0.2205 \times 18.5 = 16.85 \text{ Tons.}$$

This is equivalent to an average stress of

$$p = \frac{P}{b \cdot t} = \frac{16.85}{12.02 \times 0.2205} = 6.36 \text{ Tons/in}^2$$

over the whole column area.

That is the overall column load at which the flange will collapse is

$$P = pA = 6.36 \times 7.95 = 50.6 \text{ Tons.}$$

which compares favourably with the experimental value of 52.9 tons.

APPENDIX No. 5.

NOTE ON THE DESIGN OF CONCENTRICALLY
LOADED THIN WALLED COLUMNS.

38.

NOTE ON THE DESIGN OF CONCENTRICALLY LOADED THIN WALLED

COLUMNS.

The Perry-Robertson formula

$$p_c = \frac{p_r + (\eta + 1)p_e}{2} - \sqrt{\left(\frac{p_r + (\eta + 1)p_e}{2}\right)^2 - p_r p_e}$$

is the basis of column design in this country. It was originally developed for integral column action, that is on the basis of overall stability.

The analysis of the experimental work presented in Part II of the Thesis indicated that the formula gives good agreement with the experimental results in the component failure range also, provided the values of p_e and η correspond to the strength characteristics of the weakest plate component.

The value of p_e recommended for use in design is the elastic buckling stress of the plate component and not the stress corresponding to its ultimate collapse load. The main reason for this recommendation is that in ordinary structural engineering it is considered highly desirable to eliminate all possibility of crinkling under working conditions even if this involves some sacrifice in load carrying capacity.

The line of demarcation between integral column and plate component failure is obtained by equating the Euler column critical stress with the weakest plate component critical stress giving the linear relationship

$$\frac{L}{r} = \sqrt{\frac{k_1(1-\sigma^2)}{k_2}} \left(\frac{b}{t}\right)$$

where $\frac{L}{r}$ = slenderness ratio of column
 $\frac{b}{t}$ = weakest plate component dimension ratio
 k_1 = column constant depending on end conditions
 k_2 = plate constant depending on edge conditions.

Hence for any given section of known b/t value the slenderness ratio and consequently the "optimum" length L_0 corresponding to simultaneous column and component collapse may be calculated. The section under consideration will fail due to failure of the plate component if used on a length less than L_0 and it will fail due to integral column failure if its length is greater than L_0 .

The following values of p_e and η recommended for use with channel sections, within the approximate limiting values of the characteristic dimension ratios specified. /

specified.

Type of Failure:	Ideal Critical Stress p_e	Imperfection Factor η
<u>Integral Column</u> (as per B.S.S. 449) $\frac{b}{t}$ not greater than about 20.	$K_1 \frac{E}{(\frac{L}{r})^2}$ (Euler Column Stress)	$0.003 \frac{L}{r}$ (Robertson's value).
<u>Plate Component</u> $\frac{L}{r}$ not greater than about 100.	$K_2 \frac{E}{1-\sigma^2} \left(\frac{t}{b}\right)^2$ and $\frac{b}{t}$ $K_2 = \frac{b/t}{46 + 0.15 \frac{b}{t}}$ from $\frac{b}{t} = 20$ to $\frac{b}{t} = 60$	$0.0025 \frac{b}{t}$ (based on experiments of section II Part I)

The above described procedure applies over the whole range of structural behaviour encountered in thin walled columns. While in practice considerations other than purely structural strength may be the deciding factor it is emphasised that maximum strength, minimum weight, and economy results from the use of "equal" strength sections, that is sections designed for simultaneous integral column and plate component collapse. This can be effected by utilising a given section only on its optimum length L_0 .

In view of the great variety of thin walled columns available, it is possible to draw up design tables which by presenting alternative sections rather than only alternative sizes of the same section enable structural designers to use "equal" strength columns and to satisfy the practical construction requirements at the same time.

700.

APPENDIX No. 6.

FLANGE DEFLECTION VARIATION WITH AXIAL

LOAD.

Graphs additional to typical variation
incorporated in the text.

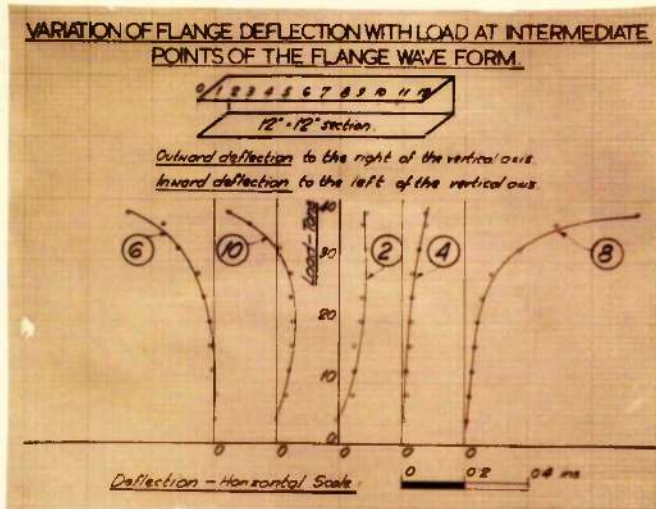


Fig. 55.

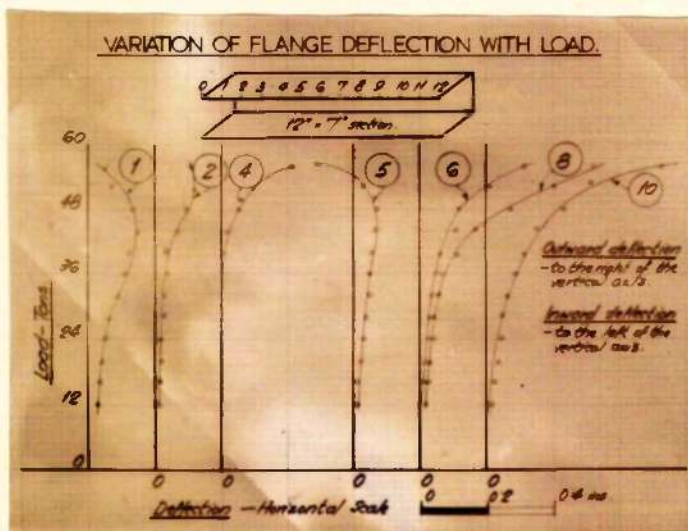


Fig. 56.

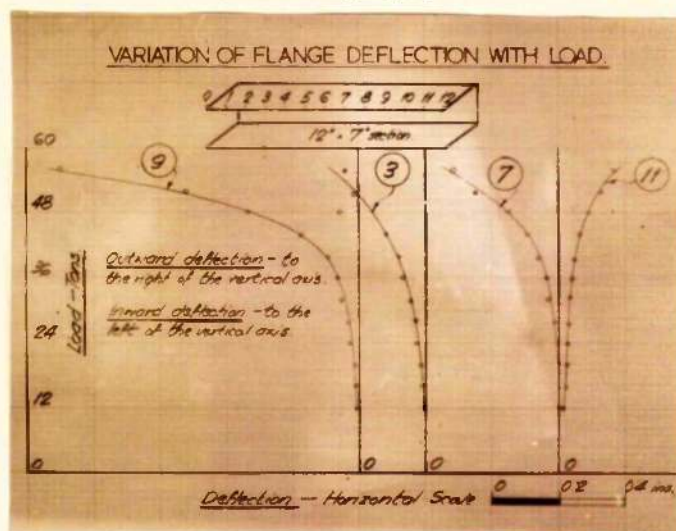


Fig. 57.